HARMONIA
International network for harmonization of atmospheric aerosol retrievals from ground based photometers

HARMONIA CA21119

Deliverable 3.3

Radiometric Measurements of Aerosol Optical Properties: Applications, Current State, and Needs

Authors

Ilias Fountoulakis[1,2], Stavros Solomos[1,2], Sophie Vandenbussche[3], Africa Barreto[4], Sara Basart[5], Hugues Brenot[3], Monica Campanelli[6], Georgia Charalampous[7,8], Maria João Costa[9], Pavla Dagsson-Waldhauserová[10], Henri Diémoz[11], Lionel Doppler[12], Victor Estelles[13], Antonis Gkikas[1], Marilena Gidarakou[14,15], Sara Herrero Anta[16,17], Celia Herrero del Barrio[16,17], Angelos Karanikolas[18], Stefan Kinne[19], Dimitra Kouklaki[20,21], Maria Elisavet Koukouli[22], Natalia Kouremeti[18], Maja Kuzmanoski[23], Franco Marenco[24], Anna Moustaka[18], Anca Nemuc[25], Kyriakoula Papachristopoulou[18], Alkistis Papetta[24], Emmanouil Proestakis[20,26], Ioannis-Panagiotis Raptis[27], Roberto Román[16,17], Carlos Toledano[16,17], Stelios Kazadzis[18]

Affiliations

[1] Research Centre for Atmospheric Physics and Climatology, Academy of Athens, Athens, Greece

[2] Biomedical Research Foundation, Academy of Athens, Athens, Greece

[3] Royal Belgian Institute for Space Aeronomy (BIRA-IASB), Brussels, Belgium

[4] Izaña Atmospheric Research Center (IARC), Agencia Estatal de Meteorología (AEMET), Santa Cruz de Tenerife, Spain

[5] World Meteorological Organization (WMO), Geneva, Switzerland

[6] National Research Council of Italy (CNR), Institute of Atmospheric Sciences and Climate (ISAC), Rome, Italy

Funded by the European Union

[7] Department of Resilient Society, Eratosthenes Centre of Excellence, Limassol, Cyprus

[8] Department of Civil Engineering and Geomatics, Cyprus University of Technology, Limassol, Cyprus

[9] University of Évora, Center for Sci-Tech Research in Earth System and Energy (CREATE) and Department of Physics, School of Sciences and Technology, Évora, Portugal

[10] Agricultural University of Iceland, Iceland

[11] Regional Environment Protection Agency (ARPA) of the Aosta Valley, Saint-Christophe, Italy

[12] Deutscher Wetterdienst (DWD), Meteorologisches Observatorium Lindenberg – Richard-Aßmann-Observatorium (MOL-RAO), Lindenberg (Tauche), Germany

[13] Department of Earth Physics and Thermodynamics, University of Valencia, Burjassot, Spain

[14] Laser Remote Sensing Unit (LRSU), Physics Department, National Technical University of Athens, Zografou, Greece

[15] Laboratory of Atmospheric Processes and Their Impacts, School of Architecture, Civil and Environmental Engineering, École Polytechnique Fédérale de Lausanne, Lausanne, Switzerland

[16] Group of Atmospheric Optics (GOA-UVa), Universidad de Valladolid, Spain

[17] Laboratory of Disruptive Interdisciplinary Science (LaDIS), Universidad de Valladolid, Spain

[18] World Optical Depth Research and Calibration Centre (WORCC), Physikalisch-Meteorologisches Observatorium Davos/World Radiation Center (PMOD/WRC), Davos Dorf, Switzerland

[19] Max Planck Institute for Meteorology, Hamburg, Germany

[20] Institute for Astronomy, Astrophysics, Space Applications and Remote Sensing, National Observatory of Athens, Athens, Greece

[21] Department of Geology and Geoenvironment, National and Kapodistrian University of Athens, Athens, Greece

[22] Department of Physics, Aristotle University of Thessaloniki, Thessaloniki, Greece

[23] Institute of Physics Belgrade, National Institute of the Republic of Serbia, Belgrade, Serbia

[24] Climate and Atmosphere Research Centre (CARE-C), The Cyprus Institute, Nicosia, Cyprus

[25] National Institute of R&D for Optoelectronics (INOE), Romania

[26] School of Chemical and Environmental Engineering, Technical University of Crete, Chania, Greece

[27] Institute for Environmental Research and Sustainable Development, National Observatory of Athens, GR15236 Athens, Greece

Date: 16 October 2026

Funded by the European Union

Abstract 4
1. Introduction 5
2. Current Capabilities 10
2.1. Ground based 10
2.2. Satellite and model data 23
2.3. Complementarity and challenges 27
3. User Requirements Across Disciplines 29
3.1. Solar radiation and radiative transfer modelling 29
3.2 Solar Energy 30
3.3. Atmospheric modelling and data assimilation 34
3.4. Satellite validation 39
3.5. Health Applications 41
3.6. Aviation 47
4. Gaps and Challenges 50
4.1. Geographic coverage gaps 50
4.2. Solar radiation and solar energy 56
4.3. Atmospheric Modelling and Data Assimilation 58
4.4. Satellite Validation 59
4.5. Health applications 61
4.6. Aviation 63
4.7. Other emerging needs 64
5. Way forward 67
Appendix 1: Measurement principles of radiometric retrieval of aerosol optical properties 70
Appendix 2: Satellite instruments used to retrieve aerosol parameters 75
References 78

Abstract

Atmospheric aerosols influence Earth's radiative balance and weather and play a key role in many processes related to human welfare and health, and the function of the ecosystems. Radiometric measurements of the aerosol optical properties are not only key for the understanding of the impact of aerosols on climate, but also useful for a wide range of applications and activities. Despite the progress that has been achieved in the last three decades in the development of instruments and networks for the monitoring of aerosol optical properties, there is still much space for improvement. This review examines the current state of radiometric observing systems and networks, and considers how these observations complement satellite products, lidar measurements, atmospheric models and reanalyses, and how they support satellite validation, data assimilation and climate monitoring. User requirements are assessed across a wide range of applications. Current capabilities of the sun-photometric systems to cover existing needs are also assessed, and finally, gaps and emerging needs are identified to construct a roadmap for the future. The review identifies priorities for sustained reference measurements, traceable calibration, harmonized protocols, transparent uncertainty estimates and improved integration across observing systems. Addressing these needs will strengthen aerosol datasets and their use in environmental research and operational services.

1. Introduction

Atmospheric aerosols are among the most important yet complex constituents of the Earth system. Despite their relatively short atmospheric lifetime compared to greenhouse gases, they exert profound influences on the climate system, atmospheric composition, ecosystem functioning, and human health. Aerosols interact directly with solar radiation through scattering and absorption processes, thereby modifying the Earth's radiation budget and the amount of biologically active solar radiation reaching the surface (IPCC, 2023). They also affect climate indirectly by acting as cloud condensation and ice nuclei, altering cloud microphysical properties, cloud lifetime, and precipitation processes (Rosenfeld et al., 2014). Beyond climate, aerosols influence numerous environmental and socio-economic sectors (IPCC, 2021). They attenuate and spectrally modify the solar radiation reaching the Earth's surface, thereby influencing photovoltaic and concentrating solar power generation, solar resource assessment, and the accuracy of solar irradiance and power forecasting (e.g., Gueymard et al., 2018). At the surface, particulate matter remains one of the major environmental health hazards, with fine particles (PM2.5) continuing to rank among the leading causes of premature mortality worldwide (WHO, 2021). Aerosols also participate in stratospheric chemistry and ozone depletion (Fahey et al., 1993), influence atmospheric visibility, affect aviation safety during volcanic eruptions and dust events (Jónsdóttir, 2011), and play an increasingly important role in numerical weather prediction, atmospheric composition monitoring, and climate services (Benedeti et al., 2018; Remi et al., 2019). Owing to their multiple interactions with the atmosphere and society, aerosols remain one of the largest sources of uncertainty in estimates of anthropogenic radiative forcing (IPCC, 2023) and continue to motivate the development of increasingly accurate observational systems.

Aerosols are an exceptionally heterogeneous atmospheric constituent, comprising particles that originate from both natural and anthropogenic sources and span several orders of magnitude in size, with highly variable chemical composition, shape, hygroscopicity, and optical behaviour. Their atmospheric abundance and properties can change substantially over spatial scales of a few kilometres and temporal scales of only a few hours, making their characterization considerably more challenging than that of well-mixed atmospheric gases (Seinfeld and Pandis, 2016). Although in-situ measurements (Quincey and Batterfield, 2009) provide highly accurate information on aerosol physical, chemical and microphysical properties, they are representative only of the local sampling volume and therefore provide limited information about the vertical distribution and column-integrated aerosol burden. Such observations alone are generally insufficient for studying aerosol transport, aerosol–cloud interactions, aerosol radiative forcing, or for validating satellite products and constraining atmospheric models. These challenges have driven the development of passive and active remote sensing techniques capable of observing aerosols over much larger spatial domains. Among them, passive radiometric observations have become the cornerstone of global aerosol monitoring because they provide continuous, non-destructive, and highly accurate measurements of the interaction between aerosols and solar radiation, enabling the retrieval of column-integrated aerosol optical and microphysical properties (e.g., Munro et al., 2016; Hassinen et al., 2016; Veefkind et al., 2012; Litvinov et al., 2025).

The interaction between aerosols, and solar (or thermal) radiation is commonly described through a complementary set of aerosol optical and microphysical properties (AOPs), each characterizing a different aspect of aerosol–radiation interactions. The most fundamental parameter is the aerosol optical depth (AOD), which quantifies the total extinction of solar radiation caused by aerosols throughout the atmospheric column and therefore represents the overall aerosol burden (WMO, 2003). The spectral dependence of AOD in a certain wavelength range is commonly described by the Ångström Exponent (AE) (Eq. 1.1). AE provides valuable information on the dominant aerosol particle size, with lower values generally indicating coarse-mode particles and higher values corresponding to fine-mode aerosols.

$$\tau = \beta \cdot \lambda^{-\alpha} \tag{1.1}$$

where τ denotes the aerosol optical depth, β is the turbidity coefficient, λ is the wavelength, and α is the Ångström exponent.

Although AOD and AE provide a first-order description of aerosol loading and particle size, they are insufficient to fully characterize aerosol radiative effects. Additional optical and microphysical properties are required to describe aerosol absorption and scattering behaviour, and particle composition. Among these, the single scattering albedo (SSA), defined as the ratio of aerosol scattering to total extinction, describes the balance between scattering and absorption, ranging from 0 (purely absorbing) to 1 (purely scattering), and is mostly related to aerosol chemical composition and particle size and, to a lesser extent, particle shape (Moosmüller and Sorensen, 2018; Wang et al., 2021; Huang et al., 2023). The complex refractive index further characterizes the intrinsic optical properties of aerosol particles, with its real part controlling scattering and its imaginary part describing absorption. The angular redistribution of scattered radiation is described by the aerosol phase function, while the asymmetry factor summarizes the relative importance of forward and backward scattering, depending primarily on particle size, morphology and orientation, although hygroscopic growth and chemical composition may also influence its value (Zhao et al., 2018; Huang et al., 2023).

Because atmospheric aerosols consist of particles spanning a wide range of sizes rather than a single characteristic diameter, their size is commonly represented by the column-integrated aerosol volume size distribution (VSD), which is generally approximated by a bimodal lognormal distribution (Dubovik and King, 2000). The VSD provides information on the volume concentration and characteristic radius of both the fine and coarse aerosol modes, while derived quantities such as the total aerosol volume concentration and modal AOD offer additional insight into aerosol loading and dominant particle populations (O'Neill et al., 2003;Dubovik and King, 2000). Together, these aerosol optical and microphysical properties provide a comprehensive description of aerosol abundance, size, composition and radiative behaviour, forming the basis foraerosol remote sensing, radiative transfer calculations, climate studies, atmospheric composition monitoring and an increasing number of operational environmental applications (IPCC, 2013).

The ground-based comprehensive characterization of aerosol optical properties relies primarily on passive radiometric observations of direct solar irradiance and diffuse sky radiance acquired

at multiple wavelengths. Unlike most atmospheric observing techniques, which provide either local in-situ measurements or information on individual aerosol parameters, multi-spectral radiometric measurements simultaneously constrain both the aerosol burden and its optical and microphysical characteristics through physically based inversion algorithms (e.g., Nakajima et al., 2020; Dubovik and King, 2000). Direct solar irradiance measurements provide accurate retrievals of AOD, the AE, and precipitable water vapour (PWV), whereas diffuse sky radiance measurements contain additional information on aerosol scattering properties and particle microphysics. By combining these complementary measurements, inversion algorithms can retrieve aerosol VSD, the real and imaginary parts of the refractive index, SSA, aerosol phase function, asymmetry factor, and, in some retrieval schemes, particle depolarization and modal aerosol properties. Consequently, passive radiometric observations provide one of the most complete descriptions currently achievable of the atmospheric aerosol column from a single observing system.

Over the last three decades, this measurement principle has become the foundation of several international observing networks. The AErosol RObotic NETwork (AERONET) remains the largest and most widely used global network, providing standardized aerosol products through inversion of measurements acquired by CIMEL Sun–Sky radiometers (Holben et al., 1998; Dubovik and King, 2000). Other international networks, including SKYNET (Nakajima et al., 1996) and the WMO Global Atmosphere Watch Precision Filter Radiometer (GAW-PFR) network (Nyeki et al., 2015), provide comparable aerosol products using different instrumentation, calibration strategies and processing methodologies. More recently, major advances in inversion algorithms, particularly the Generalized Retrieval of Atmosphere and Surface Properties (GRASP) (Dubovik et al., 2011), have considerably expanded the information that can be extracted from radiometric observations.

The growing reliance on aerosol optical properties for climate research and operational environmental services has substantially increased the requirements for the accuracy, traceability, and interoperability of aerosol observations. Recent studies showed that the aerosol optical property uncertainty accounts for one-third to half of the total direct SW uncertainty (Elsey et al., 2024). Aerosol optical depth has been designated by the Global Climate Observing System (GCOS) (GCOS, 2022) as one of the Essential Climate Variables (ECVs) (Bojinski et al., 2014) under the aerosol domain, reflecting its central role in constraining aerosol radiative forcing, which remains one of the largest uncertainties in estimates of anthropogenic climate forcing. GCOS specifies demanding observational requirements, including goal-level uncertainties of 4% or 0.02 (whichever is larger), long-term stability better than 2% per decade, high spatial resolution, and near-continuous temporal sampling. While ground-based sun photometer networks routinely achieve or exceed these accuracy requirements, their spatial coverage remains sparse and geographically uneven, whereas satellite observations and atmospheric reanalyses provide excellent spatial coverage but generally with larger uncertainties and greater dependence on retrieval assumptions and model parameterizations. Reconciling these complementary strengths and weaknesses remains one of the major challenges in modern aerosol observing systems.

Ground-based radiometric observations therefore play a unique role within the global Earth observation system (Fig. 1). Owing to their high accuracy, traceability and long-term stability, networks such as AERONET, GAW-PFR, and SKYNET constitute the primary reference datasets for the calibration and validation of satellite aerosol products developed by major international space agencies, including ESA, NASA, JAXA, NOAA and EUMETSAT (e.g., Sayer et al., 2013; GCOS, 2022; Schutgens et al., 2020). Their role closely follows the concept of Fiducial Reference Measurements (FRMs), providing SI-traceable observations with rigorously characterized uncertainty budgets that serve as independent references for satellite missions and atmospheric composition services. At the same time, these measurements provide the observational basis for the evaluation of numerical weather prediction systems, atmospheric reanalyses, climate models and aerosol data assimilation frameworks, including operational services such as CAMS and MERRA-2 (Benedetti et al., 2018; Rémy et al., 2019; Randles et al., 2017).

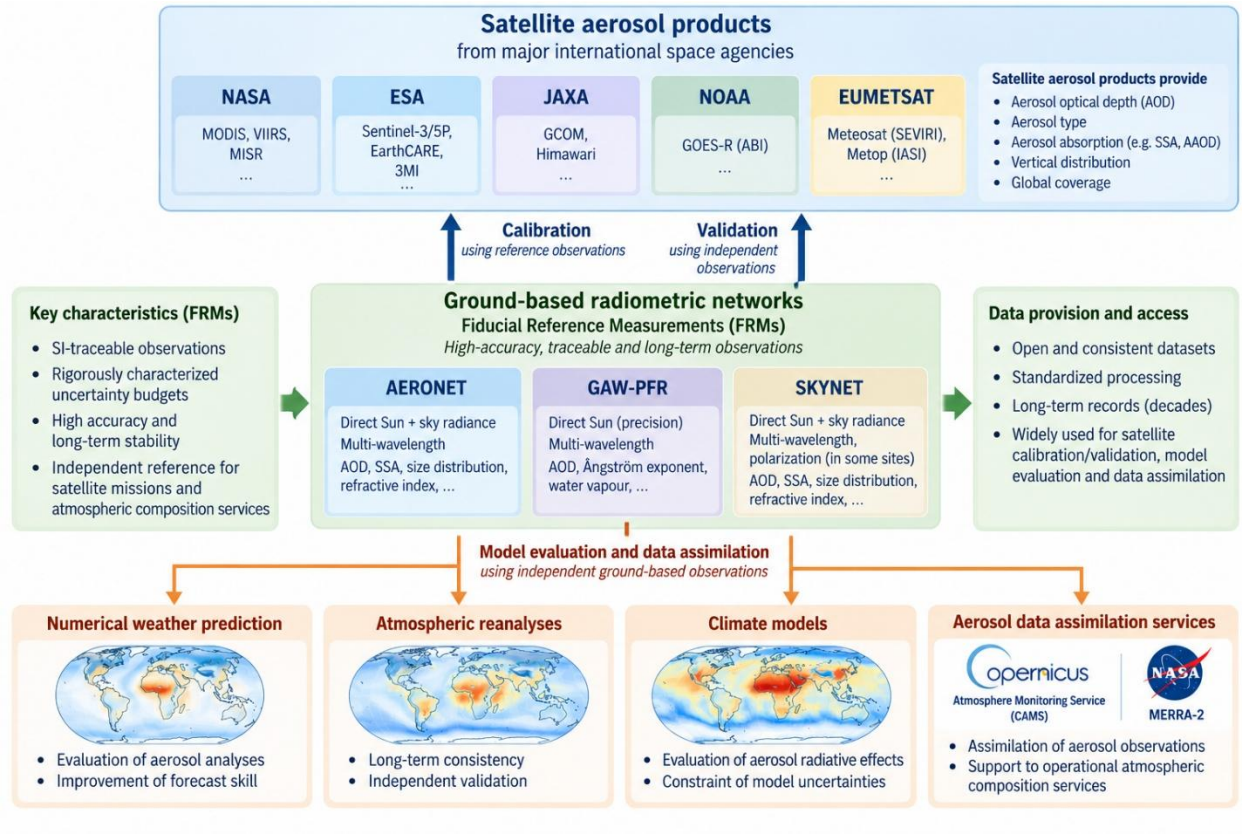


Figure 1. *The role of ground-based observation networks in the Earth observation system.*

Despite the remarkable progress achieved during the last three decades, important challenges remain. Significant differences still exist among international observing networks regarding instrumentation, calibration strategies, cloud-screening methodologies, inversion algorithms, uncertainty characterization, quality-control procedures and data products. These differences

complicate the direct comparison and combined exploitation of aerosol datasets, limit the interoperability between observing systems, and ultimately reduce the consistency of long-term climate records and operational aerosol products (e.g., Dubovik et al., 2019; Nakajima et al., 2020; Laj et al., 2024). Addressing these challenges has become a major objective of international initiatives including the WMO Global Atmosphere Watch programme (GAW), ACTRIS, ESA's FRM programme and collaborative networking activities such as COST Action HARMONIA, which aim to improve harmonization, traceability and standardization of aerosol observations across different instruments, networks and applications.

Beyond atmospheric research, aerosol optical properties play a central role in studies of the Earth's radiation budget, radiative transfer, biologically active solar radiation and solar energy applications (Häder and Sinha., 2005; Grant, 2007; Chen and Blankenship, 2011; Wild, 2012; Bais et al., 2018; Papachristopoulou et al., 2024; Bais et al., 2005; Ansari et al., 2025; Taylor et al., 2015; Hamill et al., 2016; Krishnaveni et al., 2025), epidemiological studies and exposure assessment (van Donkelaar et al. 2010, 2016), aviation safety (e.g.,Prata & Tupper, 2009; Horwell & Baxter, 2006), and contribute to agricultural and ecosystem studies by improving the understanding of aerosol-induced changes in diffuse radiation, vegetation productivity and carbon uptake (e.g., Mercado et al., 2009; Kanniah et al., 2012).

Against this background, the present review provides a comprehensive assessment of ground-based radiometric measurements of aerosol optical properties. Rather than focusing exclusively on measurement techniques or retrieval algorithms, the review adopts an application-oriented perspective that links aerosol observations with the requirements of user communities. Building upon recent advances, the review evaluates the capabilities and limitations of current observing systems, discusses ongoing harmonization and standardization efforts, and identifies the remaining scientific, technological and operational challenges. Emphasis is placed on the complementarity of ground-based observations, satellite measurements and atmospheric models, the evolving requirements of different user communities, and the opportunities offered by next-generation retrieval algorithms, integrated observing systems and operational environmental services. It aims to summarize the current state of the art, and to provide a roadmap for the future development of harmonized, traceable and application-oriented aerosol observing systems capable of supporting both scientific research and operational decision-making in the coming decades.

2. Current Capabilities

2.1. Ground based

2.1.1. Measurement principles

Ground-based passive radiometric observations of aerosol optical properties rely primarily on direct-solar irradiance and diffuse sky-radiance measurements at multiple wavelengths (Wendisch et al., 2004). Direct-Sun observations AOD after accounting for molecular and gaseous contributions, while the Langley-plot method is widely used for calibration and determination of extraterrestrial signals (Shaw, 1983; Toledano et al., 2018). Spectral AOD measurements allow derivation of the Ångström exponent (AE), which provides an approximate indication of aerosol particle size but depends on the wavelength range over which it is derived (Eck et al., 1999; Schuster et al., 2006; Kaskaoutis et al., 2007). Because direct-Sun measurements primarily constrain aerosol extinction, diffuse sky-radiance observations are required to retrieve additional properties such as SSA, VSD and refractive index (Wang and Gordon, 1993; Nakajima et al., 1996; Dubovik and King, 2000). Angular measurements using almucantar, principal-plane and hybrid scanning geometries provide complementary information on aerosol scattering and microphysical properties, although their performance depends on scattering-angle coverage and cloud contamination (Holben et al., 1998; Tonna et al., 1995; Sinyuk et al., 2020; Herrero-Anta et al., 2025). Measurements at multiple wavelengths improve sensitivity to different aerosol size modes, while polarimetric observations provide additional constraints on particle size, refractive index and non-sphericity (Dubovik et al., 2006; Dubovik et al., 2019). Advanced inversion frameworks such as GRASP can combine intensity and polarization measurements to improve the retrieval of aerosol microphysical and optical properties (Dubovik et al., 2019). More analytical information on measurement principles, calibration, retrieval equations, scanning geometries, cloud screening and associated limitations is provided in **Appendix 1**.

2.1.2. Data availability, coverage, and accessibility.

Main Global GB networks

Three major international networks currently provide extensive ground-based passive radiometric observations of aerosol optical properties: **AERONET, SKYNET and the WMO Global Atmospheric Watch Precision Filter Radiometer network (GAW-PFR)**. Although the three networks share the common objective of providing long-term observations of aerosol optical depth and related atmospheric properties, they differ substantially in their instrumentation, measurement geometries, calibration approaches, processing algorithms, data products and operational philosophies (e.g., Karanikolas et al., 2024). These differences are important when observations from different networks are combined or used for long-term intercomparison and validation.

AERONET (AErosol RObotic NETwork) (Holben et al., 1998) is the largest of the three networks and was developed by NASA Goddard Space Flight Center in collaboration with the PHOTONS programme. With observations extending back to the early 1990s and hundreds of

active sites distributed globally, AERONET provides one of the most extensive long-term datasets of ground-based aerosol observations. Its principal instrument is the CIMEL CE318 series of automatic sun-and-sky photometers, which has evolved through several generations and configurations. Standard instruments measure direct solar irradiance and diffuse sky radiance at multiple wavelengths, typically covering 340–1020 nm, while extended configurations can include longer wavelengths and additional capabilities such as polarization, ocean-colour observations and surface bidirectional reflectance characterization. The combination of direct-Sun and sky-radiance observations allows AERONET to provide spectral AOD and AE measurements together with a broad range of aerosol optical (e.g., SSA, asymmetry parameter) and microphysical properties (e.g., VSD) obtained through inversion of sky-radiance observations (Holben et al., 1998;Dubovik and King, 2000,Sinyuk et al., 2020). The network also provides TWV and quantities such as lidar ratio and radiative fluxes.

AERONET has progressively evolved from a primarily research-oriented observing network into a highly standardized operational infrastructure, with a strong emphasis on satellite validation, long-term monitoring and the provision of quality-controlled data products. Direct-Sun measurements are calibrated through determination of the extraterrestrial signal using Langley-plot calibration for reference instruments and calibration transfer for field instruments. Sky-radiance measurements are calibrated independently using laboratory radiance standards, with the calibration procedure traceable to radiometric standards. The current AERONET processing chain applies standardized cloud screening, calibration and inversion procedures and provides data at different quality levels, ranging from unscreened near-real-time observations to fully cloud-screened and quality-assured products.

SKYNET is another major international sun-and-sky radiometer network, developed primarily through Japanese research groups and coordinated through several regional subnetworks (Nakajima et al., 1996, 2020). It includes more than 100 observation sites, with particularly extensive coverage in Asia and Europe. Its principal aerosol instrument is the PREDE-POM series of sun-and-sky radiometers, which are available in several configurations and measure direct solar irradiance and diffuse sky radiance at wavelengths extending from the near-ultraviolet to the near-infrared (NIR). Depending on the instrument configuration, the measurable spectral range can extend from 315 to 2200 nm. SKYNET therefore provides spectral AOD and AE from direct-Sun observations, while inversion of sky-radiance measurements provides aerosol VSD, refractive index, SSA, phase function, asymmetry factor, lidar ratio and related aerosol properties. The instruments can additionally provide total-column ozone and TWV. Historically, SKYNET operated through relatively decentralized regional subnetworks, each with its own processing and quality-control procedures. More recently, data management has become increasingly centralized through the International SKYNET Data Center (ISDC), facilitating more consistent access to the observations and products. SKYNET also differs from AERONET in its calibration philosophy. In particular, the Improved Langley Plot method is widely used for on-site calibration, although Langley calibration at high-altitude sites and comparisons with reference instruments are also employed. Sky-radiance calibration is based on an on-site solar-disk scanning approach.

The **WMO Global Atmosphere Watch Precision Filter Radiometer network (GAW-PFR)** (Nyeki et al., 2015; Wehrli, 2000; Kazadzis et al., 2018) provides a complementary observing system focused primarily on accurate and stable measurements of direct solar irradiance and long-term aerosol optical depth. The network is based on the Precision Filter Radiometer developed at the World Radiation Monitoring Center (PMOD/WRC) and comprises core and associated stations distributed globally, with many sites located in relatively remote environments where the influence of local pollution sources is limited. The standard PFR model measures direct solar irradiance at four wavelengths, nominally 368, 412, 500 and 862/863 nm, and has been incorporated into the WMO reference framework for AOD observations. Compared with AERONET and SKYNET, the PFR does not routinely acquire angular sky-radiance measurements and consequently has a more limited set of operational aerosol products, principally AOD and AE. Nevertheless, its emphasis on radiometric stability and long-term observations makes GAW-PFR particularly valuable for climate monitoring and network intercomparison.

All three networks provide observations across a wide range of environments, including urban, rural, coastal, high-altitude, desert-influenced and remote sites, and have overlapping spectral channels that facilitate intercomparison. In particular, AOD observations around 500 nm and 862–870 nm provide useful common reference points among the networks. Despite these common features, the networks are **not directly interchangeable**. Differences occur in nominal and effective wavelengths, field of view (FOV), instrument optical characteristics, calibration procedures, ancillary atmospheric information, cloud-screening algorithms, temporal sampling, retrieval algorithms and data-quality criteria. The main differences between the three networks are summarized in Table 2.1. These methodological differences are particularly important because even apparently comparable AOD observations can exhibit systematic differences when measured by different instruments or processed using different algorithms. This issue, together with differences in calibration and retrieval procedures, has motivated a large number of dedicated intercomparison campaigns and long-term collocated observations and is discussed in detail in the following Section.

Table 1. Description of the main radiometric networks measuring aerosol optical properties.

Network	**AERONET**	**SKYNET**	**WMO GAW-PFR**
Network leadership	Developed by NASA GSFC and PHOTONS collaboration	Developed mainly by Japanese research groups led by Chiba University	Developed at PMOD WRC after the decision of WMO experts (WMO, 1993)
Operational philosophy/Primary role	Satellite validation and long-term monitoring	Research and long-term monitoring	Reference/climate monitoring

Number of active instruments and geographic distribution	About 500 active sites, >600 instruments, global distribution.	>100 sites, mainly in Asia and Europe (Nakajima et al., 2020)	12 belonging to the GAW PFR network and 30 PFRs used by individual scientists/stations, global distribution
Manufacturer/ instrument models	Cimel Electronique; CE318 series with constant evolution and several variations (polarisation, ocean color, BRDF). (Barreto et al., 2016)	Prede Co., Ltd.; POM series (POM-01, POM-02, POM-02 Moon, POM-01 Moon, POM for ship). (Nakajima et al., 1996; 2020)	PMOD WRC (Wehrli, 2000)
Direct-Sun	yes	yes	yes
Sky radiance	yes	yes	no
Polarization	yes	no	no
Typical measurement wavelengths (nm)	340, 380, 440, 500, 675, 870, 940, 1020, 1640 for standard configuration.	380, 400, 500, 670, 870, 940, 1020, for standard configuration. Additional wavelengths: 315, 340, 1225, 1600, 2200	368, 412, 500, 863 for standard configuration.
FOV	Nominal: 1.2º. Determined in the PMOD laboratory (MAPP project) for reference instruments, within the manufacturer specifications.	0.95° to 1.0° (Uchiyama et al., 2018b) Solar disk scan method, point-source or lamp scan method, and diffuse plate method (Nakajima et al., 1986, 1996; Boi et al., 1999)	~2.5 degrees (Kazadzis et al., 2018b)

FWHM	2nm in the UV. 10nm up to 1020nm 25 nm for 1640nm.	λ <=380: 3 nm λ = 400-940: 10 nm λ >=1020: 20 nm	3.8–5.4 nm
Main products	Direct sun/moon: AOD, AE (Giles et al., 2019) Inversions: AOD, SD, RI, sphericity. Derived: phase function, SSA.	Direct sun/moon: AOD, AE (Direct sun: Sunrad algorithm, Estellés et al., 2012; Moon: Uchiyama et al., 2018) Diffuse sky: VSD, RRI and IRI, SSA, phase function, ASY, LR, DEP	Direct sun: AOD, AE (Kazadzis et al., 2018)
Additional products	Radiation fluxes, radiative forcing, lidar ratio, columnar water vapor, water leaving radiances (Ocean color).	Not officially provided: Cloud properties (optical thickness, effective radius, water/ice phase (Kikuchi et al., 2006;Khatri et al., 2019), PWV (Campanelli et al., 2018;Momoi et al., 2020;Kudo et al., 2021), columnar ozone (Khatri et al., 2014)	Not officially provided: Aerosol size distribution parameters (Karanikolas et al., 2025)
Sky scans	Almucantar (two sides), principal plane (now in disuse), hybrid (two sides), aureole scan for cloud screening.	Almucantar (one side, but both sides are possible), principal plane, zenith	no

Sky radiance inversion	Sinyuk et al., 2020.	Skyrad pack 4.2 (Nakajima et al., 1996), for solar calibration constant; Skyrad pack MRI v2 (Kudo et al., 2021)	no
Radiometric calibration strategy	AOD: Langley method (reference instruments) or intercalibration (field instruments). Sky radiance: laboratory calibration with spectral radiance reference (integrating sphere), traceable to NIST.	On-site, Improved Langley (Campanelli et al., 2007; 2024). Langley at high-altitude sites and inter-comparison with reference instruments	Based on the WMO reference triad of PMODWRC (Kazadzis et al., 2018)
Non-spherical particles	Spheroid model included, the inversion provides fraction of spherical particles (Dubovik et al., 2006;Sinyuk et al., 2020).	Only accounted for in Skyrad MRI (Kudo et al., 2021). Spheroids from Dubovik et al. 2006.	no
Cloud screening	Giles et al. 2019. (version 3 processing).	Smirnov et al. (2000), Estellés et al. (2012) and Song et al. (2014); Khatri and Takamura (2009), Irie et al., 2019., Kaufman et al., 2006	Kazadzis et al., 2018
Data quality levels	Level 1.0: AOD, no cloud screening. Level 1.5: cloud-screened AOD and inversions.	L2A, L2 for ESR-MRI and SUNRAD inversions L2 for Ceres inversion	L3 for calibrated and post processed data

	Level 2: cloud-screened and quality assured AOD and inversions.		
Data access	https://aeronet.gsfc.nasa.gov	https://www.skynet-isdc.org/	https://ebas.nilu.no/

Other sensors and networks

In addition to the three major global radiometric networks discussed above, several complementary instruments and observing systems provide aerosol optical measurements for specific applications, environments or measurement geometries. These systems range from spectral irradiance instruments and compact zenith-viewing radiometers to portable sun photometers and imaging systems. Although they generally provide a more limited set of aerosol products than the principal sun-and-sky photometer networks, their lower cost, portability, extended spectral coverage or ability to operate in environments where conventional sun photometers are difficult to deploy makes them valuable components of the broader aerosol observing system.

Zenith-viewing radiometers and multifilter rotating shadowband radiometers (MFRSRs) (Alexandrov et al., 2008; Almansa et al., 2017) provide an important complementary approach to conventional sun-tracking photometers. A rotating shadowband can alternatively expose and shade the detector, allowing measurements of GHI and diffuse horizontal irradiance (DHI). DNI can subsequently be derived from these measurements and used to retrieve AOD through the Beer–Bouguer–Lambert law, together with appropriate corrections for molecular scattering and gaseous absorption and an instrument calibration based on Langley-plot techniques. This approach provides a relatively simple alternative to conventional sun-tracking systems and has the additional advantage that the same observations can be used for surface-radiation applications. The **MFRSR** is the most established example of this measurement concept. It combines measurements at several narrow spectral bands in the VIS and NIR spectral regions with automated separation of the direct and diffuse radiation components (Harrison et al., 1994). Spectral AOD is retrieved with typical uncertainties of about 0.01. MFRSRs have been deployed within long-term radiation-monitoring programmes, including the **Atmospheric Radiation Measurement (ARM)** programme and the **Surface Radiation Budget Network (SURFRAD)**, providing observations that can be exploited simultaneously for aerosol characterization and surface-radiation studies. The use of several narrow spectral channels also allows the spectral dependence of aerosol extinction to be characterized through AOD and AE retrievals. Recent developments have further extended the spectral capabilities of this approach into the ultraviolet (UV). Michalsky and McConville (2024) demonstrated the retrieval of both ozone and aerosol optical depth using an ultraviolet MFRSR.

A related but simpler approach is represented by the **ZEN** system developed by Sieltec Canarias in collaboration with the Izaña Atmospheric Research Center (Almansa et al., 2017). Unlike

conventional sun photometers, ZEN uses a narrow-band radiometer viewing the zenith and therefore does not require solar tracking. The ZEN-R41 measures zenith sky radiance at 440, 500, 675 and 870 nm, while the later ZEN-R52 additionally includes a 940 nm channel for TWV measurements. The original **ZEN-LUT** retrieval approach uses a radiative-transfer look-up table generated with *libRadtran*, containing zenith sky-radiance values simulated for different aerosol optical depths and dust conditions. Observed zenith sky radiances are compared with the look-up table to estimate AOD, avoiding the need for direct-Sun measurements. Almansa et al. (2020) subsequently extended the ZEN system and demonstrated the ZEN-R52 configuration, including the water-vapour channel. The reported uncertainty of the ZEN-LUT AOD retrieval is approximately ± 0.01 + 0.13 × AOD. More recently, the **GRASP-ZEN** approach introduced by Herrero-Anta et al. (2023) substantially expanded the information that can be obtained from zenith-viewing measurements. Instead of restricting the retrieval to dust aerosol and AOD, GRASP-ZEN uses the four-channel ZEN-R52 zenith sky-radiance measurements at 440, 500, 675 and 870 nm as input to the GRASP inversion framework. The methodology allows AOD to be retrieved for different aerosol types and additionally provides estimates of the fine- and coarse-mode aerosol volume concentrations and their total volume concentration. Reported AOD uncertainties are approximately ±0.03 at 440 and 500 nm and ±0.02 at 675 and 870 nm.

Brewer spectrophotometers provide another complementary source of aerosol observations, particularly in the UV spectral range (e.g., López-Solano et al., 2018). Originally developed for routine measurements of total-column ozone and spectral UV irradiance, Brewers provide spectrally resolved direct-Sun observations that can also be exploited to retrieve AOD (e.g., Meleti and Capellani, 2000). Over the past two decades, several methodologies have been developed for retrieving AOD in the UV (Meleti and Capellani, 2000; Cheymol and de Backer, 2003; Sellito et al., 2006; Kazadzis et al., 2007) and, in some approaches, aerosol absorption-related properties such as SSA (Bais et al., 2005; Fountoulakis et al., 2019). Brewer MkIV instruments are particularly valuable in this context because their extended spectral range includes measurements in the visible region, allowing AOD retrievals at wavelengths around 425–453 nm in addition to the UV (Diemoz et al., 2016). The long observational records of Brewer instruments (longer, in some cases, than most synchronous radiometers), together with their extensive deployment within global atmospheric monitoring networks, provide an important opportunity to combine aerosol and UV observations and to extend long-term aerosol records toward shorter wavelengths (Lopez-Solano et al., 2018). The European Brewer Network (EuBrewNet) provides a coordinated framework for Brewer observations, centralized processing and quality control, further enhancing the consistency and accessibility of these measurements (Rimmer et al., 2018). Nevertheless, compared with dedicated sun–sky photometers, Brewer-based aerosol products remain more uncertain, and more limited in terms of the number of aerosol optical and microphysical properties that can be retrieved routinely (e.g., Lopez-Solano et al., 2018).

All-sky cameras represent a complementary technology for aerosol observations. By recording the angular distribution of sky radiance over a very large portion of the sky, they can provide information traditionally obtained from scanning sun-and-sky photometers, while offering the

additional capability of characterizing cloud conditions simultaneously (e.g., Olmo et al., 2008; Antuña-Sánchez et al., 2021; Logothetis et al., 2023). Both, empirical and physically based retrieval approaches have been demonstrated. Cazorla et al. (2008) used neural-network methods to estimate AOD from sky-imager observations, while Román et al. (2022) demonstrated the use of normalized, uncalibrated sky radiances with the GRASP inversion framework to retrieve AOD and particle-size information. More recently, machine-learning approaches have been applied to partially cloudy scenes, demonstrating the potential of all-sky cameras to extend aerosol retrievals beyond the clear-sky conditions required by conventional sky-radiance inversions (Scarlatti et al., 2024). All-sky cameras are also particularly promising for **nighttime aerosol observations**. Lunar sky-radiance measurements can be combined with lunar AOD observations to retrieve aerosol microphysical properties, while stellar photometry provides a complementary approach that does not depend on the phase or visibility of the Moon. Román et al. (2017) demonstrated retrievals of aerosol refractive index, spherical fraction and size distribution using lunar almucantar measurements from high-dynamic-range sky-camera images combined with lunar photometry. More recently, Román et al. (2025) developed a star-photometry approach based on observations of predefined stars, including cloud screening and Langley-plot calibration, and demonstrated its potential for obtaining nighttime AOD without requiring laboratory calibration. This approach has been implemented in the **GOA-SCAN** network, where camera observations have been validated against independent Sun–sky–Moon photometers at several stations.

Compact portable sun photometers provide another important extension of aerosol observations, particularly for shipborne and distributed measurements. The **Microtops II** (Ichoku et al., 2002) is a handheld multichannel sun photometer capable of measuring AOD and total-column water vapour and is the standard instrument used within the **Maritime Aerosol Network (MAN)** (Smirnov et al., 2009), a component of AERONET. MAN provides shipborne AOD measurements over the oceans, where fixed ground-based networks are necessarily sparse. Microtops instruments are calibrated using transfer procedures linked to AERONET reference instruments and are processed using standardized AERONET algorithms, with reported AOD uncertainties generally not exceeding approximately ±0.02. MAN therefore provides an important complement to continental ground-based networks and contributes to the characterization of aerosol distributions over oceanic regions.

Calitoo (*Temun*) is a handheld sun photometer (Djossou et al., 2018; Bayat and Assarenayati, 2023) that represents an even more compact and low-cost approach. Developed in the context of the GLOBE educational programme, the handheld instrument provides AOD at 465, 540 and 619 nm and has been shown to retrieve AOD with an estimated uncertainty of approximately ±0.02 (Léon et al., 2021; García et al., 2025). Its low cost makes it particularly attractive for distributed observations and citizen-science or educational networks. Calitoo observations have also been used for dust-monitoring applications and are now collected in the CALINET database, providing an example of how inexpensive instruments can contribute to spatially dense aerosol observations when appropriate calibration and quality-control procedures are applied (Bayat and Assarenayati, 2023; Masoumi et al., 2025).

Other sensors: Other passive remote-sensing systems can provide complementary aerosol information beyond conventional filter-based sun photometers. Multi-Axis Differential Optical Absorption Spectroscopy (**MAX-DOAS**) instruments (Wagner et al., 2004, 2011) measure scattered solar radiation at multiple elevation angles and exploit differential absorption features, particularly of O_4, to retrieve aerosol extinction profiles and aerosol optical depth (e.g., Irie et al., 2009; Karagkiozidis et al., 2022). Their principal advantage is the ability to provide information on the vertical distribution of aerosols, which is generally unavailable from column-integrated direct-Sun measurements. For example, Gratsea et al. (2021) retrieved aerosol extinction profiles at 477 nm from MAX-DOAS measurements over Athens and found good agreement with independent lidar profiles, while the corresponding AOD showed satisfactory agreement with AERONET observations. **Pandora** spectrometers, originally developed for high-resolution measurements of atmospheric trace gases such as O_3, NO_2 and HCHO, provide another potentially valuable source of aerosol information (Herman et al., 2009). Pandora systems perform high-resolution direct-Sun and sky-radiance measurements in the UV–visible spectral range, and dedicated developments have demonstrated the retrieval of AOD and column-integrated water vapour from Pandora observations. The use of Pandora measurements also provides an important synergy for aerosol observations because accurate, high-frequency NO_2 measurements can be used to account for the variable NO_2 absorption contribution to AOD retrievals in the UV and short-visible spectral range, where the effect can be significant (Masoom et al., 2024). **Array spectroradiometers** and dedicated solar spectroradiometers (Zuber et al., 2018; Gröbner et al., 2023) provide another complementary approach by measuring the direct solar spectrum over a broad wavelength range. The **UVBTS/BTS-Solar system**, based on the Gigahertz-Optik BTS array spectroradiometer, can be configured for direct spectral solar irradiance measurements in the UV and extended into the visible and near-infrared . Spectral AOD can be derived from the direct irradiance using Beer–Lambert–Bouguer/Langley-type approaches. Recent intercomparison work has demonstrated the potential of BTS spectroradiometers for SI-traceable spectral AOD measurements, including wavelengths extending from the UV into the near-infrared. The BTS AOD measurements have been evaluated in Gröbner et al., (2023) and Karanikolas et al., (2025) showing uncertainties of less than 2%. The **EKO MS-711** grating spectroradiometer, which measures direct spectral normal irradiance over approximately 300–1100 nm can be also used for aerosol observations. García et al. (2020) demonstrated good agreement with a reference AERONET-Cimel sun photometer, although the relatively large 5° field of view of the MS-711 introduces enhanced circumsolar radiation that can bias AOD, particularly at shorter wavelengths and under high aerosol loading. Applying radiative-transfer-based circumsolar-radiation corrections substantially improved the agreement with AERONET. Subsequent work using EKO MS711/MS712 spectroradiometers further demonstrated simultaneous retrievals of AOD and precipitable water vapour from direct-Sun measurements, with AOD correlations exceeding 0.99 against a reference CE318 sun photometer at 380–1020 nm.

Other specialized systems include **Sun/Moon photometers**, which extend aerosol observations into the nighttime using lunar irradiance, and astronomical photometers, which can exploit

stellar observations to characterize atmospheric extinction and retrieve nighttime AOD (e.g., Barreto et al., 2013, 2017). Together, these systems broaden the temporal, spectral and vertical information available from ground-based aerosol observations and illustrate the increasing convergence between aerosol, trace-gas, solar-radiation and astronomical atmospheric-monitoring infrastructures.

2.1.3. Intercomparison and standardization efforts.

Despite the common objective of providing accurate and long-term aerosol observations, the major ground-based radiometric networks have historically developed largely independently, resulting in differences in instrumentation, calibration procedures, ancillary atmospheric information, cloud screening, retrieval algorithms and data processing. As a consequence, AOD measurements obtained from nominally equivalent wavelengths and collocated instruments may exhibit systematic differences that are not necessarily related to actual atmospheric variability. Intercomparison activities are therefore essential for quantifying instrumental and methodological differences, establishing traceability to common references and identifying procedures that can improve the consistency and interoperability of aerosol observations (e.g., Kazadzis et al., 2018; Toledano et al., 2019).

Many dedicated campaigns and long-term colocated measurements have been conducted to evaluate the consistency of the principal aerosol photometers and networks (e.g. Cuevas et al., 2019). These include campaigns addressing both daytime and nighttime observations, different instrument types and calibration approaches. The first multi-instrument nocturnal intercomparison campaign at the Izaña Atmospheric Observatory in 2017 compared two lunar photometer types and a stellar photometer and provided an assessment of the influence of calibration procedures and lunar irradiance models on nocturnal AOD retrievals (Barreto et al., 2019). Earlier work at Izaña had also demonstrated the importance of lunar irradiance modelling and calibration for obtaining consistent nighttime AOD observations (Barreto et al., 2017). More recent daytime intercomparison activities have included the QUATRAM campaigns in Rome and Davos (Karanikolas et al., 2024;Campanelli et al., 2024), as well as campaigns at Ny-Ålesund, Lindenberg and other reference sites (e.g., Mazzola et al., 2012; Doppler et al., 2023). These experiments have provided controlled datasets for assessing differences between CIMEL, PREDE and PFR instruments under a range of aerosol and atmospheric conditions. The HARMONIA COST Action has subsequently brought these existing campaigns together within a common framework through Working Group 1 (WG1), with the objective of developing a scientific roadmap for the homogenization of aerosol measurements and retrievals (Doppler et al., 2023, 2024, 2025).

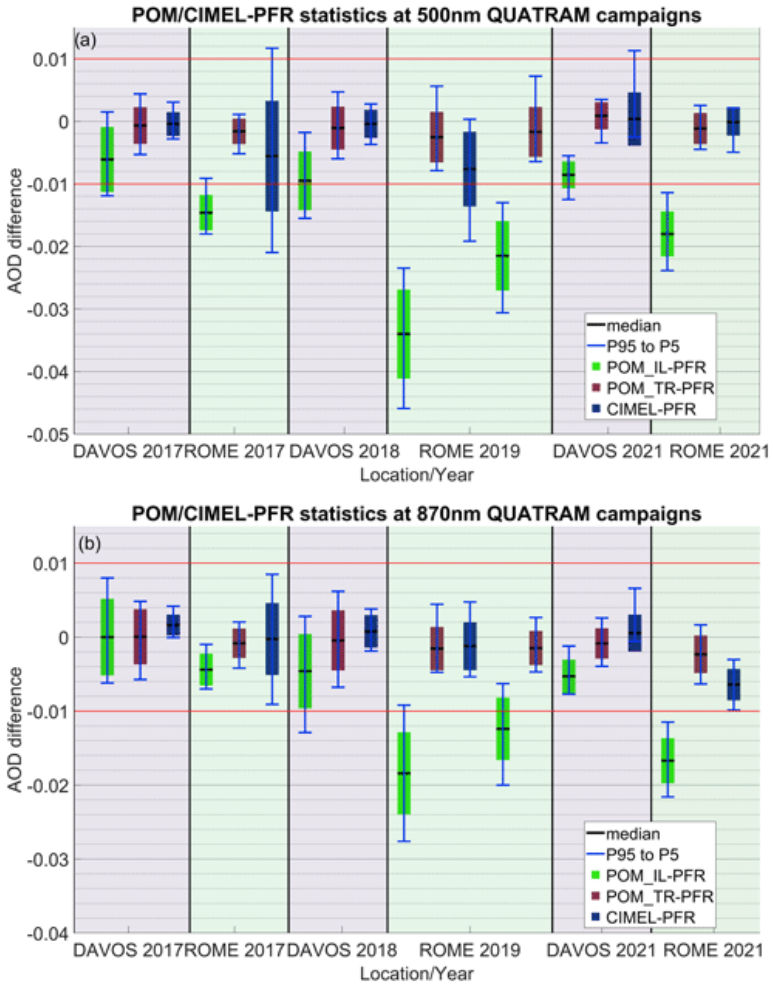


Figure 2. *Boxplot of the statistics of AOD differences for all instrument comparisons at both locations during the three QUATRAM campaigns. Panel* ***(a)*** *shows the results for 500 nm, while panel* ***(b)*** *shows those for 870 nm. In all cases, the PFR is used as the reference instrument. The black line indicates the median difference, the size of the boxes represents the distance between the median and the standard deviation, and the error bars indicate the 5th and 95th percentiles of the AOD differences. The green boxes correspond to the differences between the original POM AOD and the reference, while the red boxes represent the POM AOD differences obtained using the calibration retrieved through transfer from the PFR. The blue boxes correspond to the differences between CIMEL and PFR. For the Rome 2019 campaign, two different POMs were compared with the same PFR, with POMCNR shown on the left and POMSPZ on the right. Figure originally published in Karanikolas et al. (2024).*

One of the most comprehensive long-term comparisons has been performed between GAW-PFR and AERONET-CIMEL observations. Using more than 70,000 synchronous one-minute measurements collected between 2005 and 2015, Cuevas et al. (2019) found generally good agreement between the two networks at their common wavelengths, with more than 95% of the observations satisfying the relevant WMO traceability criteria at 440 and 500 nm and approximately 98% at 870 nm. Nevertheless, systematic differences were identified at shorter

wavelengths and under conditions dominated by coarse aerosols. Differences in instrument field of view were found to be particularly relevant under dust-dominated conditions because the larger contribution of forward-scattered radiation can affect the measured direct irradiance and consequently the retrieved AOD (Cuevas et al., 2019).

Intercomparisons involving SKYNET have provided further evidence that differences between networks can originate not only from the instruments themselves but also from calibration and retrieval procedures. Karanikolas et al. (2024) compared AOD retrievals from GAW-PFR and SKYNET at 500 and 870 nm using measurements acquired in Davos and Rome during the 2017–2021 period. The study showed that the SKYNET AOD obtained using the Improved Langley Plot (ILP) calibration was systematically lower than the corresponding PFR AOD, with differences varying between the two sites and campaigns. In contrast, when PFR calibration transfer was used to recalculate the SKYNET/PREDE AOD, the absolute median differences were generally below 0.005, demonstrating that a substantial part of the observed discrepancy was associated with calibration rather than intrinsic instrument performance. Comparisons with colocated CIMEL instruments also showed generally good agreement, with most median differences below 0.01. Ongoing efforts within SKYNET aim to further improve the Improved Langley Method. Recent advances by Kumar et al. (2026) indicate that using a more recent radiative transfer model (Skyrad MRI v2, Kudo et al., 2021) together with an iterative technique can improve the accuracy of calibration factors and lead to closer agreement with AOD measurements from AERONET and GAW-PFR.

Differences may arise at several stages of the observation and retrieval chain (Kim et al., 2008; Khatri et al., 2016; Karanikolas et al., 2024). Although the principal networks use physically similar formulations for converting direct-solar measurements into AOD, differences in the ancillary datasets and computational conventions adopted in these steps can introduce systematic discrepancies. This is particularly important when long-term observations from different instruments or networks are merged, because methodological changes may appear as artificial temporal discontinuities and compromise the homogeneity of derived climate records. An important approach for separating instrumental from retrieval-related differences is therefore to reprocess measurements from different instruments using common equations, ancillary information and computational conventions. This approach has been explored using long-term colocated datasets such as the Lindenberg observations, where CIMEL, PREDE and PFR measurements are available under essentially identical atmospheric conditions (Doppler and Becker, 2025). Such datasets allow differences between instruments to be examined first using the original network-specific processing and subsequently using a common retrieval framework. The comparison therefore provides a means of determining which component of the observed differences is attributable to the instrument and which originates from calibration, ancillary data or retrieval methodology.

The accumulated evidence from intercomparison campaigns indicates that the major ground-based networks are generally consistent within their stated uncertainties, particularly for AOD in the visible and near-infrared spectral ranges, but that systematic differences remain under specific conditions, including low aerosol loading, high solar zenith angles, strong coarse-mode

aerosol loading and at shorter wavelengths. Future standardization efforts should focus on establishing common reference procedures, traceable calibration standards, harmonized retrieval conventions, transparent uncertainty characterization and interoperable data products. Such an approach would maximize the scientific value of combining observations from different networks for climate monitoring, satellite validation, atmospheric composition studies and operational aerosol services.

2.2. Satellite and model data

2.2.1. Satellite sensors

Satellite remote sensing provides the spatial coverage required to characterize the distribution and evolution of aerosols from regional to global scales. Unlike ground-based radiometric networks, which provide highly accurate but spatially localized column-integrated observations, satellite instruments can map aerosol properties over remote regions and oceans where surface observations are sparse or unavailable (Remer et al., 2008). Depending on the observing geometry, spectral coverage and polarization capabilities, satellite instruments can provide information on AOD, AE, fine- and coarse-mode contributions, aerosol type, absorption, particle size and shape, and, for active sensors, aerosol vertical distribution (e.g., Mishchenko et al., 2009; Li et al., 2009; Cairns et al., 2009; Winker et al., 2013; Tsikerdekis et al., 2022;Fu et al., 2023; Yang et al., 2023; Donovan et al., 2024). The retrieval of these properties nevertheless depends strongly on surface reflectance, cloud screening, aerosol models, viewing geometry and the availability of suitable ancillary information. Consequently, ground-based observations remain essential for calibration, validation and uncertainty characterization of satellite aerosol products (e.g., Su et al., 2023). A wide range of satellite instruments has been developed for aerosol remote sensing. A list of the main satellite-born instruments is provided in Table A2.1 in **Appendix 2**.

The **Moderate Resolution Imaging Spectroradiometer (MODIS)** instruments aboard Terra and Aqua have provided one of the longest and most widely used global records of satellite AOD, with retrievals adapted to dark vegetated and bright surfaces and ocean environments (Remer et al., 2008; Levy et al., 2013). The **Visible Infrared Imaging Radiometer Suite (VIIRS)** on Suomi-NPP and NOAA-20 extends this capability with improved spatial coverage and spectral information, supporting AOD, aerosol-type retrievals and detection of smoke and dust (Pei et al., 2025). **Multi-angle and polarimetric observations** provide additional constraints beyond conventional single-view multispectral measurements. The **Multi-angle Imaging SpectroRadiometer (MISR)** retrieves AOD together with information on aerosol size, type and, under favourable conditions, particle shape and plume characteristics (Kahn & Gaitley, 2015). The **POLDER** series demonstrated the added sensitivity of multi-angle polarimetry to aerosol microphysical properties, including particle size, refractive index and non-spherical particle fractions (Waquet et al., 2013). Building on this heritage, the European **Multi-viewing, Multi-channel, Multi-polarisation Imager (3MI)** on MetOp-SG is designed to exploit combined spectral, angular and polarization measurements to better constrain aerosol optical and microphysical properties (Fougnie et al., 2018). **Ultraviolet observations** provide complementary information, particularly for absorbing aerosols. The **Ozone Monitoring**

Instrument (OMI) and **TROPOspheric Monitoring Instrument (TROPOMI)** have been widely used to derive UV aerosol indices and monitor absorbing aerosol, including mineral dust and biomass-burning plumes. Their sensitivity to absorbing particles and reduced dependence on visible/near-infrared surface-reflectance assumptions makes UV measurements complementary to conventional AOD retrievals (Torres et al., 2007;Trees et al., 2025). **Thermal IR observations**, (e.g. from the **Infrared Atmospheric Sounding Interferometer or IASI** onboard the Metop satellite series) allow intrinsic sensitivity to only mineral aerosols, such as desert dust and volcanic ash. In addition, it allows a limited sensitivity to the aerosol altitude (Vandenbussche et al., 2026).

Active satellite sensors provide information that passive radiometers generally cannot, most importantly the vertical distribution of aerosol. **CALIOP** aboard CALIPSO established a multi-year global record of aerosol backscatter and extinction profiles and polarization-based aerosol typing (Winker et al., 2009). The next generation is represented by **ATLID aboard EarthCARE**, a high-spectral-resolution, polarization-sensitive lidar providing aerosol extinction, backscatter, depolarization, optical depth and aerosol classification profiles. EarthCARE's multispectral imager (MSI) provides complementary measurements of clouds and aerosol (van Zadelhoff et al., 2024; Hünerbein et al., 2024). **Geostationary observations** provide a complementary advantage through high temporal sampling. Instruments such as **Himawari AHI, GOES ABI and Meteosat SEVIRI** enable observations at intervals of minutes to tens of minutes, supporting the monitoring of rapidly evolving dust and smoke plumes, aerosol transport and diurnal variability, as well as air-quality and solar-energy applications (Ceamanos et al., 2023; Fu et al., 2023; Gueymard et al., 2023). Their retrieval accuracy, however, remains dependent on surface characterization, cloud screening and viewing geometry.

Together, these systems demonstrate the increasing diversity of satellite aerosol observations. While conventional multispectral sensors provide robust AOD records, multi-angle and polarimetric instruments add constraints on aerosol microphysics, active lidar provides vertical structure, and geostationary platforms provide high temporal resolution.

2.2.2. Reanalysis datasets

CAMS EAC4 (Innes et al., 2019) provides an independent global atmospheric composition reanalysis based on the ECMWF Integrated Forecasting System and an aerosol model coupled to the atmospheric composition system. The system assimilates satellite aerosol observations and provides total and component-resolved aerosol properties, including AOD associated with dust, sea salt, sulfate, black carbon and organic matter, together with AE and aerosol absorption and scattering properties (Inness et al., 2019). **MERRA-2** is NASA's global atmospheric reanalysis for the satellite era, based on the GEOS-5 Earth system model coupled to the GOCART aerosol module. It assimilates bias-corrected aerosol optical depth (AOD) observations from ground- and space-based remote-sensing platforms and provides globally consistent information on aerosol loading, including component-resolved distributions of dust, sea salt, sulfate, black carbon and organic carbon, as well as aerosol optical thickness and vertical aerosol properties (Randles et al., 2017; Buchard et al., 2017). The different

assimilation strategies and model formulations used by **MERRA-2** (Gelaro et al., 2017; Randles et al., 2017; Buchard et al., 2017) and CAMS are important when comparing their products because differences between the datasets do not necessarily represent differences in the actual atmospheric aerosol field but may arise from model assumptions, emissions, assimilation methodology and the observations assimilated.

AOD and AE evaluations against AERONET have generally demonstrated that both MERRA-2 and CAMS reproduce the broad spatial and temporal variability of aerosol optical properties, although systematic differences remain. In particular, underestimation can occur during episodes of very high aerosol loading, while the performance of AE is generally more variable than that of AOD (Sun et al., 2018; Mukkavilli et al., 2019; Shi et al., 2019; Gueymard et al., 2020; Ansari and Ramachandran, 2023; Su et al., 2023; Moustaka et al., 2026). Their long temporal coverage has nevertheless made these datasets particularly valuable for studies of long-term changes in total and species-resolved aerosol optical depth (Che et al., 2019; Sun et al., 2019; Cao et al., 2021; Yao et al., 2021; Yousefi et al., 2021).

In addition to operational reanalyses, coordinated model intercomparison activities provide another important source of information on the global aerosol distribution. **AeroCom (Aerosol Comparisons between Observations and Models)** is an open international initiative that coordinates aerosol modelling experiments and evaluates global aerosol simulations against available observations, including ground-based and satellite-derived aerosol optical properties (Gliß et al., 2021). **AeroCom** experiments provide a framework for examining differences among aerosol models arising from emissions, transport, chemistry, removal processes, aerosol microphysics and assumptions linking aerosol mass and size to optical properties. A major strength of AeroCom is therefore not the production of a single best aerosol dataset, but the systematic quantification of model diversity and the identification of processes responsible for differences between simulations.

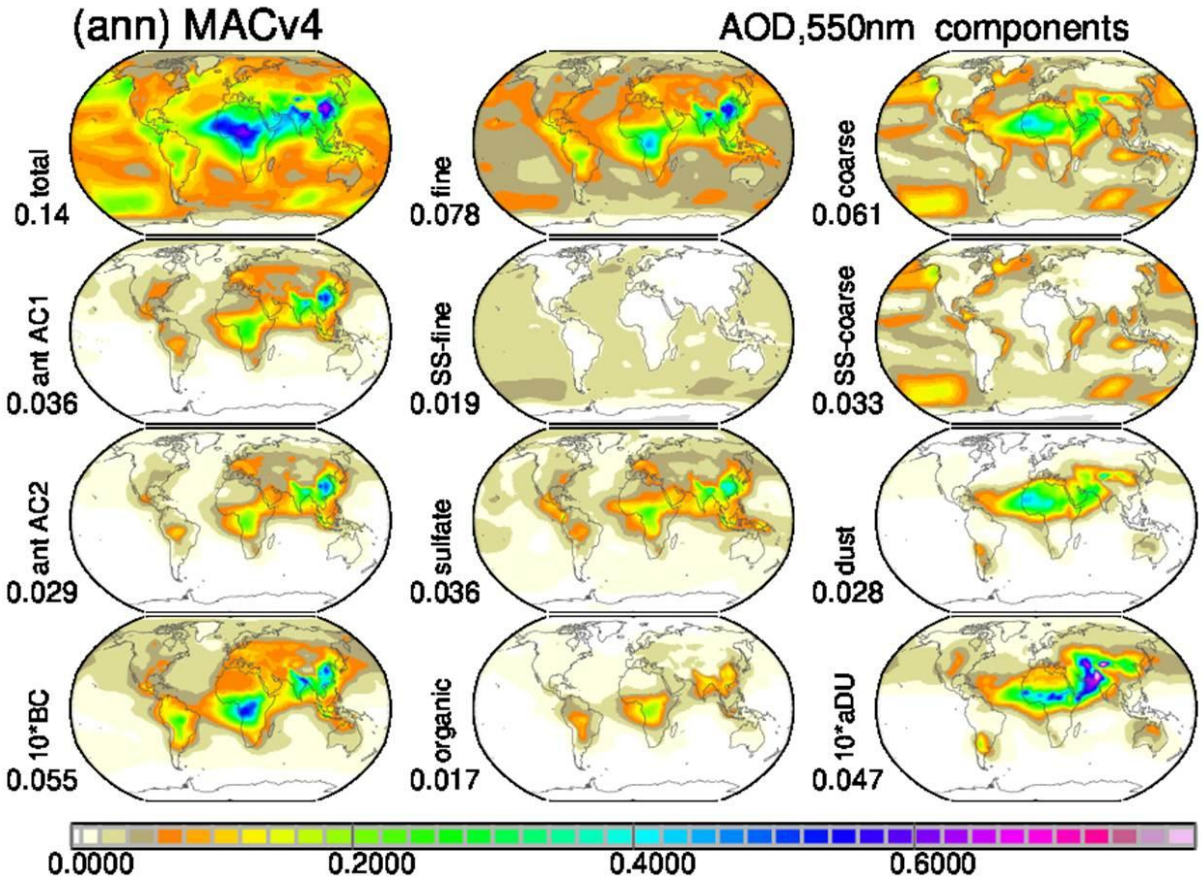


***Figure 3**. Annual maps of the MACv4 aerosol climatology at current conditions for the mid-visible AOD (550nm wavelength). The top row presents maps for total AOD and contributions from (sub-micrometer) fine-mode (AODf) and (super-micrometer) coarse mode (AODc) aerosol. Below the AODc map (col3) are its contributions from seasalt and mineral dust. Below the AODf map (col2) are its contributions from seasalt, sulfate, organic matter and soot (col1/row4). For comparison to AOD and AODf, anthropogenic fine mode estimates since 1750 (using AeroCom 1 emission data, 'ant_AC1') and since 1850 (using AeroCom 2 emission data, 'ant_AC2') are offered. Also shown are estimates for anthropogenic coarse mode mineral dust AOD ('aDU') from land-use changes. Values to the lower left indicate annual global averages. Note, that maps and global averages for BC and aDU (anthropogenic dust) are artificially multiplied by 10 to fit the common color scale.*

A further development is represented by the **MACv4 aerosol climatology** (Kinne, 2019; Vogel et al., 2022), which combines information from AeroCom modelling with long-term ground-based sun-photometer observations, particularly AERONET observations over land and Maritime Aerosol Network (MAN) observations over oceans. The methodology uses observations to constrain regional patterns of total, fine-mode and coarse-mode AOD and absorption AOD and subsequently derives contributions from major aerosol components, including sulfate, organic matter, soot, mineral dust and sea salt. Because the component contributions are associated with prescribed size distributions and refractive indices, the

resulting climatology can provide not only AOD but also related single-scattering properties such as SSA and the asymmetry factor for radiative-transfer applications. The current MACv4 framework additionally provides spectral and temporal information suitable for climate and radiative-effect studies.

AeroCom and MACv4 therefore occupy a different position from satellite retrievals and operational reanalyses. Satellite products provide observations with broad spatial coverage, reanalyses provide dynamically consistent four-dimensional fields through data assimilation, while AeroCom provides a framework for model evaluation and intercomparison and MACv4 provides an observation-constrained aerosol climatology. Together, these resources substantially extend the information available from ground-based observations and provide essential datasets for climate modelling, atmospheric composition studies, satellite validation and radiative-transfer applications.

2.3. Complementarity and challenges

Ground-based observations, satellite retrievals and numerical models provide complementary information on atmospheric aerosols and their interactions with radiation. Their respective strengths and limitations arise from differences in spatial and temporal sampling, measurement geometry, retrieved quantities and dependence on assumptions or ancillary information. No single observing system can therefore provide a complete description of the highly variable aerosol field, making their integration essential for comprehensive aerosol monitoring and modelling.

Ground-based networks such as AERONET, SKYNET and GAW-PFR provide accurate, traceable and temporally resolved measurements of column-integrated aerosol optical properties. Observations at intervals of minutes to tens of minutes allow short-term variability and transport processes to be resolved, while sky-radiance and polarization measurements can provide additional information on aerosol size distribution, refractive index, SSA and particle shape. Their main limitation is spatial representativeness: individual stations characterize relatively small areas and provide limited information on horizontal distribution and vertical structure. International networks partially compensate for this limitation, but their spatial sampling remains much sparser than that of satellite observations (Li et al., 2020; Kahn et al., 2023).

Satellite observations provide extensive spatial coverage, including remote continental regions and oceans where ground-based measurements are sparse (Urraca et al., 2025; Dong et al., 2026). They are particularly valuable for investigating aerosol transport, emission sources and plume evolution. Multi-angle and polarimetric sensors provide additional constraints on aerosol size, absorption and type, thermal IR sensors provide dust and ash specific data, active lidar provides vertical information, and geostationary platforms offer high temporal sampling for rapidly evolving dust and smoke events. However, satellite retrievals are affected by cloud contamination, surface reflectance, viewing geometry and assumptions concerning aerosol properties (Dubovik et al., 2019;Winker et al., 2009;Cho et al., 2024;Remer et al., 2024;Levy et al., 2013). Polar-orbiting sensors also sample the atmosphere only at discrete overpass times

(Remer et al., 2024). While AOD retrievals are relatively mature, products such as SSA, refractive index, size distribution and particle shape remain considerably more uncertain and less standardized (Dubovik et al., 2019; Dong et al., 2026).

Airborne platforms can be also used to complement ground-based remote sensing because they can be employed for sampling the upper atmosphere using in-situ payloads. These include aircraft, balloons and Unmanned Aerial Vehicles (UAVs). Different aerosol and cloud in-situ instrument packages can be deployed to provide insight into, e.g., the particle size and the composition. Remote sensing retrievals of volume size-distribution such as the one used in SKYRAD have been validated, amongst others, against such type of observations (e.g., Nakajima et al, 2020; Kudo et al, 2021). Moreover, the combination of airborne in-situ observations with remote sensing can be used for closure on the aerosol properties to gain a more holistic view (e.g., Tsekeri et al, 2017). It is generally important to design experiments such as to combine remote sensing observations to airborne in-situ methods, as it allows to close the uncertainty gap.

Numerical models and reanalysis systems provide a complementary perspective by representing aerosol emissions, transport, chemical transformation, cloud interactions and removal processes within a physically consistent framework. They provide continuous four-dimensional fields and can therefore overcome many observational sampling limitations. Models also support source attribution, emission-scenario analysis, radiative-effect estimates and forecasting, while systems such as MERRA-2 and CAMS combine simulations with observations through data assimilation. Their uncertainties arise from emissions, aerosol microphysics, chemical processes, deposition and parameterizations, as well as from the quality and representativeness of the observations used for model evaluation or assimilation (Yumimoto et al., 2024;Zhang et al., 2026).

The complementarity of these approaches is particularly evident for key aerosol parameters. **AOD** can be accurately measured by ground-based sun photometers, mapped spatially by satellites and continuously represented by models through vertically integrated aerosol extinction. **AE** can be derived from spectral AOD measurements and modelled aerosol size distributions. **Aerosol size distributions** are constrained in greater detail by advanced ground-based sky-radiance and polarimetric observations, while satellite multi-angle and polarimetric measurements provide spatially distributed but generally less constrained information. **SSA**, which is critical for aerosol absorption and radiative effects, remains sensitive to aerosol loading and measurement uncertainty. **Vertical aerosol profiles**, meanwhile, require complementary observations such as ground-based or satellite lidar because they cannot be reliably obtained from conventional column-integrated measurements alone.

3. User Requirements Across Disciplines

3.1. Solar radiation and radiative transfer modelling

3.1.1 User requirements and aerosol inputs for radiative transfer modelling

Accurate radiative transfer (RT) simulations require a realistic representation of atmospheric aerosol conditions, as aerosols constitute one of the dominant sources of variability in surface solar irradiance (SSI) under cloud free skies (Gueymard, 1993). Through scattering and absorption processes, aerosols attenuate the incoming solar radiation beam, redistribute energy between the direct and diffuse components, and modify the spectral distribution of solar radiation reaching the Earth's surface. Consequently, aerosol effects influence not only the magnitude of global horizontal irradiance (GHI), but also direct normal irradiance (DNI), and diffuse horizontal irradiance (DHI), all of which are essential inputs for solar-energy applications and atmospheric studies (e.g., Eltbaakh et al., 2012; Obregón, M.A. et al., 2018; Kosmopoulos et al., 2017). Because RT models explicitly describe aerosol-radiation interactions, their performance depends directly on the quality and representativeness of the aerosol information used as input (e.g., Raptis et al., 2018; Ruiz-Arias & Gueymard, 2018; Ruiz-Arias et al., 2015; Belluardo et al., 2016; Witthuhn et al., 2021; Elsey et al., 2024).

Sensitivity analyses by Obregón et al. (2018) identified AOD as the most influential atmospheric parameter controlling irradiance under cloudless skies. SSA determines the fraction of extinction due to scattering relative to absorption and therefore governs the partitioning of solar radiation between atmospheric heating and surface irradiance. Under certain atmospheric conditions, SSA can be equally significant with the AOD, especially at shorter visible and UV wavelengths, and at environments where strongly absorbing aerosol species dominate (Kazadzis et al., 2005; Raptis et al., 2018; Fountoulakis et al., 2019; Witthuhn et al., 2021). The aerosol phase function, commonly approximated by the asymmetry parameter (g), controls the angular redistribution of scattered radiation and is particularly important for accurately simulating diffuse irradiance. Spectrally resolved AOD, SSA and g (or, if available, the phase function instead of g) are required to reproduce wavelength-dependent irradiance and to support applications relying on spectral solar radiation. Increasing aerosol loading strongly reduces DNI, while the reduction in GHI is smaller because part of the attenuated direct beam is redirected into the diffuse component. Although the vertical distribution of aerosols has only a minor effect on shortwave irradiance at the surface and at the top of the atmosphere, it strongly influences radiometric quantities and heating rates within the atmosphere. These differences can be large during episodes with elevated aerosol layers, such as dust intrusions (Fountoulakis et al., 2022). Since default extinction profiles are commonly used in RT models, vertically resolved information from lidar and ceilometer networks, spaceborne lidars or atmospheric composition models can reduce this source of uncertainty (Granados-Muñoz ET AL., 2019; Bazo et al., 2023)

The required aerosol information also depends on the intended application and the desired accuracy (e.g., Belluardo et al., 2016; Ruiz-Arias et al., 2018; Kahn et al., 2023). Climatological aerosol datasets may be sufficient for long-term climatological studies. In contrast, operational

applications increasingly require observations with high spatial and temporal resolution that capture the strong variability of aerosol properties. This is especially true during mineral dust outbreaks, biomass-burning episodes, and pollution events, when rapid changes in aerosol loading and composition can substantially alter surface irradiance within a few hours (e.g., Gueymard, 2012; Masoom et al., 2023; Kouklaki et al., 2026).

3.1.2 Accuracy requirements and uncertainty propagation

The value of aerosol observations for radiative transfer applications depends not only on the availability of aerosol optical properties but also on their accuracy, temporal resolution, and representativeness. Although relatively few studies have systematically quantified the propagation of aerosol uncertainties into simulated surface solar irradiance (SSI) (Belluardo et al., 2016; Witthuhn et al., 2021; Roman et al., 2014 a,b), they consistently demonstrate that the required accuracy depends on the irradiance quantity of interest. In particular, uncertainties in AOD have a substantially larger impact on DNI and DHI than on GHI, because changes in the direct and diffuse components partially compensate when integrated into global irradiance. Consequently, applications relying on DNI, such as concentrating solar power (CSP), impose considerably stricter accuracy requirements on aerosol products than applications based primarily on GHI.

The highest simulation accuracy is currently achieved when RT models are driven by high-quality ground-based aerosol observations. Under these conditions, uncertainties associated with individual aerosol optical properties can be below 1% (Belluardo et al., 2016), while the combined uncertainty in broadband GHI, accounting for aerosol properties, water vapour, ozone, surface albedo, solar zenith angle and the extraterrestrial solar spectrum, is approximately 3–6% (Roman et al., 2014a,b). In contrast, simulations based on satellite-derived aerosol products generally exhibit larger uncertainties because of retrieval errors, reduced temporal sampling, and the use of temporally averaged aerosol fields. Reported uncertainties reach approximately 4–10% for broadband shortwave irradiance and 8–17% for ultraviolet irradiance, highlighting the sensitivity of RT simulations to the quality of aerosol inputs (Roman et al., 2014b). Uncertainties in the AOD from CAMS reanalysis, quantified against collocated AERONET observations, translate into relative uncertainties in clear-sky GHI that generally remain below 5–6 %. DNI is considerably more sensitive, with relative uncertainties frequently above18% over major aerosol source regions, such as areas affected by desert dust, biomass burning and persistent anthropogenic pollution, and can reach 25–35% in certain seasons under high aerosol loading (Moustaka et al. Prepr, 2026).

3.2 Solar Energy

3.2.1 Why the solar-energy sector needs aerosol observations

Atmospheric aerosols influence the performance of both photovoltaic (PV) and concentrating solar power (CSP) systems by modifying the quantity, angular distribution, and spectral composition of solar radiation reaching the Earth's surface (Papachristopoulou et al., 2022). Through scattering and absorption processes, aerosols attenuate the direct solar beam,

enhance diffuse irradiance, and alter the spectral distribution of incoming radiation, thereby affecting the energy available for solar conversion. In addition to these direct radiative effects, aerosols influence cloud formation and cloud optical properties, introducing further variability in the available solar resources (e.g., Varga, 2025, Varga et al., 2026).

The magnitude of these effects depends strongly on aerosol loading, composition, and optical properties. Different aerosol types, including mineral dust, biomass-burning smoke, urban pollution, and marine aerosols, affect solar-energy production in different ways, with episodic dust and smoke events often producing the largest short-term reductions in available solar irradiance (e.g., Kouklaki et al., 2023, 2026).

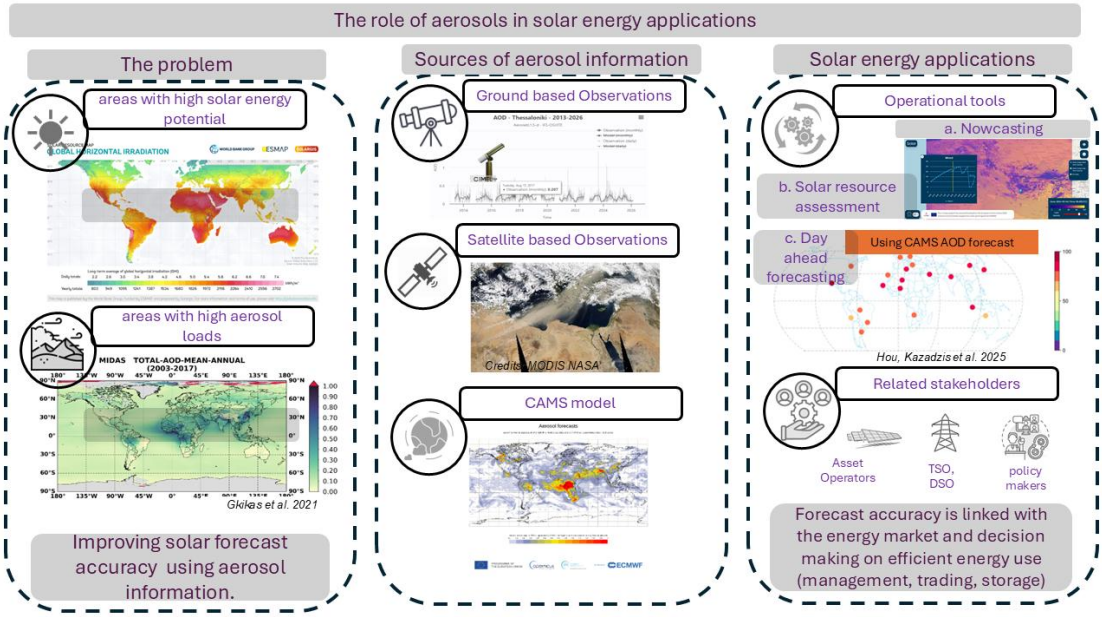


Figure 4. *Overview of the role of atmospheric aerosol in solar energy applications.*

Radiometric measurements provide the primary means for quantifying aerosol optical properties (AOPs), forming the basis (Fig. 3.1) for improved solar resource assessment, performance modeling, and forecasting of solar energy systems (Papachristopoulou et al., 2024). Conventional fixed-tilt PV systems utilize both global and diffuse irradiance and thus direct and scattered light are both important (e.g., Papadimitriou et al., 2026; Ruiz-Arias et al., 2018). Such systems are usually sensitive to photons with wavelengths that are shorter than ~ 1200 nm. Thus, measurements of the spectral AOD and the spectral SSA in this range are necessary for applications related to such systems.

AOD, specially for high solar zenith angles.In contrast, CSP and tracking systems depend predominantly on DNI, making them considerably more sensitive to Furthermore, CSP systems use irradiance in the entire spectral range (i.e., including the solar infrared spectral region) which introduces an additional need for spectral AOD measurements at wavelengths longer than 1200 nm. CSP installations experience an additional atmospheric loss because reflected radiation is further attenuated along the optical path between heliostat mirrors and the central

receiver (e.g., Hanrieder et al., 2017). As a result, accurate characterization and forecasting of aerosol optical properties are essential for reliable solar resource assessment, power forecasting, plant operation, and investment planning, particularly in regions frequently affected by desert dust or severe pollution events.

3.2.2 Aerosol information requirements for solar-energy forecasting

Solar-energy nowcasting and forecasting have become essential components of modern power-system operation, enabling improved grid stability, energy trading, plant operation, and maintenance scheduling (Yang et al., 2022; Sengupta et al., 2021). Although clouds are the dominant source of variability in SSI , aerosols become equally important under clear-sky conditions, particularly in regions (see Fig. 4) with high solar-energy potential where cloudiness is limited but aerosol loads are frequently elevated, such as regions that are in the proximity of large deserts (e.g., Kosmopoulos et al., 2017; Fountoulakis et al., 2021). Consequently, operational forecasting systems increasingly require accurate predictions of aerosol optical properties in addition to cloud information. Forecast aerosol information can be incorporated into solar-energy prediction systems through several approaches. These include aerosol climatologies, persistence forecasts derived from ground-based observations, satellite-based retrievals, chemical transport models coupled with numerical weather prediction (NWP) systems, and fully integrated global atmospheric composition forecasting systems (Breitkreuz et al., 2009; Jimenez et al., 2016; Razagui et al., 2021). Table 3.1 summarizes the principal sources currently used in solar-energy applications.

Table 2. Main aerosol property sources currently used in solar-energy applications

Source of aerosol forecast	**Dataset**	**Citation**
Global atmospheric models	Copernicus Atmosphere Monitoring Service (CAMS)	*Flemming et al., 2017; Eskes et al., 2024*
	Goddard Earth Observing System, Version 5 (GEOS-5)	*Molod et al., 2015*
Ground or satellite based observations • persistence forecasts • calculated climatological values	AErosol RObotic NETwork (AERONET)	*Holben et al., 1998; Giles et al., 2019*
	MODerate resolution Imaging Spectroradiometer (MODIS)	*Levy et al., 2013; Wei et al., 2019*
aerosol climatologies	Tegen	*Tegen and Fung, 1994;* *Tegen et al., 1997*

	MACv2	*Kinne, 2019*

3.2.3 Operational aerosol forecasting systems and applications

Among the currently available global atmospheric composition forecasting systems, the Copernicus Atmosphere Monitoring Service (CAMS) and NASA's Goddard Earth Observing System Version 5 (GEOS-5) are the two systems most widely used for solar-energy applications. Both provide operational forecasts of aerosol optical depth together with aerosol speciation and additional optical and microphysical properties through freely available services (Flemming et al., 2017; Molod et al., 2015; Eskes et al., 2024). Early work by Schroedter-Homscheidt et al. (2013) quantified the aerosol forecast accuracy required to support CSP applications and demonstrated that substantial improvements in aerosol prediction were needed before day-ahead DNI forecasts could reach operational accuracy requirements.

More recently, Hou et al. (2025) evaluated CAMS day-ahead AOD forecasts using AERONET observations and quantified the propagation of aerosol forecast errors into clear-sky DNI forecasts through radiative transfer modelling. CAMS generally outperformed persistence methods at urban and industrial locations, while persistence forecasts remained superior during several intense dust episodes, highlighting the continuing difficulty of forecasting mineral dust transport. The study further showed that none of the evaluated approaches consistently achieved the aerosol forecast accuracy necessary to limit day-ahead DNI errors below approximately 5%, particularly over dust-prone regions. Similar conclusions have been reported using GEOS-5 aerosol forecasts (Bunn et al., 2020) and WRF-Solar simulations incorporating forecast aerosol fields (Yoon et al., 2026), confirming that dynamic aerosol forecasts consistently outperform climatological assumptions but that forecast errors remain a limiting factor during rapidly evolving aerosol events.

Forecast aerosol products have also been successfully integrated into operational solar-energy nowcasting systems. The NextSENSE2 platform (Papachristopoulou et al., 2024) incorporates CAMS aerosol forecasts together with cloud observations to produce 15-minute solar irradiance forecasts up to three hours ahead. Evaluation over Europe and North Africa demonstrated only a small positive CAMS AOD bias (~10%), corresponding to a mean GHI bias below 1%. Independent validation during a one-year field campaign in Athens (Raptis et al., 2023) further showed that CAMS forecasts perform close to observational uncertainty under typical conditions, while wildfire events remain challenging because rapidly changing local emissions are difficult for operational forecasting systems to capture.

Overall, these studies demonstrate that aerosol forecasting has progressed considerably during the past decade, although further improvements remain necessary, particularly for applications relying on accurate DNI prediction in desert and biomass-burning regions.

3.2.4 Spatial and temporal observation requirements

The temporal and spatial requirements of aerosol observations depend strongly on the intended application. For process studies, aerosol measurements should resolve rapid variations

associated with dust fronts, pollution plumes, wildfire smoke, and boundary-layer evolution. Such studies ideally require observations with sampling intervals of the finest possible temporal resolution, together with simultaneous measurements of solar irradiance and power production.

For operational nowcasting, aerosol optical properties should be available in near real time with temporal resolutions of approximately 5–15 minutes, consistent with current operational photometer networks such as AERONET and SKYNET. Such temporal resolution is generally sufficient for use in operational solar irradiance nowcasting systems (Papachristopoulou et al., 2024). Operational forecasting typically requires updates every 1–3 hours, matching the frequency of current global atmospheric composition models.

Spatial representativeness constitutes an equally important requirement. Aerosol properties may vary substantially over relatively short distances owing to local emission sources, coastal influences, complex terrain, or elevation gradients. Consequently, urban and industrial environments may require observation spacing of approximately 5–10 km to adequately represent local aerosol variability. Conversely, in desert regions dominated by mineral dust, aerosol fields are generally more homogeneous, and longer station spacing can be sufficient to characterize regional aerosol conditions relevant for solar-energy applications. For climatological solar-resource assessments, hourly aerosol observations are generally adequate because long-term averages rather than short-term fluctuations dominate the uncertainty. Similar spatial representativeness requirements apply, although more dense observations remain desirable over complex terrain and polluted metropolitan areas where aerosol gradients can remain significant over relatively small spatial scales (e.g., Teri et al., 2025).

3.2.5 Current capabilities for solar energy applications

Current observing and forecasting capabilities already provide much of the aerosol information required by operational solar-energy applications. Ground-based networks such as AERONET and SKYNET routinely provide high-quality observations of AOD and other aerosol properties, while satellite instruments including MODIS, VIIRS, Sentinel-3, and geostationary platforms deliver regional aerosol monitoring with near-global coverage. Operational atmospheric composition services such as CAMS and GEOS-5 further provide forecasts of aerosol optical properties ready to use into solar-energy forecasting systems.

3.3. Atmospheric modelling and data assimilation

3.3.1 Radiometric aerosol observations for atmospheric composition monitoring

Accurate monitoring of atmospheric aerosols is essential for understanding their sources, transport, transformation and removal, as well as their impacts on air quality, weather, and climate. Radiometric measurements are a cornerstone of atmospheric composition monitoring, providing long-term, quality-assured observations of aerosol optical properties that support research, operational services and climate applications (Benedetti et al., 2018; IPCC, 2021). Unlike in situ observations, which sample aerosols locally, radiometric measurements characterize the atmospheric column, making them particularly valuable for atmospheric composition modelling and data assimilation (Holben et al., 1998; Dubovik et al., 2002; Benedetti et al., 2018). Ground-based sun-photometers routinely retrieve products that provide

key constraints for aerosol transport models, radiative-transfer calculations and aerosol climatology (Kahn et al., 2023; Benedetti et al., 2018).

Observational requirements vary according to the application. Operational forecasting primarily requires near-real-time AOD observations with well-characterized uncertainties and sufficient spatial coverage for data assimilation (Benedetti et al., 2018; Kahn et al., 2023), whereas climate applications demand long-term stability, calibration traceability and temporal consistency to detect multi-decadal changes (GCOS, 2022; IPCC, 2021; Weatherhead et al., 1998). Process studies additionally require comprehensive aerosol optical and microphysical properties, including aerosol absorption and particle size, for investigating aerosol processes and evaluating numerical models (Samset et al., 2018; Kahn et al., 2023). No single observing system satisfies all these requirements, making complementary observations from multiple platforms essential (Benedetti et al., 2018; GCOS, 2022).

Ground-based networks such as **AERONET** and **SKYNET** provide the most accurate and internally consistent aerosol optical observations available and serve as the primary reference for validating satellite products, evaluating atmospheric composition models and supporting aerosol data assimilation. Satellite sensors, including MODIS, VIIRS, MISR, POLDER and the latest geostationary imagers, complement these measurements by providing near-global spatial coverage, although generally with larger retrieval uncertainties and more limited sensitivity to aerosol absorption and vertical structure (Levy et al., 2013; Benedetti et al., 2018).

3.3.2 Aerosol data assimilation and operational forecasting systems

Aerosol data assimilation has become a fundamental component of modern atmospheric composition forecasting, combining observations with physically based numerical models to produce the most realistic estimate of the atmospheric aerosol state. By continuously correcting model initial conditions, data assimilation reduces uncertainties associated with emissions, transport, deposition, aerosol properties and meteorological forcing, thereby improving both short-term forecasts and long-term atmospheric analyses (Benedetti et al., 2009; Bocquet et al., 2015; Benedetti et al., 2018). It now underpins operational services such as the Copernicus Atmosphere Monitoring Service (CAMS), NASA's Global Modeling and Assimilation Office (GEOS), the Navy Aerosol Analysis and Prediction System (NAAPS) and several regional forecasting systems (e.g., Carrassi et al., 2018).

Radiometric aerosol observations provide the principal observational constraint for these systems. AOD remains the most widely assimilated aerosol variable because it is routinely retrieved from both ground-based sun-photometer networks and numerous satellite sensors, has well-characterized uncertainties and provides a robust measure of atmospheric aerosol loading (Benedetti et al., 2009; Moustaka et al., 2026; et al., 2020; Eskes et al., 2024). While AERONET observations primarily serve as reference measurements for calibration, validation and independent evaluation, satellite retrievals from sensors such as MODIS, VIIRS and geostationary imagers provide the spatial coverage required for global operational analyses (Levy et al., 2013; de Leeuw et al., 2015; Shi et al., 2014).

Current operational systems generally assimilate retrieved AOD using variational (3D-Var and 4D-Var), Ensemble Kalman Filter (EnKF) or hybrid ensemble-variational approaches that optimally combine observations with model forecasts while accounting for uncertainties in both (Schwartz et al., 2014). The assimilation updates aerosol mass concentrations and, indirectly, emissions and transport pathways. More recently, developments have focused on direct radiance assimilation and inverse modelling of aerosol emissions, reducing retrieval-related uncertainties and improving the consistent use of observations from multiple satellite sensors (Benedetti et al., 2009; Carrassi et al., 2018). **Figure 5** illustrates the aerosol 4D-Var assimilation framework implemented within the ECMWF Integrated Forecasting System (IFS).

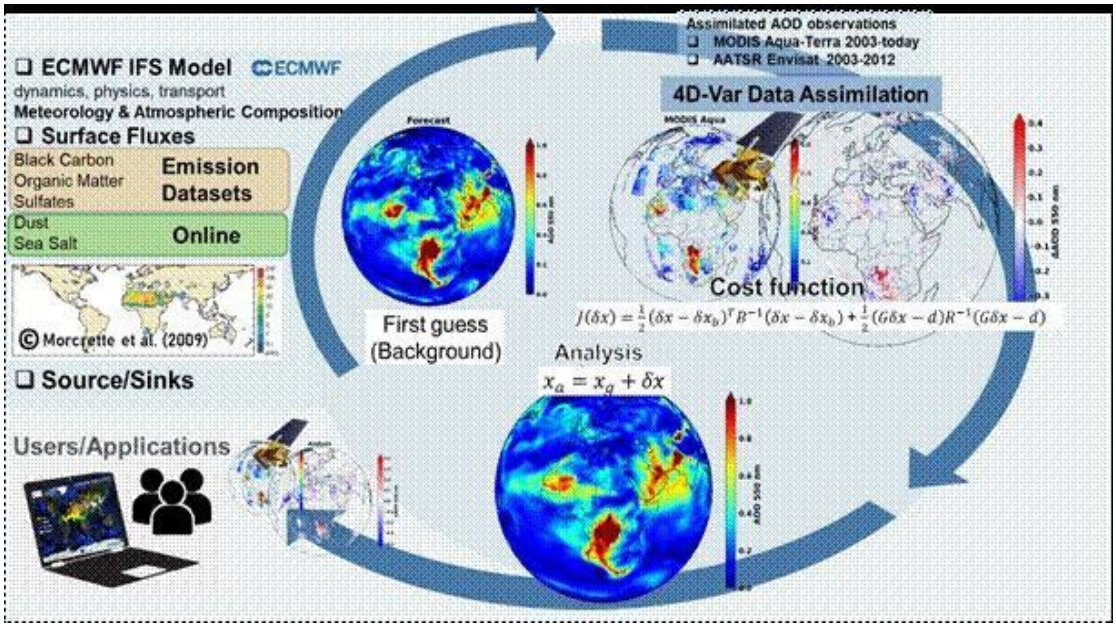


Figure 5: *Schematic overview of the ECMWF Integrated Forecasting System (IFS) aerosol 4D-Var data assimilation procedure.*

Despite these advances, operational assimilation still relies predominantly on AOD, which provides only limited information on aerosol composition, absorption, particle size and vertical distribution. Consequently, several aerosol properties that strongly influence atmospheric chemistry and radiative effects remain only weakly constrained (Kahn et al., 2023; Yang et al., 2023; Segers et al., 2023). Emerging observations from multi-angle polarimeters, lidar systems and advanced ground-based inversion products offer the potential to assimilate additional variables—including SSA, aerosol layer height and particle size distribution—thereby improving both aerosol forecasts and radiative-transfer simulations (Benedetti et al., 2018; Bond et al., 2018; Kahn et al., 2023).

Forecast quality depends not only on assimilation algorithms but also on the quality, latency and representativeness of the assimilated observations. Although satellite observations provide the global coverage required for operational assimilation, these improvements ultimately depend on high-quality ground-based observations. Networks such as AERONET provide the reference measurements required to calibrate and validate satellite retrievals and independently

evaluate assimilated products, ensuring the long-term reliability of operational forecasting systems (Levy et al., 2013; Sayer et al., 2019; Popp et al., 2016; Inness et al., 2019; Moustaka et al., 2026).

The benefits of assimilating radiometric aerosol observations are clearly illustrated by comparisons between the CAMS EAC4 reanalysis, which assimilates satellite-derived AOD, and a control simulation without aerosol assimilation (CTRL) (Moustaka et al., 2026). As shown in Figure 6a, assimilation substantially improves agreement with independent AERONET observations, with positive differences in the correlation coefficient (ΔR) at almost all stations and enhanced temporal variability over Europe, North Africa and South Asia. Overall, approximately 98% of the evaluated stations exhibit improved correlation coefficients following assimilation. Similarly, Figure 2b demonstrates a substantial reduction in systematic bias, with 75% of stations showing improved relative mean bias statistics compared with the control simulation. These results demonstrate that radiometric aerosol observations provide one of the strongest observational constraints on aerosol transport and significantly improve operational analyses and forecasts.

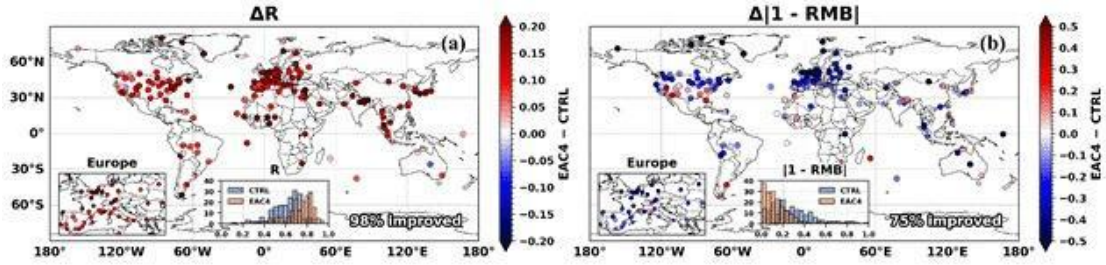


Figure 6: *Spatial distribution of the statistical performance differences between EAC4 and CTRL relative to AERONET observations. Panels show (a) the difference in the correlation coefficient (ΔR) and (b) the difference in the relative mean bias metric (Δ|1−RMB|). Positive ΔR values and negative Δ|1−RMB| values indicate improved performance following aerosol assimilation* (updated from Moustaka et al., 2026).

Future aerosol data assimilation is expected to evolve towards integrated multi-sensor frameworks combining radiometric observations with lidar, polarimetric satellite measurements, in situ observations and machine-learning techniques. Such systems will provide stronger observational constraints on aerosol optical and microphysical properties, improve the representation of aerosol sources and transport, and enhance operational services supporting air-quality forecasting, aviation, renewable-energy management and climate applications (Benedetti et al., 2018; Carrassi et al., 2018; Kahn et al., 2023).

3.3.3 Aerosol reanalyses, climate data records and operational products

Aerosol reanalyses and operational forecasting products have become indispensable resources for atmospheric composition research, climate studies and environmental services. By combining atmospheric models with observations through data assimilation, they provide spatially and temporally consistent descriptions of aerosol distributions that cannot be obtained from observations alone. Reanalyses offer continuous global aerosol fields over periods ranging

from years to decades, whereas operational systems provide near-real-time information for environmental monitoring and decision support (Benedetti et al., 2009; Inness et al., 2019; Eskes et al., 2024).

Major international products include CAMS, MERRA-2, NASA GEOS, NAAPS and several regional forecasting systems. These datasets routinely provide AOD, speciated aerosol concentrations, radiative properties, deposition fluxes, surface particulate matter and associated meteorological variables for applications spanning air quality, climate, renewable energy and atmospheric research (Randles et al., 2017; Gelaro et al., 2017; Inness et al., 2019; Eskes et al., 2024).

Beyond operational forecasting, radiometric observations also provide essential constraints for evaluating aerosol reanalyses, atmospheric composition models and Earth system models. Measurements of AOD and inversion products are routinely used to assess simulated aerosol loading, particle size distributions and optical properties, improving estimates of aerosol radiative forcing and increasing confidence in climate projections (Benedetti et al., 2018; Kahn et al., 2023). The long-term stability and traceability of ground-based observations are critical for ensuring the temporal consistency of aerosol reanalyses and climate data records, enabling the identification of retrieval drifts and the merging of observations from successive satellite missions (GCOS, 2022).

3.3.4 Machine learning applications supported by radiometric aerosol observations

The rapid development of machine learning (ML) has transformed atmospheric composition research by enabling new approaches for aerosol retrieval, forecasting, data fusion and model emulation. Unlike traditional numerical models, which explicitly represent aerosol processes through physical parameterizations, ML algorithms learn complex relationships directly from observations and model outputs. The increasing availability of long-term radiometric aerosol measurements, together with satellite observations, meteorological reanalyses and chemical transport model outputs, has created unprecedented opportunities for data-driven methods that complement conventional atmospheric modelling (Reichstein et al., 2019; Irrgang et al., 2021; Peng et al., 2023). Ground-based radiometric networks provide the high-quality reference observations required for most supervised ML applications. Their long-term, accurately calibrated measurements of aerosol AOD, AE, SSA, VSD and other products serve as training, validation and benchmark datasets for aerosol retrievals, bias correction and predictive modelling (Chen et al., 2020; Chen et al., 2022; Irrgang et al., 2021; Awais and Wang, 2025; Mishra et al., 2025; Logothetis et al., 2024; Akgül et al., 2026).

One of the most mature ML applications is the improvement of satellite aerosol retrievals. Deep learning and other statistical approaches have been used to retrieve AOD from multispectral and hyperspectral imagery, reduce errors associated with surface reflectance, cloud contamination and aerosol type, and combine observations from multiple satellite platforms. AERONET observations remain the primary reference for both algorithm training and independent evaluation (Chen et al., 2020; Kahn et al., 2023). Machine learning is also

increasingly applied to aerosol forecasting, where neural networks, random forests, gradient-boosting algorithms and hybrid physics-informed models combine radiometric observations with meteorological variables, satellite retrievals and numerical model outputs to predict aerosol loading, particulate matter concentrations and surface solar irradiance. The performance of these algorithms depends critically on the availability of representative, long-term radiometric observations spanning diverse aerosol regimes (Reichstein et al., 2019; Irrgang et al., 2021).

3.4. Satellite validation

3.4.1 Role of radiometric observations in operational validation

Satellite-based aerosol properties offer the huge benefit of global coverage, usually once or twice daily from polar orbits (respectively for visible and thermal infrared observations) or even every half hour from geostationary platforms. Those space instruments however require thorough calibration, and the data retrieved from them require evaluation at least, validation at best. This allows to assess the satellite data quality, and also guide further algorithm developments. Established global networks such as AERONET (Holben et al., 1998; Giles et al., 2019; Sinyuk et al., 2020) and SKYNET (Takamura et al., 2004; Nakajima et al., 2020) have deployed sun-photometers delivering reference aerosol observations suitable for assessing the performance of spaceborne aerosol retrievals. Among the aerosol optical properties obtained by satellite instruments, the majority of the evaluation studies have focused on AOD, a measure of aerosols' columnar load expressed in optical terms, which is the most common retrieved aerosol parameter across various satellite instruments.

3.4.2 Validation of satellite aerosol products

Global and regional evaluation studies of MODIS AOD versus AERONET have been performed to assess the evolution of the developed retrieval algorithms applicable over dark land and ocean surfaces (Tripathi et al., 2005; Levy et al., 2007; Remer et al., 2008; Levy et al., 2013; Tao et al., 2015; Mhawish et al., 2017; Wei et al., 2019), over bright surfaces (Hsu et al., 2013; Sayer et al., 2013a), excluding ice/snow covered areas, as well as on the "merged" products, which combine the three algorithms (Sayer et al., 2013b).

Similar studies have evaluated AOD retrieved from passive sensors such MISR (; Kahn et al., 2005; Jiang et al., 2007; Garay et al., 2017; Ruonan et al., 2023), VIIRS (Jakson et al., 2013; Hsu et al., 2019; Sayer et al., 2018; Sayer et al., 2019; He et al., 2021; Wang et al, 2023; Lee et al., 2024), AVHRR (Hauser et al., 2005a; Hauser et al., 2005b; Riffler et al., 2010; Tao et al., 2020), Sentinel-3 (Liu et al., 2021; Lipponent et al., 2022; Sogacheva et al., 2022;), Sentinel -2 (Obregón et al., 2019; Yang et al., 2021; Kumar et al., 2024), SPEXone (Fu et al., 2025) and MSI (Docter et al., 2023). The GRASP algorithm (Dubovik et al., 2014; Dubovik et al., 2021) has been applied to observations derived from satellite instruments such as POLDER/PARASOL (Li et al., 2019; Chen et al., 2020; Schutgens et al., 2021), Sentinel 3-A/OLCI (Chen et al., 2022), Sentinel 5P/Tropomi (Litvinov et al., 2024; Chen et al., 2024), OMI (Ahn et al., 2014) and Himawari-8 (Li et al., 2025) providing a set of aerosol properties including AOD, its fine and coarse counterparts, AE and SSA. Validation of GRASP-derived

aerosol products against AERONET measurements and retrievals has demonstrated very good performance for aerosol-load-related parameters and moderate performance for optical properties related to aerosol size and origin.

Evaluation studies (Tang et al., 2023; Cao et al., 2023) relying on SKYNET aerosol measurements are substantially fewer than those based on AERONET measurements because the network comprises only a limited number of stations in Europe and Asia. Aerosol measurements over the oceans have also been obtained through the Marine Aerosol Network (MAN; Smirnov et al., 2009; Smirnov et al., 2011), in which sunphotometers have been deployed aboard vessels and ships, extending observational capabilities beyond continental areas to remote maritime regions and enclosed seas. Numerous assessment studies based on t hese measurements have been conducted (Sayer et al., 2012; Schutgens et al., 2013; Shen et al., 2018; Pei et al., 2023; Pearson et al., 2025), contributing substantially to the identification of the strengths and limitations of spaceborne aerosol retrievals. In addition to assessments of individual satellite instruments, joint evaluations of various spaceborne aerosol retrievals have been conducted, facilitating their intercomparison within a common validation framework, as demonstrated in numerous studies (; Kahn et al., 2007; Su et al., 2021; Bibi et al., 2015; Xiao et al., 2016; Chen et al., 2022; Su et al., 2021; Wang et al., 2020; Osgouei et al., 2022).

3.4.3 Validation of advanced aerosol products

Spaceborne aerosol properties deriving information about aerosol particles' size, fine/coarse fraction, shape and composition have also been validated against AERONET measurements/retrievals. These studies have focused on the AE (Levy et al., 2010; Schutgens et al., 2013; Sayer et al., 2013; Sayer et al., 2018; Chen et al., 2020; Ma et al., 2026; Si et al. 2017; Fu et al., 2025; Sogacheva et al., 2022; Litvinov et al., 2021; Chen et al., 2024; Litvinov et al., 2025), fine mode fraction (Li and Ginoux, 2025; Sogacheva et al., 2022), single scattering albedo (Si et al. 2017; Mok et al., 2018; Jethva, H. and Torres, 2019; Litvinov et al., 2021; Chen et al., 2024; Fu et al., 2025; Litvinov et al., 2025), and the asymmetry parameter (). The main conclusion emerging from comparisons between AOD and non-AOD evaluation studies is that passive satellite sensors retrieve aerosol load satisfactorily, whereas their performance in retrieving other aerosol optical properties is poorer.

Most existing validation studies of aerosol retrievals from passive spaceborne instruments have focused on total-column aerosol optical depth, which represents the combined extinction of the aerosol mixture, whose composition and optical properties vary geographically and seasonally (; Tesche et al., 2019). Evaluating retrievals of individual aerosol types therefore requires the combined use of AERONET direct-Sun measurements and derived size or optical-property products to select cases in which the aerosol type of interest dominates the atmospheric column (). Mineral-dust-dominated cases are commonly characterized using coarse-mode AOD retrieved with the spectral deconvolution algorithm (SDA; O'Neill et al., 2003) at AERONET sites within or near major dust-source and transport regions (Klüser et al., 2011; Capelle et al., 2018; Vandenbussche et al., 2026). Alternative approaches exclude observations with moderate-to-high Ångström-exponent values, which indicate substantial fine-mode

contributions (Eck et al., 1999; Basart et al., 2009), or apply simultaneous thresholds to AOD and the Ångström exponent to distinguish high-loading dust events from low-AOD coarse marine aerosol conditions (). Within this context, Gkikas et al. (2021) proposed the combined use of total and coarse-mode AOD, the Ångström exponent between 440 and 870 nm, and single-scattering albedo at 440 and 675 nm to identify AERONET observations in which dust dominates the entire atmospheric column. These dust-dominated observations were subsequently used to evaluate the mid-visible dust optical depth at 550 nm provided by the satellite-based MIDAS dataset (; 2022). This approach demonstrates how multiple ground-based aerosol properties can be combined to isolate specific aerosol types and support the evaluation of aerosol-type-specific satellite products beyond conventional total-AOD validation.

3.5. Health Applications

3.5.1. Urban air quality

Urban air pollution is a major environmental and public-health concern, with particulate matter ($PM_{2.5}$ and PM_{10}) among the most important pollutants associated with adverse health effects. Conventional air-quality monitoring networks provide accurate measurements of near-surface PM concentrations, but their spatial coverage is often limited. Radiometric observations provide complementary information by characterizing the aerosol burden over much larger areas. In particular, AOD retrieved from satellite observations and ground-based networks such as AERONET can provide valuable information for estimating surface PM concentrations and mapping urban air quality with high spatial and temporal coverage (Chu et al., 2016; Liu et al., 2020; Zhu et al., 2023; Lolli, 2025).

However, AOD represents the integrated optical effect of aerosols throughout the atmospheric column and therefore cannot be directly equated with surface PM. The relationship between AOD and near-surface PM depends strongly on planetary boundary-layer height, aerosol vertical distribution, relative humidity, particle size and composition, and the contribution of elevated aerosol layers such as transported dust or smoke (Zhu et al., 2023; Lolli, 2025). Recent observations further demonstrate that the AOD–PM relationship can vary substantially according to aerosol layering and atmospheric conditions, with elevated aerosol layers potentially becoming decoupled from surface concentrations (Rogozovsky et al., 2026).

Radiometric measurements can contribute to urban air-quality monitoring through several complementary approaches, including spatial mapping of aerosol loading, estimation of $PM_{2.5}$ and PM_{10} concentrations, identification of pollution episodes, and characterization of aerosol transport into and across urban areas. The combination of satellite AOD with surface PM observations, meteorological parameters, chemical transport models and statistical or ML methods is increasingly used to improve the spatial and temporal resolution of urban PM estimates (Chu et al., 2016; Liu et al., 2020; Zhu et al., 2023; Padimala and Matli, 2024; Lolli, 2025). Recent reviews emphasize that integrated approaches can substantially extend the information provided by conventional monitoring networks, while persistent challenges remain

related to cloud contamination, missing satellite observations, spatial resolution, aerosol vertical structure and uncertainty quantification (Zhu et al., 2023; Padimala and Matli, 2024; Lolli, 2025).

3.5.2. Dust impacts on health

To-date atmospheric dust is increasingly recognized for its substantial contribution to air quality degradation and adverse impacts to human welfare and health. The reason behind these negative impacts is mainly twofold. First, mineral dust particles emitted and entailed in the atmosphere, originating both from natural sources (Kok et al., 2023) and anthropogenic activities (Ginoux et al., 2012), account to several thousands of teragrams (Tg) (1 Tg= 1 billion kilograms) per year, making this type of aerosol one of the most abundant aerosol types in terms of mass at a global scale (Gliß et al., 2021). This translates to frequently considerable amounts of dust accumulating close to the Earth's surface (Proestakis et al., 2024; 2025), even across regions hundreds or thousands of kilometers downwind from main dust emission sources, frequently exceeding World Health Organization Air Quality Guideline (WHO, 2021) recommended safety thresholds for $PM_{2.5}$ and PM_{10} (Table 3.2). Second, several extensive experimental campaigns focusing on the investigation of atmospheric dust properties through the exploitation of in-situ instrumentation measurements report on dust particle size distribution spanning over several orders of magnitude, from less than 0.1 μm to more than 100 μm in diameter (Weinzierl et al., 2017; Ryder et al., 2018; van der Does et al., 2018; Papetta et al, 2026). In this context of particles' size, an increasing body of epidemiological and dust studies underline the multifaceted risks that high concentrations of mineral particles pose to human health. More specifically, coarse dust particles are considered of low potential for harmful health effects, mainly causing mild skin irritation and/or non-severe allergic reactions even under conditions of prolonged exposure to high particle concentrations (Sandstrom and Forsberg, 2008; Goudie, 2014). However, fine dust particles due to their small size can infiltrate the lower respiratory system and even accumulate within the lungs and alveoli; thereby increasing the risk to trigger allergic reactions (Watanabe et al., 2011) and more serious conditions such as respiratory diseases (Wiggs et al., 2003; Middleton, 2020), cardiovascular disorders (Martinelli et al., 2013; Middleton et al., 2008), carcinogenic outcomes (Giannadaki et al., 2014; Steenland and Ward, 2014), while have even been associated with enhancement of meningitis pandemic outbreaks (Pérez García-Pando et al., 2014).

Table 3. World Health Organization (WHO) air quality guidelines (AQGs) for $PM_{2.5}$ and PM_{10}.

$PM_{2.5}$:	5 μg m^{-3} annual mean
	15 μg m^{-3} 24-hour mean
PM_{10}:	15 μg m^{-3} annual mean

	45 µg m^{-3}	24-hour mean

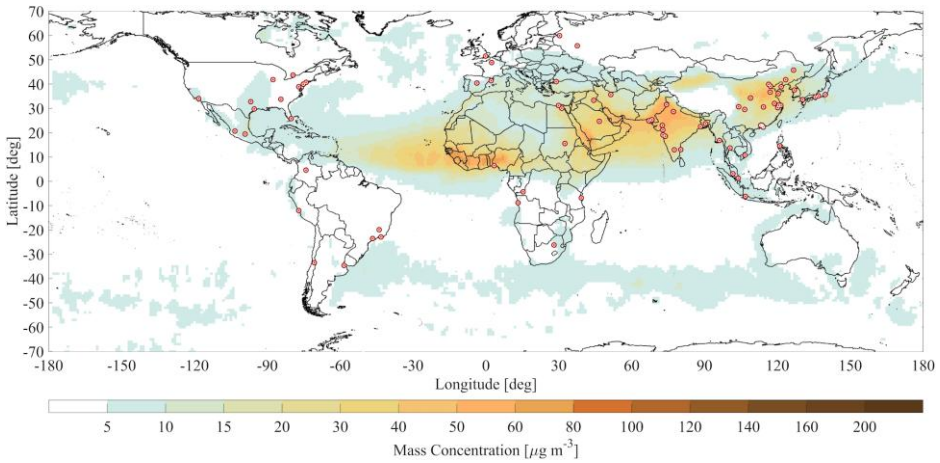


Figure 7: *CALIOP-based dust mean mass concentration (PM_1; µg m^{-3}), corresponding to the altitudinal range 0–500 m a.m.s.l. for the temporal period 06/2006-07/2023. Cycles denote major urban centers of population greater than 5 million (UN, 2018).*

Radiometric observations provide an important observational framework for monitoring atmospheric dust and improving its representation in atmospheric models. Ground-based sun-photometer measurements can be used to detect dust events, characterize their intensity and duration, distinguish coarse-dominated dust from mixtures with fine-mode pollution, and evaluate satellite retrievals and dust-forecasting systems. Comparisons between sun-photometer and lidar observations and regional dust models have demonstrated that radiometric measurements can reveal biases in simulated dust loading, particle-size distributions and transport, while also helping to identify uncertainties associated with dust emission parameterizations (Pérez et al., 2006; Rubin et al., 2017; Xian et al., 2019).

Assimilation of satellite and ground-based AOD observations can further improve the initial aerosol fields and subsequent dust forecasts, with demonstrated benefits extending to approximately 48 h in some regional forecasting applications (Choi et al., 2020). Importantly, assimilation of AOD alone provides limited information on the vertical distribution of dust. The combination of sun-photometer observations with ground-based and spaceborne lidar measurements can provide complementary information on the altitude, thickness and vertical structure of dust layers, and assimilation of vertically resolved dust extinction profiles has been shown to provide additional improvements in dust analyses and forecasts (Wang et al., 2014; Di Tomaso et al., 2022; Yang et al., 2023). Such observations are particularly valuable for health applications because they can help distinguish elevated transported dust layers from dust located within the planetary boundary layer, where the potential for population exposure is greater. Combining columnar AOD, vertically resolved aerosol observations and surface PM

measurements can therefore improve the interpretation of dust episodes and the assessment of population exposure.

Radiometric observations also support the characterization of dust impacts on radiation and climate, visibility, aviation, ecosystems and agriculture, while measurements of aerosol optical properties and solar irradiance can be used to quantify the effects of dust on photovoltaic and other solar-energy systems (Mamouri et al., 2026). Finally, sustained multi-platform observations provide a basis for evaluating dust emission, transport, deposition and removal processes, identifying systematic model deficiencies, and developing more reliable operational dust early-warning and impact-assessment systems.

3.5.3. Bioaerosols

Beyond mineral dust, atmospheric particulate matter also contains a diverse biological fraction, including bioaerosols, which introduce additional complexity in terms of exposure pathways, health effects, and measurement constraints.

Airborne biological particles, including bacteria, viruses, fungal spores, pollen, fragments of organisms, and biologically active macromolecules such as endotoxins and allergenic proteins, represent a diverse and ubiquitous component of atmospheric particulate matter. Globally, bioaerosol emissions arise from natural sources (vegetation, soil, oceans, wildfires) and anthropogenic activities (agriculture, waste handling, building ventilation), producing concentrations that vary widely in space and time and often peak seasonally during pollen release, fungal sporulation, or agricultural operations (Després et al., 2012; Fröhlich-Nowoisky et al., 2016; Katsivela et al., 2025; Gidarakou et al., 2026a). Because bioaerosols span a broad size range (from submicron fragments and virus-laden particles to intact pollen grains exceeding 10–50 μm), their environmental persistence, atmospheric transport, and human exposure patterns are highly variable.

The health impacts of bioaerosols are complex and depend on particle size, composition, viability, and accompanying chemical contaminants. Intact coarse particles such as pollen commonly provoke allergic rhinitis, conjunctivitis, and non-life-threatening hypersensitivity reactions in sensitized individuals (Martikainen et al., 2023; Reponen et al., 1996; Zemmer et al., 2024). In contrast, fragmented pollen, fungal fragments, and microbial cell debris that fall into the fine mode (<2.5 μm) can penetrate the lower respiratory tract, increase asthma morbidity, and contribute to severe asthma episodes, particularly in at-risk populations (D'Amato et al., 2017; Lake et al., 2017; Peden and Bush, 2015). Infectious risks are associated with viable pathogens suspended in aerosols, as particles smaller than ~5 μm can remain airborne for extended periods, disperse over distances, and penetrate deep into the lungs, increasing the transmission risk of respiratory viruses and bacteria (Griffin, 2007). Non-viable biological material, including endotoxins and mycotoxins, may also induce inflammatory responses, while interactions with chemical pollutants can further enhance bioaerosol toxicity and associated respiratory and cardiovascular effects (Pöschl and Shiraiwa, 2015; Šantl-Temkiv et al., 2022).

Long-range transport processes further complicate the public health picture, since bioaerosols may be entrained into dust plumes, biomass burning smoke, or convective updrafts and carried across regional to intercontinental scales, extending exposures far from emission sources and potentially introducing novel allergens or pathogens to susceptible populations (Griffin, 2007; Prospero and Mayol-Bracero, 2013). In particular, the mixing of dust with wildfire smoke can enhance the complexity and toxicity of aerosol mixtures, due to the presence of organic compounds, black carbon, and associated biological material (Bond et al., 2013; Gidarakou et al., 2026b; Kanakidou et al., 2005; Masoom et al., 2023; Pöschl, 2005; Pöschl and Shiraiwa, 2015). Vulnerable groups, including children, the elderly, and individuals with pre-existing respiratory or cardiovascular disease, are particularly high-risk during episodes such as high-pollen days, fungal spore peaks, and intense smoke/dust events, as well as under chronic exposure to inflammatory biological components. Quantifying these risks remains challenging, however, due to the complex interplay between aerosol composition, long-range transport, and the limited biological specificity of current measurement techniques.

Radiometric measurements contribute in studies focused on atmospheric bioaerosols, although their application remains considerably less mature than for mineral dust, smoke, or anthropogenic aerosols. Aerosol optical properties from ground-based sun photometers and satellite observations can be used to identify periods favorable for enhanced biological aerosol concentrations when interpreted together with meteorological conditions, land-cover information, and transport modelling (Noh et al., 2013; Sofiev, 2022; Vélez-Pereira et al., 2022).

3.5.4. UV modelling for health purposes - the role of aerosol uncertainties

The identical optical parameterizations used to derive surface PM maps from column observations, such as single scattering albedo (SSA) and size distribution, simultaneously dictate the transmission of solar ultraviolet radiation to the Earth's surface, impacting human health through an entirely different biological pathway. Exposure to solar ultraviolet (UV) radiation is essential for many biological processes and human health, including vitamin D production and regulation of physiological functions. Nevertheless, excessive UV exposure is associated with adverse health effects such as erythema, skin cancer, cataracts, and immune system suppression (WHO, 2002; Munakata et al., 2006; Fountoulakis et al., 2025). For this reason, accurate estimation and forecasting of surface UV radiation and the UV Index (UVI) are critical for public health services, awareness campaigns, and early warning systems.

Surface UV radiation levels are controlled by several atmospheric and environmental parameters, including total ozone, clouds, aerosols, surface albedo, solar zenith angle, and altitude. Among these factors, aerosols represent one of the largest uncertainty sources in UV radiation modelling due to their strong temporal and spatial variability and their diverse optical and microphysical properties (Balis et al., 2004; Raptis et al., 2018). Absorbing aerosols such as mineral dust, smoke, and black carbon can significantly reduce surface UV irradiance, while highly scattering aerosols modify the diffuse-to-direct radiation ratio and the angular distribution of radiation. Accurate characterization of aerosol absorption properties is therefore essential for reliable UV simulations and radiative transfer calculations (e.g., Bais et al., 2005).

Spectral UV measurements can also be exploited to retrieve aerosol absorption properties and improve the representation of aerosol effects in UV modelling applications (Fountoulakis et al., 2019). The Mediterranean region and other aerosol-prone areas are frequently affected by desert dust outbreaks, biomass burning episodes, and urban pollution events, resulting in substantial and rapidly changing aerosol-related UV attenuation. Under such conditions, uncertainties in aerosol optical properties can lead to significant errors in UV simulations and UVI forecasts. In particular, incorrect assumptions regarding aerosol absorption properties and aerosol type may result in either overestimation or underestimation of biologically effective UV radiation (Raptis et al., 2018).

Radiative transfer models used for UV simulations require accurate atmospheric inputs in order to produce reliable UV estimates and forecasts. Ground-based spectral UV measurements and aerosol observations are therefore essential for the validation and improvement of these models (Kazadzis et al., 2001, Fountoulakis et al., 2025, Raptis et al., 2018). Operational UV forecasting systems currently combine radiative transfer modelling with satellite observations, atmospheric composition forecasts, and numerical weather prediction products. For example, services such as the CAMS provide global UV forecasts through the synergistic use of Earth observation products, chemistry transport modelling, and radiative transfer simulations. The overall workflow linking aerosol observations, aerosol optical characterization, radiative transfer modelling, and operational UV forecasting applications is summarized in Figure 8. However, aerosol and cloud uncertainties remain among the major sources of error in these operational systems, especially over polluted regions, mountainous terrain, coastal areas, and highly reflective surfaces (Fountoulakis et al., 2025).

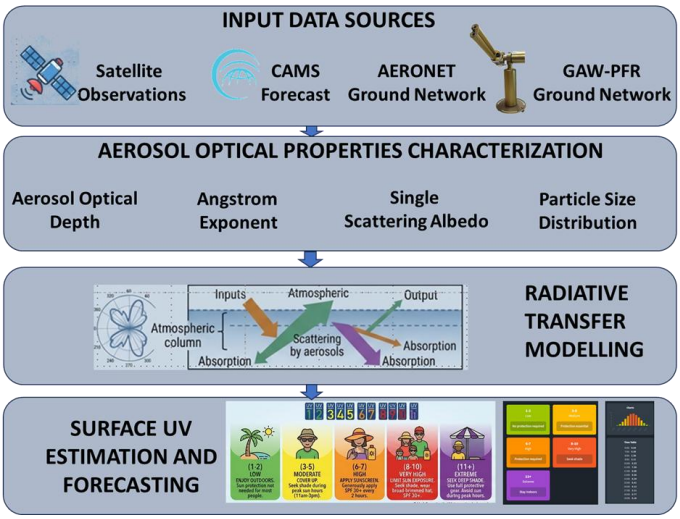


Figure 8. *Conceptual workflow illustrating the integration of satellite observations, aerosol monitoring networks, atmospheric composition forecasts, and radiative transfer modelling for surface UV irradiance and UVI estimation.*

Satellite-based UV products provide broad spatial coverage and are widely used for climatological and operational applications. Nevertheless, their accuracy is limited by factors such as the finite satellite pixel size, limited sensitivity to lower tropospheric aerosol layers, and uncertainties in the representation of aerosol-cloud-radiation interactions (e.g., Kazadzis et al., 2005). Ground-based monitoring networks therefore remain indispensable for validation and quality assurance purposes.

Ground-based radiometric observations provide high-quality aerosol optical properties that are particularly valuable for UV modelling applications. In addition, dedicated UV monitoring stations equipped with spectroradiometers and broadband radiometers provide highly accurate measurements of surface UV irradiance and UVI values. The high stability, traceability, and calibration standards of Precision Filter Radiometer (PFR) measurements make them especially suitable for long-term aerosol and UV climatology studies and for satellite validation activities. Recent results from the Cyprus Erythemal Irradiance Forecasting System (CERYFOS) further demonstrate the sensitivity of operational UV forecasts to aerosol uncertainties (Charalambous et al., 2026, preprint). In particular, underestimation of AOD resulted in systematic overestimation of UVI values, highlighting the critical importance of accurate aerosol characterization for reliable UV forecasting applications.

Near-real-time aerosol observations are particularly important for operational UV forecasting and warning systems. Timely information on aerosol loading and aerosol type can improve the representation of rapidly evolving events such as dust storms, wildfire smoke transport, and pollution episodes, which may otherwise lead to substantial forecast errors. Continuous operation of well-maintained ground-based UV and aerosol monitoring stations is therefore essential not only for public information and health protection, but also for the validation and improvement of satellite products, atmospheric composition models, and operational UV forecasting systems (Fountoulakis et al., 2025).

3.6. Aviation

AOD retrievals from ground-based instruments and satellite platforms play an important role in aviation hazard assessment and, more indirectly, in contrail-related studies, although their utility differs substantially between these applications.

3.6.1. Aviation hazard monitoring using aerosol optical properties

Ground-based and satellite AOD measurements support aviation hazard monitoring by providing information on atmospheric aerosol loading, which is essential for detecting and tracking volcanic ash plumes, wildfire smoke, and dust outbreaks that can affect aviation safety through reduced visibility, air quality degradation, and potential hazards to aircraft systems (Prata and Tupper, 2009; Clarisse et al., 2013). Among satellite products, the Moderate Resolution Imaging Spectroradiometer (MODIS) instruments onboard the Terra and Aqua satellites have historically been among the most widely used global aerosol datasets, providing near-daily global coverage with aerosol retrievals at spatial resolutions of approximately 10 km for standard products and 3 km for enhanced products (Levy et al., 2013). More recently, the Visible Infrared Imaging Radiometer Suite (VIIRS) onboard Suomi-NPP, NOAA-20, and

NOAA-21 has become a key operational sensor for aerosol monitoring, offering improved retrieval performance and near-global daily coverage with spatial resolutions ranging from approximately 750 m to 6 km depending on the product configuration (Jackson et al., 2013; Huang et al., 2016). While these satellite AOD products provide valuable information for aviation hazard monitoring, they remain limited by the lack of vertical resolution, since AOD represents a column-integrated quantity and does not provide direct information on aerosol altitude or layering.

Ground-based and active remote sensing observations complement satellite AOD products by providing vertically resolved aerosol information. Sun photometer networks such as AERONET deliver high-quality AOD measurements widely used for aerosol characterisation and satellite validation (Holben et al., 1998). In Europe, the E-PROFILE network integrates operational atmospheric profiling systems, including ceilometers and lidar instruments, to provide continuous monitoring of aerosol and boundary-layer structure (Haeffelin et al., 2016). Similarly, the European Aerosol Research Lidar Network (EARLINET) provides advanced aerosol profiling capabilities using coordinated high-performance lidar systems designed to retrieve aerosol vertical distributions, optical properties, and long-range transport patterns across Europe (Pappalardo et al., 2014). The vertical information from lidar systems is essential for aviation applications because it allows identification of aerosol layer height and structure, which cannot be inferred from column-integrated AOD alone. (Mona and Marenco, 2016) (Marenco and Hogan, 2011; Ansmann et al, 2011)

Spaceborne lidar observations extend these capabilities to global scales. The Cloud-Aerosol Lidar with Orthogonal Polarization (CALIOP) instrument onboard the CALIPSO satellite has provided global aerosol and cloud vertical profiling since 2006 (end of operations on 1 August 2023), enabling observation of aerosol layer heights, volcanic ash transport, smoke plumes, and dust outbreaks relevant to aviation safety (Winker et al., 2009). More recently, the EarthCARE mission introduces the Atmospheric Lidar (ATLID; commissioning phase in May 2024), a high-spectral-resolution lidar designed to improve aerosol and cloud vertical characterisation through enhanced sensitivity and improved aerosol typing capabilities (Illingworth et al., 2015, Donovan et al., 2024). Together, these spaceborne lidar observations provide critical global information on aerosol vertical structure that complements both satellite AOD retrievals and ground-based profiling networks.

For aviation decision-making, situational awareness requires not only column-integrated aerosol indicators such as AOD, but also information on near-surface conditions, vertical aerosol distribution, and particle type. Operational systems therefore combine surface meteorological observations (e.g., visibility and runway visual range measurements), numerical weather prediction products, and remote sensing data. Ground-based profiling networks (e.g., E-PROFILE and EARLINET) are particularly valuable in this context because they provide real-time information on aerosol layer height and boundary-layer structure, which directly determines whether aerosols impact flight levels or remain confined near the surface. Satellite AOD products (e.g., MODIS and VIIRS) provide regional-scale information on plume extent and evolution, while spaceborne lidars (e.g., CALIOP and ATLID) add global-scale vertical

structure information. Together, these complementary observing systems support integrated aviation situational awareness and decision-support systems for hazard mitigation (ICAO, 2005; WMO, 2018; Scherllin-Pirscher et al., 2025).

Beyond column-integrated AOD, emerging retrieval frameworks are increasingly addressing the lack of vertical aerosol information in passive satellite observations. In this context, the MAPIR (Mineral Aerosol Profiling from Infrared Radiances) algorithm provides vertically resolved aerosol concentration profiles derived from thermal infrared satellite radiances, enabling improved characterisation of aerosol vertical structure (Vandenbussche et al., 2026). Such approaches demonstrate the added value of moving beyond AOD-only products toward integrated datasets that combine aerosol optical depth with vertical concentration profiles, which is particularly relevant for applications requiring knowledge of aerosol layering in the upper troposphere and lower stratosphere.

Mineral dust represents a particularly important aviation hazard due to its strong impacts on visibility, flight safety, and aircraft integrity. Dust outbreaks can lead to hazardous reductions in visibility at airports and along flight routes, as well as increased turbulence, wind shear, and degraded operational safety during take-off and landing. In addition, dust particles can cause abrasion and corrosion of aircraft surfaces and contribute to engine degradation through ingestion and high-temperature melting processes, resulting in increased maintenance requirements and operational risk. Recent synthesis studies highlight that dust-related hazards have contributed to multiple aviation incidents and can significantly affect both short-term flight safety and long-term aircraft performance, particularly in regions influenced by major dust source areas and long-range transport pathways (Scherllin-Pirscher et al., 2025). These findings reinforce the need for dedicated dust monitoring and prediction capabilities integrated into aviation decision-support systems, combining satellite observations, ground-based measurements, and atmospheric modelling frameworks.

3.6.2. Contrail detection, aerosol properties, and radiative forcing assessment

Contrail detection and monitoring rely primarily on multi-spectral satellite radiometry from polar-orbiting and geostationary platforms. Key sensors include MODIS, VIIRS, and geostationary imagers such as ABI (GOES), AHI (HIMAWARI), SEVIRI (MSG) and recently FCI onboard MTG-I1. These instruments enable contrail identification through combined visible, near-infrared, and thermal infrared radiances, with thermal infrared window channels (10–12 μm) and brightness temperature difference techniques widely used to detect optically thin ice clouds. Visible reflectance channels provide additional sensitivity during daytime conditions. Geostationary observations are particularly valuable for contrail lifecycle analysis due to their high temporal resolution (5–15 min), allowing continuous monitoring of formation, spreading, and transition into contrail cirrus. Early developments in automated tracking, such as the algorithm of Vázquez-Navarro et al. (2010), demonstrated the feasibility of following contrail evolution in satellite imagery.

Recent progress is strongly driven by machine learning approaches, which improve robustness under complex atmospheric conditions such as cirrus contamination and variable illumination.

Deep learning models applied to GOES-16 ABI data and trained on the OpenContrails dataset have demonstrated strong performance in contrail segmentation and detection across different regions and viewing conditions (Ng et al., 2023; Ortiz et al., 2025). These approaches increasingly rely on multi-sensor radiance inputs and spatio-temporal learning strategies to improve generalisation across satellite platforms.

A complementary aspect of current detection workflows is the use of RGB composite imagery, particularly "aerosol" and "dust" RGB schemes, which enhance the contrast of thin ice clouds and improve visual discrimination of contrails from surrounding cirrus and aerosol structures. Although originally developed for aerosol and dust applications, these products are widely used in contrail analysis because they enhance subtle cloud features and support both qualitative interpretation and semi-automated detection. Combined with spectral methods and machine learning approaches, they form a hybrid framework integrating physical and data-driven information.

Quantification of contrail radiative forcing remains a central component of aviation climate impact assessment. Contrail radiative effects depend on optical properties such as optical depth, ice crystal effective radius, and cloud geometry, as well as solar geometry and background atmospheric conditions (Schumann, 2005). Satellite-based approaches have enabled regional-scale estimation of contrail radiative forcing using retrieved cloud properties combined with radiative transfer modelling. Ortiz et al. (2024) demonstrated satellite-based quantification of contrail radiative forcing over Europe using multi-spectral observations and aviation activity data, highlighting strong spatial and temporal variability in aviation-induced climate effects. In parallel, Dimitropoulou et al. (2026) proposed a rapid estimation approach for high-altitude ice cloud radiative forcing based on satellite observations, enabling efficient assessment of aviation climate impacts. Within broader climate assessments, Lee et al. (2021) and the IPCC Sixth Assessment Report (IPCC, 2021) discuss aviation climate forcing and the contribution of non-CO_2 effects, including contrail cirrus, while emphasising uncertainties in their quantification.

4. Gaps and Challenges

4.1. Geographic coverage gaps

Despite the remarkable expansion of ground-based radiometric networks over the past three decades, with AERONET alone growing from a handful of prototype stations in the mid-1990s to more than 700 active sites worldwide today, the spatial coverage of the global aerosol observing system remains strongly uneven. Station density is concentrated predominantly in populated continental areas of Europe, North America and East Asia, reflecting the historical alignment of network development with scientific and institutional capacity rather than with the geographic distribution of aerosol sources or the requirements of the applications discussed in the preceding sections. As a result, significant observational gaps persist over regions where aerosol variability is highest, where the impacts on climate, health and solar energy are most acute, and where the absence of ground-based reference data most severely limits the ability to

constrain satellite retrievals, validate transport models and support operational services. Three categories of region merit particular attention.

4.1.1. Polar regions

High-latitude environments present a distinctive combination of scientific importance and observational difficulty. The Arctic lower troposphere is subject to a distinctive seasonal phenomenon known as Arctic haze (Fig. 9): the accumulation, between late autumn and early spring, of long-range transported anthropogenic pollution, dominated by sulfate, black carbon, and nitrate, that builds up under stable atmospheric conditions and reduced wet scavenging during the polar winter (Schmale et al., 2021; Willis et al., 2018; Quinn et al., 2007). Scattering aerosol components reduce the amount of solar radiation reaching the surface, while absorbing particles enhance atmospheric heating within the haze layer. Although anthropogenic emission reductions in Europe and Russia since the 1990s have reduced background Arctic aerosol loading, wildfire contributions have increased during the past decade, introducing additional variability that remains insufficiently captured by current observing systems. This makes sustained, year-round aerosol optical depth monitoring in high-latitude environments particularly important.

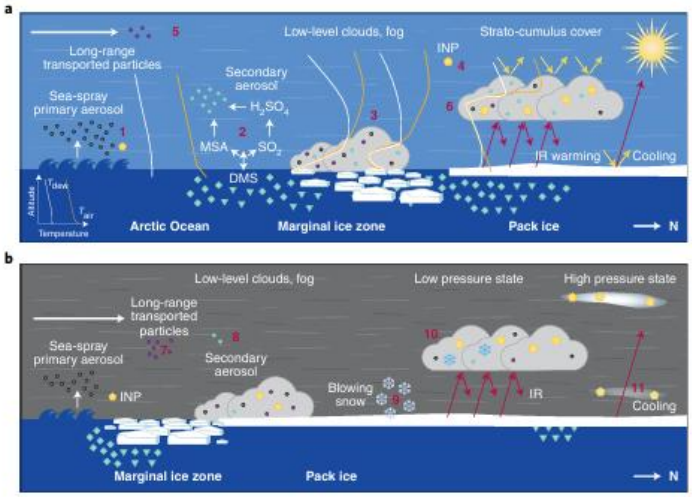


Figure 9. Aerosol processes during polar day and night. *a,b, Schematic showing aerosol processes of climate relevance in the Arctic for polar day (a) and night (b). DMS, dimethyl sulfide; MSA, methanesulfonic acid; CCI, cloud condensation nuclei; INP, ice nucleating particle; IR, infrared. Illustrative temperature profiles are shown as white (T_air, dewpoint temperature) and orange (T_air, air temperature) curves, representing different atmospheric states during polar day in a. Yellow arrows indicate short-wave radiation, and red arrows indicate long-wave radiation. Light-blue shapes in the ocean represent various species of marine microorganisms. Circles in atmosphere and clouds represent secondary aerosols formed from marine microorganisms. Yellow pentagons in atmosphere and clouds represent INPs (figure originally published in Schmale et al. 2021).*

The austral polar environment is comparably challenging, with episodic intrusions of mineral dust from Patagonia and Australia and biomass-burning smoke adding to a background of marine aerosol and sea salt (González et al., 2020; Pulimeno et al., 2026). In both polar regions, extended periods of low solar elevation, polar night, and severe weather limit the operational window of standard sun photometers and impose stringent requirements on instrument autonomy, power supply, and remote maintenance. The majority of aerosol observations have historically relied on daytime measurements, leaving a substantial gap during polar winter and night-time periods, particularly in the Arctic (Herber et al., 2002; Mazzola et al., 2012; Graßl and Ritter, 2019). Lunar and stellar photometry is beginning to address this limitation: the 20-year homogenised solar–stellar record at Ny-Ålesund demonstrates the feasibility of year-round continuous aerosol monitoring (Graßl et al., 2024). Extreme events also highlight the value of coordinated multi-instrument observations; for example, the 2019 Svalbard aerosol episode, involving wildfire smoke, volcanic emissions and anthropogenic pollution up to 16 km, was characterised through combined photometric, airborne and trajectory observations (Herrero-Anta et al., 2026).

The Polar-AOD programme has made important progress in consolidating long-term aerosol optical depth measurements from Arctic and Antarctic stations (Pulimeno et al., 2026). Multi-decadal records reveal a statistically significant decrease in background Arctic aerosol loading associated with emission reductions in Europe and Russia, while episodic wildfire contributions have increased markedly during the past decade. Nevertheless, characterisation of aerosol variability across the full annual cycle remains uneven, particularly during polar winter and night-time periods. The extension of photometric measurements through lunar and stellar observations offers an important route towards closing this gap and establishing continuous, long-term records across the polar annual cycle (Graßl et al., 2024).

High latitudes and Polar Regions also contain important mineral-dust sources, accounting for at least 5% of the global atmospheric dust budget and covering more than 1.6 million km² across both hemispheres (UNCCD, 2022; Meinander et al., 2022). High-latitude dust can travel thousands of kilometres within the Arctic and towards Europe, while Saharan, Middle Eastern and Aral–Caspian dust can also reach the Arctic and northern Europe (Groot Zwaaftink et al., 2016; Moroni et al., 2018, 2024; Varga et al., 2021, 2023). Monitoring remains sparse and is strongly constrained by harsh conditions and limited solar illumination; vertical aerosol profiling is also limited, despite evidence of high-latitude dust reaching several kilometres altitude during polar-vortex conditions. Satellite observations provide useful complementary information, but AOD products are currently less reliable for high-latitude dust sources, highlighting the need for additional ground-based and profiling observations.

High-latitude dust storms can be frequent and intense, particularly in Iceland, where up to 135 dust days per year have been reported and PM10 concentrations can exceed 1,000 μg m^{-3}, with much higher values at dust hotspots (Dagsson-Waldhauserova et al., 2014; Meinander et al., 2022). These events represent important natural hazards, impair air quality and visibility, and disrupt transportation and vulnerable ecosystems. The sparse observational network limits the

assessment of their environmental and health impacts and constrains reliable monitoring of their spatial and vertical evolution.

The most pronounced climate changes are occurring at high latitudes, where high-latitude dust (HLD) is an important climate driver (IPCC, 2019; AMAP, 2021). HLD deposited on snow and glaciers reduces albedo and accelerates melting, while airborne dust affects atmospheric radiation and cloud microphysics (Meinander et al., 2022; Baldo et al., 2023; Di Biagio et al., 2026). Its indirect radiative forcing through cloud interactions is also important, as HLD can act as an efficient ice-nucleating particle in mid- and high-latitude mixed-phase clouds (Sanchez-Marroquin et al., 2020). Instantaneous radiative forcing of HLD in the Arctic has been estimated at 0.09 W m^{-2} at the top of the atmosphere, with an additional 0.07 W m^{-2} associated with HLD deposited on snow (Kylling et al., 2018). Icelandic dust is also substantially more absorbing in the near-infrared than African and Asian dust (Baldo et al., 2023), underlining the need for accurate measurements of aerosol optical properties and their vertical distribution.

Frequent dust storms at high latitudes impair air quality, reduce visibility, disrupt transportation, and disturb vulnerable ecosystems (Meinander et al., 2022). In Iceland, severe dust storms have been associated with road-safety incidents, including fatalities (Jenssen et al., 2019), while increased emergency hospital visits have been reported in Reykjavík in association with dust storms and other particle sources (Carlsen et al., 2015). The scarcity of observations therefore limits not only understanding of the climate effects of high-latitude dust, but also the assessment of its environmental, health and societal impacts.

4.1.2. Maritime, remote and resource-limited environments

Open-ocean environments represent perhaps the most persistent gap in the global aerosol observing system. Marine aerosol observations are important for ocean-colour atmospheric correction, for the characterisation of marine boundary-layer aerosol and its interaction with clouds, for the validation of satellite retrievals over ocean surfaces, and for understanding aerosol deposition to marine ecosystems. The Marine Aerosol Network (MAN) (Smirnov et al., 2009), operating hand-held sun photometers aboard volunteer observing ships, has provided valuable data over many ocean basins, but its measurements are logistically constrained to daytime, fair-weather conditions and are not continuous. More recently, the adaptation of a standard CIMEL sun photometer to operate aboard the French research vessel Marion Dufresne using an automated motion-compensation system demonstrated that AERONET-compatible, continuous aerosol observations can be maintained over the open ocean for multi-year periods, substantially expanding the available marine aerosol climatology and providing reference data for satellite validation over the Indian Ocean (Torres et al., 2025). Synergistic shipborne observations combining photometry and micro-pulse lidar further demonstrated the value of profiling the vertical aerosol structure in marine environments, where clean background conditions are frequently interrupted by transported aerosol plumes from distant continental sources (Sánchez-Barrero et al., 2026).

4.1.3. Desert and arid regions

North Africa and the Middle East are the most active dust source regions on Earth and represent a major source of uncertainty in both climate forcing estimates and operational aerosol forecasting (Kok et al., 2021; Moustaka et al., 2026). Despite their importance, the density of ground-based radiometric observations across these source regions remains markedly insufficient. Importantly, this observational gap has deteriorated over time rather than improved. The scarcity of observations over desert and arid regions is particularly problematic because it forces satellite retrieval algorithms and atmospheric transport models to rely on poorly constrained assumptions about aerosol properties, particle size distributions, and spectral behaviour precisely in the environments where these properties are most variable and where retrieval conditions are most challenging due to bright desert surfaces.

Recent efforts to address this gap through the coordinated use of satellite products have demonstrated both the potential and the limitations of space-based approaches in the absence of adequate ground-based reference data. An analysis of twelve years of A-Train satellite observations over North Africa and the Middle East revealed strong spatial and seasonal gradients in dust lidar ratio and aerosol radiative properties that are not reproduced by current observing network configurations, with lidar ratio estimates differing by up to 30–40% between sub-regions, translating into corresponding uncertainties in aerosol optical depth retrievals and radiative effect estimates (Moustaka et al., 2026). The study explicitly identified the absence of distributed ground-based measurements as the primary limitation preventing validation of these satellite-derived gradients. Complementary field observations from the A-LIFE campaign, which targeted Saharan and Arabian dust events over the eastern Mediterranean, further illustrated that aerosol optical properties of dust from different source regions differ substantially and that accurate aerosol characterisation in regions relevant for both climate modelling and solar energy applications requires site-specific long-term observations rather than regionalised climatologies alone (Mateos et al., 2026). Expanding ground-based coverage in desert and arid regions also has direct implications for solar energy resource assessment, since high solar irradiance potential and elevated, variable aerosol loading coexist precisely in regions where the current photometer network is weakest. Under such conditions, the uncertainty in aerosol optical depth alone can translate into direct normal irradiance uncertainties well in excess of 15–20% (Moustaka et al., 2026), rendering reliable long-term solar resource assessment difficult without dedicated local observing infrastructure.

Chen et al. (2026) revealed a structural bias in the global aerosol validation framework that has gone largely unrecognised. Although AERONET grew from 284 to 497 active sites between 2008 and 2018, this expansion was heavily skewed toward vegetated and urban regions: the fraction of observations from desert and bare soil surfaces (NDVI ≤ 0.2) actually declined from 25.9% to 23.9%, even though satellite data show that more than 45% of global aerosol retrievals originate from these same dryland areas. The apparent improvement in satellite–AERONET agreement over this period is therefore largely a statistical artefact: when stratified by surface type, MODIS performance over drylands remained consistently poor (RMSE > 0.16; GCOS

fulfillment < 33%), compared with RMSE < 0.13 and GCOS fulfillment > 45% over vegetated surfaces. Nearly half of all global grid cells with elevated disagreement between MODIS and POLDER AOD products are located in drylands, where the mean TOA aerosol radiative cooling is weaker by 0.24 W m^{-2} and its uncertainty 22% higher than elsewhere — with direct consequences for global aerosol radiative forcing estimates. These authors explicitly identify sites in the Negev Desert, the Arabian Peninsula, the central Sahara, and the Sahel — represented by AERONET stations SEDE_BOKER, Mezaira, Tamanrasset_INM, and Banizoumbou — as priority locations for future ground-based validation efforts (Fig. 10).

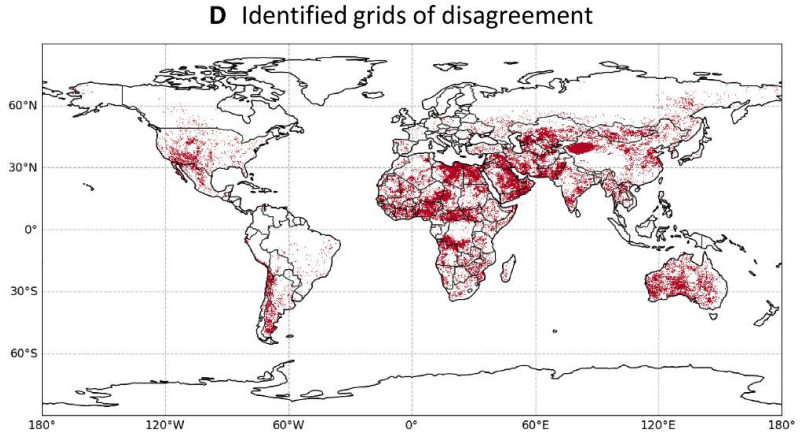


Figure 10. *Spatial patterns of agreement between MODIS and POLDER AOD retrievals in 2008 and identification of regions of disagreement. [Extracted from Chen 2026]*

These findings underscore that the need for expanded and sustained ground-based observations over remote, arid regions is not merely a question of spatial completeness: without a more geographically stratified observing strategy, global validation metrics will continue to overstate the skill of satellite aerosol retrievals in precisely the environments where aerosol–climate interactions are most uncertain and where solar energy potential is highest.

Beyond polar, desert and maritime regions, a broader category of observational gaps exists in areas where the cost and complexity of deploying and maintaining reference-grade instrumentation exceeds national or regional technical capacity. Large parts of Sub-Saharan Africa, Central Asia, tropical South America and many island environments remain without sustained ground-based aerosol observations, despite their importance for global aerosol budgets and for regional applications in health, agriculture and solar energy. Addressing these gaps requires not only the development of simpler and more autonomous observing platforms, but also investment in regional training, calibration infrastructure and data-sharing arrangements that allow locally acquired observations to be harmonised with international network standards. The deployment of low-cost or simplified instruments validated against reference-grade systems represents one pathway toward filling these geographic gaps, provided that their observational characteristics and uncertainty budgets are rigorously characterised and transparently documented.

4.2. Solar radiation and solar energy

Important limitations remain regarding the current capabilities for solar energy applications. Existing ground-based networks remain too sparse to fully characterize aerosol variability near major solar-energy facilities, particularly in regions affected by complex terrain, coastal gradients, urban pollution, and rapidly evolving wildfire smoke. Forecast models continue to experience difficulties in accurately predicting the timing, intensity, vertical distribution, and optical characteristics of mineral dust and biomass-burning aerosols. Furthermore, operational forecast systems generally provide limited information on aerosol absorption properties, spectral variability, and vertical structure, despite growing evidence that these parameters influence high-accuracy radiative transfer simulations and advanced solar energy modelling.

Future improvements are therefore expected to rely on tighter integration of ground-based radiometric observations, satellite retrievals, lidar observations, and next-generation atmospheric composition forecasting systems. Emerging observing capabilities, including missions such as EarthCARE, together with improved aerosol data assimilation into global and regional forecasting systems, are expected to substantially reduce uncertainties in aerosol radiative effects and improve operational solar-energy forecasting over the coming decade.

The main gaps and requirements for solar-radiation and solar-energy applications can be summarized as follows:

- **High temporal resolution:** aerosol observations should resolve the rapid variability associated with dust fronts, pollution plumes, wildfire smoke and other evolving aerosol events. Sampling of ~1 s may be required for process studies, while ~5–15 min is appropriate for operational nowcasting and 1–3 h for forecasts. Hourly observations are generally sufficient for climatological applications (Gueymard, 2012; Papachristopoulou et al., 2024; Teri et al., 2025).

- **Accurate and spectrally resolved aerosol properties:** high-accuracy RT simulations require not only AOD but also SSA and information on the aerosol phase function, particularly for accurately representing direct and diffuse irradiance. Accurate modeling of the different irradiance components (DNI and DHI) is critical. Aerosol uncertainties have a larger impact on DNI and DHI than on GHI (e.g., Kouklaki et al., 2026). Measurements in the UV-B and NIR spectral regions are currently less frequent and less accurate than for wavelengths between 340 and 1200 nm. Spectrally resolved AOD and SSA are required for solar-energy applications, with measurements extending beyond ~1200 nm being particularly relevant for CSP (Belluardo et al., 2016; Raptis et al., 2018; Fountoulakis et al., 2019; Witthuhn et al., 2021; Ruiz-Arias et al., 2018; Hanrieder et al., 2017; Kouklaki et al., 2023, 2026).

- **Improved aerosol typing and event characterization:** operational products should better distinguish mineral dust, biomass-burning smoke, pollution, marine aerosol and mixed aerosol conditions, particularly during rapidly evolving events, when fixed or

climatological aerosol properties may not adequately represent atmospheric conditions (Kahn et al., 2023; Elsey et al., 2024; Ruiz-Arias et al., 2015; Gueymard, 2012).

- **Improved spatial coverage:** observations should be expanded around solar-energy facilities and in arid regions, complex terrain, coastal areas and polluted environments. Spatial scales of ~5–10 km may be required in urban/industrial areas, compared with ~20–50 km in relatively homogeneous desert regions (Teri et al., 2025; Papadimitriou et al., 2026; Chen et al., 2026). Using reliable low-cost sensors can contribute towards this direction.

- **Co-located aerosol and radiation measurements:** aerosol observations should be combined with broadband and spectral solar irradiance measurements and, where possible, solar-power production data, enabling direct assessment of aerosol impacts and validation of solar irradiance estimates and forecasting systems (Papadimitriou et al., 2026).

- **Improved aerosol forecasting:** dynamic aerosol forecasts from CAMS and GEOS-5 should be further improved, particularly for mineral dust and biomass-burning events. Although forecast products generally outperform climatological assumptions, uncertainties in emissions, transport, deposition, vertical distribution and optical properties remain important, and persistence can still outperform dynamic forecasts during some intense dust episodes (Flemming et al., 2017; Molod et al., 2015; Eskes et al., 2024; Hou et al., 2025; Yoon et al., 2026).

- **Better uncertainty characterization:** uncertainties in aerosol observations and forecasts should be explicitly quantified and propagated into irradiance and solar-power predictions, particularly for DNI and DHI, where aerosol errors have a stronger influence on the resulting solar radiation estimates (Roman et al., 2014a,b; Belluardo et al., 2016; Hou et al., 2025; Moustaka et al., 2026).

- **Integrated observing and modelling systems:** future developments should combine ground-based radiometry, satellite retrievals, lidar and atmospheric composition forecasting/data assimilation to provide continuous, spatially representative and spectrally resolved aerosol information (Kahn et al., 2023; Elsey et al., 2024).

Overall, the key challenge is no longer simply the availability of aerosol observations, but their integration into an observation–modelling–forecasting framework capable of representing the rapidly changing, spectrally dependent, and spatially heterogeneous aerosol conditions that affect surface solar radiation and solar-energy production. This is particularly important for solar-energy applications, especially in regions frequently affected by mineral dust, biomass burning, and severe pollution.

4.3. Atmospheric Modelling and Data Assimilation

Although substantial progress has been achieved over the past two decades in observing atmospheric aerosols and integrating radiometric measurements into atmospheric composition monitoring, operational forecasting and climate services, important observational gaps remain. Addressing observational challenges will be essential for the next generation of atmospheric composition and climate services (IPCC, 2021; Benedetti et al., 2018; Kahn et al., 2023).

AOD alone provides limited information on aerosol composition, vertical distribution, particle size and absorption, while reliable observations of SSA, refractive index, coarse-mode particles, aerosol layer height and aerosol speciation remain comparatively sparse. These limitations constrain atmospheric composition models and operational forecasting (Benedetti et al., 2018; Kahn et al., 2023; IPCC, 2021). Multi-decadal observations of AOD, AE, VSD and absorption properties that are currently limited, also provide the basis for detecting trends associated with anthropogenic emissions, natural variability and air-quality policies, while supporting the generation of climate-quality aerosol data records (GCOS, 2022; Giles et al., 2019; IPCC, 2021). These limitations contribute to uncertainties in aerosol radiative effects, aerosol–cloud interactions and deposition processes, particularly during dust outbreaks, biomass-burning episodes and other extreme events (Inness et al., 2019; Kahn et al., 2023; IPCC, 2021). Improved observations of coarse, super-coarse and giant particles, together with vertically resolved aerosol profiles from ground-based and spaceborne lidars, are needed to reduce persistent uncertainties in dust transport, deposition, atmospheric lifetime and radiative effects that remain inadequately represented in many atmospheric and climate models (Winker et al., 2009; Ryder et al., 2019; Adebiyi and Kok, 2020; Kok et al., 2021; Fountoulakis et al., 2024; Masoom et al., 2023; Gidarakou et al., 2026).

One more key issue remains the quantification of aerosols in the traditional sense (mass concentrations) from remote sensing. The mass-extinction ratio, required for evaluating concentration from optical measurements, depends on the aerosol properties and amongst those the particle effective radius is one of the most decisive ones (Papetta et al, 2026).

The growing use of ML introduces additional observational requirements. Artificial intelligence is increasingly applied to aerosol retrieval, data fusion, uncertainty estimation, forecasting and the generation of climate-quality aerosol products, but its performance depends fundamentally on the availability of long-term, representative and accurately calibrated observations. Expanding monitoring capacity in under-sampled regions, harmonizing quality-assurance procedures and providing comprehensive uncertainty estimates will be essential for developing robust hybrid physics–machine learning systems capable of generalizing across diverse aerosol regimes and extreme events. Furthermore, most current ML applications focus primarily on AOD, whereas comparatively few exploit additional aerosol properties such as SSA, refractive index, particle size distribution or vertically resolved observations. Expanding radiometric measurements and integrating them with lidar, polarimetric observations and in situ data will be essential for developing robust hybrid physics-informed ML systems capable of supporting atmospheric composition monitoring, operational forecasting and climate services (Benedetti et al., 2018; Reichstein et al., 2019; Kahn et al., 2023).

Summarizing, future progress will thus increasingly rely on integrated multi-sensor observing systems that will provide complementary constraints on aerosol loading, absorption, composition, particle size and vertical distribution, supporting improved aerosol reanalyses, Earth system models and climate services (Winker et al., 2009; Dubovik et al., 2019; Xu et al., 2021; Papetta et al., 2026; Kahn et al., 2023).

4.4. Satellite Validation

Despite substantial progress in the validation of satellite aerosol products, important gaps remain in the ability of current reference observations to fully characterize their accuracy, representativeness and long-term consistency. These challenges are becoming increasingly important as satellite missions provide increasingly detailed information on aerosol size, type, optical properties and vertical distribution.

Representativeness of satellite–ground comparisons: A fundamental limitation arises from the different spatial and temporal sampling of satellite and ground-based observations. Aerosol properties can vary strongly in both space and time, whereas ground-based measurements are essentially point observations and satellite retrievals represent an area corresponding to the satellite pixel. Consequently, satellite–ground collocation can introduce substantial representativeness and matchup errors. Multiple reference observations per day are required to accommodate different satellite overpasses and capture diurnal variability, while year-round observations are necessary to represent seasonal aerosol cycles. Long, continuous and internally consistent time series are additionally required to assess the long-term consistency, stability and trends of satellite products.

For visible satellite observations, **AOD** remains the most directly comparable parameter with ground-based sun- and moon-photometry and therefore the most mature basis for validation. Established networks such as AERONET and SKYNET provide the main continental reference observations, while the Marine Aerosol Network extends measurements to oceanic environments (Holben et al., 1998; Takamura et al., 2004; Smirnov et al., 2009, 2011; Giles et al., 2019; Nakajima et al., 2020; Sinyuk et al., 2020). Nevertheless, the spatial distribution of these observations remains uneven, limiting the representativeness of validation datasets, particularly for specific aerosol regimes and challenging surface conditions.

Validation beyond total AOD: The validation of total-column AOD is substantially more mature than that of aerosol properties describing particle size, type and optical characteristics. Existing studies indicate generally satisfactory performance for aerosol loading but poorer performance for properties such as the AE, fine-mode fraction, SSA and asymmetry parameter (Levy et al., 2010; Sayer et al., 2013, 2018; Schutgens et al., 2013; Si et al., 2017; Mok et al., 2018; Jethva and Torres, 2019; Chen et al., 2020, 2024; Sogacheva et al., 2022; Fu et al., 2025; Litvinov et al., 2025; Ma et al., 2026).

The development of advanced retrieval approaches, including GRASP-based products from POLDER/PARASOL, Sentinel-3/OLCI, Sentinel-5P/TROPOMI, OMI and Himawari-8, further increases the need for comprehensive reference observations capable of evaluating multiple aerosol properties simultaneously (Ahn et al., 2014; Dubovik et al., 2014, 2021; Li et

al., 2019, 2025; Chen et al., 2020, 2022, 2024; Schutgens et al., 2021; Litvinov et al., 2024). The relatively limited number of independent validation studies based on SKYNET also indicates the need to broaden the observational basis beyond AERONET (Tang et al., 2023; Cao et al., 2023).

Aerosol-type-specific validation: A particularly important gap concerns the validation of aerosol-type-specific products. Reliable validation of individual aerosol types requires complementary measurements (in addition to AOD) capable of identifying periods when the aerosol type of interest dominates the atmospheric column (Shin et al., 2019). For mineral dust, existing approaches combine coarse-mode AOD, Ångström exponent and SSA to identify dust-dominated conditions (Klüser et al., 2011; Capelle et al., 2018; Groß et al., 2016; Gkikas et al., 2021, 2022). These studies demonstrate the potential of multi-parameter ground observations to support validation beyond conventional total-AOD comparisons.

A particular challenge is that coarse-mode AOD can include contributions from **marine and volcanic aerosols**, making it an imperfect reference for satellite dust products. This is especially relevant for thermal-infrared (TIR) satellite observations, such as IASI, which provide dust-related parameters including TIR AOD, mean altitude, effective radius and low-resolution vertical profiles (Capelle et al., 2018; Clarisse et al., 2019; Vandenbussche et al., 2026). There are currently no directly observed ground-based reference measurements in the TIR for these retrievals, and validation consequently relies on indirect comparisons with sun- and moon-photometer observations. At minimum, coarse-mode AOD is required, but the development of methods capable of retrieving **dust-only coarse AOD**, excluding marine and volcanic contributions, would provide a substantially more robust reference for satellite dust validation.

Spatial and environmental coverage: As discussed in Sect. 4.1, current reference networks remain unevenly distributed across aerosol environments and surface types. Further observations are needed over **under-sampled and challenging environments**, including bright deserts, high latitudes, coastal transition zones and the open ocean (Moustaka et al., 2026; Herrero-Anta et al., 2026). Joint evaluation of satellite retrievals has demonstrated the value of geographically distributed reference observations for identifying differences between products (Kokhanovsky et al., 2007; Kahn et al., 2007; Bibi et al., 2015; Xiao et al., 2016; de Leeuw et al., 2018; Wang et al., 2020; Su et al., 2021; Chen et al., 2022; Osgouei et al., 2022), but such intercomparisons remain constrained by the availability of representative reference data.

Maritime observations are particularly important because continental networks cannot adequately characterize aerosol conditions over the ocean. MAN has substantially expanded this capability (Smirnov et al., 2009, 2011; Sayer et al., 2012; Schutgens et al., 2013; Shen et al., 2018; Pei et al., 2023; Pearson et al., 2025). Recent efforts to adapt standard CIMEL systems to shipborne applications demonstrate further potential (García et al., 2025; Torres et al., 2025; Sánchez-Barrero et al., 2026), but standardized systems with improved resistance to salt, vibration and platform motion are still required.

Requirements for next-generation satellite observations: The increasing use of geostationary, multi-angle, polarimetric and hyperspectral satellite observations will require corresponding advances in ground-based validation. Higher temporal sampling is needed to support geostationary and multi-angle missions and to characterize rapidly changing aerosol conditions (Karanikolas et al., 2025). Polarimetric and hyperspectral ground systems can provide additional constraints for validating advanced retrieval algorithms, while co-located all-sky imagers and cloud sensors can improve cloud screening and reduce satellite–ground mismatch errors (Herrero del Barrio et al., 2026).

Operationalization, uncertainty and interoperability: A further gap concerns the transition from individual research-based validation studies towards systematic operational calibration and validation. Automated satellite–ground matchup services should incorporate explicit measures of spatial and temporal representativeness and collocation mismatch uncertainty, while standardized uncertainty budgets should account for both reference-measurement and satellite-retrieval uncertainties (Ichoku et al., 2002; Virtanen et al., 2018; Sayer, 2020). Near-real-time quality-controlled outputs are required to support operational validation, complemented by consistent delayed-mode products for scientific analyses and long-term assessment. Operational validation frameworks already demonstrate the value of standardized spatial and temporal matching, quality screening and expected-error criteria (NASA MODIS/VIIRS validation frameworks). Improved cloud/aerosol discrimination and interoperable data services and APIs would further facilitate the integration of reference observations into satellite cal/val systems and mission processing chains.

4.5. Health applications

One of the main challenges for health applications is to translate these column-integrated observations into quantities that are directly relevant to human exposure (Chu et al., 2016; Lolli, 2025). The relationship between columnar aerosol properties and surface PM is highly dependent on planetary boundary layer height (PBLH), relative humidity, aerosol size and composition, and the vertical distribution of aerosol layers. Elevated dust or smoke plumes may produce substantial AOD while remaining partly decoupled from surface concentrations, whereas aerosol layers that mix down into the boundary layer can rapidly increase population exposure. Recent observations highlight the importance of aerosol layering in interpreting the AOD–PM relationship (Rogozovsky et al., 2026). Consequently, AOD should not be regarded as a direct substitute for surface PM measurements; rather, it should be combined with surface observations, meteorological information, vertical-profile measurements and atmospheric models.

Vertical information is particularly important during dust and biomass-burning episodes. Ground-based and spaceborne lidar observations can complement sun-photometer measurements by providing information on the altitude, thickness and vertical structure of aerosol layers, while atmospheric composition models can describe their transport and evolution. The combination of columnar AOD, vertically resolved observations and surface PM measurements can therefore provide a much better basis for assessing whether an observed aerosol event is likely to contribute to population exposure. This is also important for evaluating

and improving dust and smoke forecasts, for which radiometric observations can constrain aerosol loading, transport and model uncertainties (Pérez et al., 2006; Rubin et al., 2017; Wang et al., 2014; Di Tomaso et al., 2022; Yang et al., 2023).

A second major challenge is the limited chemical and biological specificity of aerosol optical properties. AOD, AE, SSA and particle-size distributions provide valuable information on aerosol loading, size and optical characteristics, but they do not uniquely determine aerosol composition or source. This is particularly relevant for health applications because mineral dust, combustion aerosols, urban pollution and biological particles can have different health effects while exhibiting partly overlapping optical characteristics. The limitation is especially important for bioaerosols: although pollen and other biological particles can influence aerosol optical properties, radiometric observations alone cannot currently provide reliable quantitative estimates of biological aerosol concentrations (Noh et al., 2013). For bioaerosols, radiometric measurements therefore need to be considered as part of a broader observational framework. Biological sampling, fluorescence-based techniques, molecular measurements and atmospheric transport modelling can provide the additional information needed to identify biological components and their sources (Sofiev et al., 2022; Vélez-Pereira et al., 2022). A major research need is consequently the development of better-validated methods for linking optical observations with source-specific and biologically relevant exposure metrics. Information on aerosol source and composition could improve exposure assessment by distinguishing aerosol events with different potential health implications. For bioaerosols, however, this transition will require dedicated biological measurements and validation datasets because current optical observations lack sufficient specificity (Noh et al., 2013; Sofiev et al., 2022).

One more important challenge is to translate improved observations into operational health services and early-warning systems. Near-real-time aerosol observations can improve the representation of rapidly evolving dust, smoke and pollution events in atmospheric models and can contribute to more timely exposure information. The same aerosol characterization is also relevant to UV-related health applications, since aerosol optical properties influence the amount and spectral distribution of solar UV radiation reaching the surface. Recent work on operational UV forecasting has shown that errors in aerosol optical depth can propagate into systematic errors in predicted UV Index values (e.g., Charalampous et al., 2025). Integrating aerosol observations, atmospheric composition forecasts and radiative-transfer modelling can therefore support both particulate-exposure and UV-exposure assessments.

A particularly important observational gap concerns the lack of systematic, long-term measurements of aerosol optical properties in the UV, and especially of SSA and AOD at UVB wavelengths. Most operational aerosol networks provide robust and well-established measurements in the visible and near-infrared spectral ranges, whereas spectrally resolved measurements of aerosol absorption and SSA in the UV remain comparatively sparse (e.g., Mok et al., 2018). AOD measurements at wavelength shorter than 320 nm are also sparse (e.g., Doppler et al., 2026; Carvalho and Henriques, 2000; Gröbner et al., 2001; Marenco, 2002; Kazadzis et al., 2005; Fountoulakis et al., 2016; Hrabčák, 2018, 2025), and usually highly uncertain (e.g., Lopez-Solano et al., 2018). Uncertainties in UV aerosol optical properties, and

particularly in SSA, can propagate directly into estimates and forecasts of biologically effective UV radiation and the UV Index. Systematic measurements of UV aerosol optical properties, supported by traceable calibration and standardized retrieval methods, are therefore needed to reduce this uncertainty and improve the representation of aerosols in health-oriented radiative-transfer models.

4.6. Aviation

For aviation applications, requirements for vertically resolved aerosol products are generally more critical than those based solely on column-integrated measurements.

A key challenge for aviation hazard monitoring is the limited ability of current passive satellite aerosol products to provide vertically resolved information on aerosol type, altitude, and aviation relevance, compounded by the sparse global coverage of aerosol profiling observations and the need for stronger integration with operational forecasting and decision-support systems. Addressing these gaps will require combining passive satellite observations with ground-based and spaceborne lidar measurements, expanding operational aerosol profiling capabilities (e.g., EarthCARE/ATLID and E-PROFILE), developing vertically resolved aerosol products and data assimilation frameworks, and enhancing dedicated monitoring of dust, smoke, and volcanic ash hazards for aviation operations.

Regarding the assessment of contrails radiative forcing, the state of the art is moving toward integrated contrail detection and radiative assessment frameworks that combine multi-spectral observations and advanced retrieval techniques. Geostationary imagers enable high-frequency monitoring of contrail evolution, while polar-orbiting sensors provide global consistency and calibration continuity. Machine learning approaches increasingly enhance detection robustness and scalability across heterogeneous datasets. These observational systems rely not only on satellite-derived cloud properties but also on aerosol optical properties retrieved from radiometric satellite sensors, which provide essential background information for radiative transfer modelling and atmospheric state characterisation. They are increasingly coupled with radiative transfer modelling, which builds on established satellite-derived cloud property retrieval frameworks (Stubenrauch et al., 2010), to produce consistent estimates of contrail occurrence and radiative forcing, supporting improved quantification of aviation-induced climate effects.

A major challenge in assessing contrail-related aviation climate impacts is the large uncertainty in contrail occurrence, persistence, and radiative forcing, driven in part by limited observations of ice-supersaturated regions (ISSRs), difficulties in distinguishing contrails from natural cirrus clouds, and the absence of harmonised operational frameworks linking observations, atmospheric models, and aviation activity data. Progress will require integrating geostationary and polar-orbiting satellite observations with machine-learning detection techniques, improving monitoring and forecasting of ISSRs and upper-tropospheric conditions, coupling observations (with improved characterisation of the atmospheric background properties) with radiative transfer and contrail evolution models, and developing operational observation-based systems to support monitoring, reporting, and verification of aviation non-CO_2 climate impacts.

4.7. Other emerging needs

Agriculture, terrestrial ecosystems and the ocean are affected by aerosols through several interconnected pathways, including changes in surface radiation, modification of the direct-to-diffuse radiation ratio, aerosol deposition to vegetation and soil, and deposition of mineral dust and associated nutrients to the ocean. These processes operate over a wide range of spatial and temporal scales and remain subject to substantial observational and modelling uncertainties. An important emerging opportunity is therefore to use radiometric observations not only to characterize aerosols themselves, but also to provide constraints for models describing their environmental impacts.

4.7.1. Agriculture and terrestrial ecosystems

Aerosol-induced changes in surface radiation are particularly relevant for vegetation. Scattering aerosols can reduce direct irradiance while increasing the diffuse component, potentially enhancing the penetration of radiation into plant canopies and modifying photosynthesis and light-use efficiency (Gu et al., 2002; Cohan et al., 2002; Mercado et al., 2009). The response is not necessarily proportional to the reduction in total irradiance, since the magnitude and even the sign of the ecosystem response depend on aerosol loading, optical properties, canopy structure and meteorological conditions. Aerosol-induced cooling and changes in atmospheric moisture can further modify photosynthesis and evapotranspiration (Zhou et al., 2021).

These effects create a direct need for aerosol observations. Information on AOD, aerosol absorption and spectral properties is required to “feed” crop-growth and ecosystem models and to estimate accurately the modification of photosynthetically active radiation and its partitioning between direct and diffuse components. Observations of diffuse radiation are particularly important because changes in the diffuse fraction can alter canopy-level light-use efficiency. Recent modelling studies have demonstrated that improved estimates of diffuse radiation can substantially improve simulations of gross primary productivity, illustrating the value of observational constraints on radiation fields for ecosystem models (Zhou et al., 2021).

4.7.2. Aerosol deposition to vegetation and soil

A second, comparatively less developed application concerns the deposition of atmospheric particles onto vegetation and soil. Dry deposition depends on aerosol particle size and density, atmospheric stability and turbulence, and the structure and collecting properties of the vegetation (Pryor et al., 2008; Petroff et al., 2008). Existing measurements and modelling studies show substantial variability in deposition velocities and indicate that differences between models are strongly related to the representation of particle collection within the canopy (Petroff et al., 2008a,b; Hicks et al., 2016).

Radiometric observations cannot directly measure deposition flux, but they can provide important constraints on several of the variables controlling deposition. Spectral AOD and aerosol absorption measurements can provide information on aerosol loading and type, while measurements of particle size, lidar observations and meteorological measurements can provide complementary information on aerosol size, vertical distribution and atmospheric transport. When combined with deposition models, these observations could help improve

estimates of deposition velocity and flux, particularly during episodes dominated by coarse mineral dust or biomass-burning aerosol (e.g., Grönholm et al., 2009).

The ecological relevance of this process extends beyond particle removal from the atmosphere. Aerosol deposition represents an important pathway for the transfer of nutrients, acidifying compounds and potentially toxic substances to terrestrial ecosystems (Mahowald et al., 2008; Jickells et al., 2016; Kanakidou et al., 2012). Mineral dust, in particular, can modify nutrient availability and interact with plant physiological processes (Burkhardt, 2010; Lokshin et al., 2026). Consequently, the atmospheric aerosol burden, its optical properties and its deposition flux should not be considered as independent quantities. Connecting radiometric observations with deposition and ecosystem models could provide a more physically consistent description of the sequence from aerosol transport to surface deposition and ecosystem response.

4.7.3. Aerosol deposition to the ocean

A similar but particularly important problem occurs over the oceans. Atmospheric deposition of mineral dust provides iron and other elements to marine environments and can influence marine biogeochemistry and productivity (Jickells et al., 2005; Mahowald et al., 2009; Schulz et al., 2012). However, both the magnitude and spatial distribution of dust deposition remain poorly constrained. Model estimates over remote oceanic regions have historically differed by more than an order of magnitude, while the fraction of deposited iron that becomes biologically available remains highly uncertain (Schulz et al., 2012). This represents an important opportunity for integrating aerosol radiometry with atmospheric transport and ocean-biogeochemical modelling. Radiometric measurements, combined with lidar measurements of vertical distribution and satellite observations, can provide constraints on the atmospheric aerosol state before deposition. When combined with measurements of aerosol composition, precipitation and deposition, these observations can be used to evaluate and improve atmospheric transport and deposition models and, subsequently, the aerosol inputs used by ocean-biogeochemical models. Schulz et al. (2012) specifically identified the need for long-term measurements combining atmospheric and marine observations to address the coupled processes controlling dust deposition and its biogeochemical effects.

4.7.4. Urban applications and planning

Aerosols interact with urban radiation, boundary-layer dynamics, air quality and surface energy exchange, while the strong spatial heterogeneity of urban environments produces large gradients in aerosol concentration and radiative conditions. These processes are relevant to urban-scale assessments of air quality, thermal environment and solar-energy potential (Barlow, 2014; Li et al., 2017; Ulpiani, 2021). Radiometric observations could contribute to urban modelling by providing constraints on aerosol loading and optical properties that can be combined with satellite observations, surface PM measurements, meteorological observations and high-resolution atmospheric models. Such integrated datasets could improve estimates of surface radiation and help distinguish changes in aerosol optical depth associated with vertical redistribution from changes in near-surface aerosol concentration. They could also contribute to applications including urban air-quality assessment, photovoltaic deployment, building-

energy modelling and evaluation of urban heat-mitigation strategies (e.g., Popovici et al., 2018).

4.7.5. Insurance and environmental risk modelling

Modern catastrophe and climate-risk models increasingly combine physical hazard simulations with exposure and vulnerability information, rather than relying solely on historical loss records. Such models require spatially and temporally consistent information on the frequency, intensity and spatial extent of relevant hazards and their associated uncertainties (Steptoe et al., 2022; Ingels et al., 2024).The role of aerosol observations in this context is primarily indirect: radiometric measurements can improve the representation of aerosol processes within the atmospheric models that generate the physical variables subsequently used by risk models. Long-term observations of AOD and other optical properties can be used to evaluate aerosol climatology and model extremes, while high-temporal-resolution observations can constrain individual dust and smoke events. This is particularly relevant for sectors that are sensitive to surface radiation and aerosol episodes. For solar-energy assets, uncertainty in aerosol optical properties translates into uncertainty in irradiance and therefore expected energy production (e.g., Li et al., 2020; Kouklaki et al., 2026). For agriculture, persistent dust or smoke episodes can modify radiation and photosynthesis and may contribute to crop losses (Cohan et al., 2002; Mercado et al., 2009; Zhou et al., 2021). For urban areas, aerosol episodes can interact with heat, air quality and visibility (Li et al., 2017; Barlow, 2014; Duarte and Duarte, 2020). In each case, improved characterization of the aerosol state could reduce uncertainty in the hazard component of downstream impact models.

4.7.6. Solar Radiation Modification

A further emerging application of aerosol radiometric observations concerns Solar Radiation Modification (SRM), particularly stratospheric aerosol injection (SAI). SAI aims to increase the scattering of incoming solar radiation by introducing aerosol or aerosol precursors into the stratosphere, thereby modifying the shortwave radiation budget (e.g., Lee et al., 2026; Lange et al., 2026). The magnitude and spatial distribution of the resulting radiative effects depend strongly on aerosol amount, particle size, composition, vertical distribution and optical properties. Consequently, accurate characterization of aerosol radiative properties is an important requirement for assessing both the radiative response and the associated uncertainties (Dykema et al., 2016; Yu et al., 2023; Huynh and McNeill, 2024).

Radiometric observations could contribute to SRM monitoring at several stages of the observational chain. Spectral measurements of aerosol optical depth, aerosol extinction and absorption can provide information on the magnitude and optical characteristics of an aerosol perturbation, while lidar measurements can constrain its vertical distribution. Satellite observations provide the spatial context required to follow the evolution and transport of an aerosol layer, but ground-based measurements can provide continuous observations and independent constraints for satellite retrievals and radiative-transfer models. Recent work has demonstrated that satellite solar-occultation measurements may be capable of detecting relatively small stratospheric aerosol perturbations, although detectability depends on the magnitude and duration of the perturbation and on the natural variability of the background

aerosol layer (Lange et al., 2025). Existing pyranometer and spectroradiometer networks could provide useful observations for SRM-related research, particularly when combined with AOD, lidar, satellite and meteorological measurements (SAPEA, 2024). Recent assessments of SRM field experiments have emphasized the need for improved observations of aerosol properties, vertical distribution and radiative effects, as well as coordinated ground-based, airborne and satellite measurements (SAPEA, 2024; Kremser et al., 2016; Lange et al., 2025). Current observing systems still contain significant gaps in aerosol properties, vertical distribution and radiative effects relevant to SRM (ESA SRM Workshop, 2025; Hernandez-Galindo et al., 2026).

5. Way forward

Ground-based radiometric observations will remain indispensable for advancing our understanding of atmospheric aerosols, improving satellite retrievals, and supporting climate monitoring and operational environmental services. Despite substantial progress in instrumentation, retrieval algorithms and international observing networks, important challenges persist regarding the continuity, spatial representativeness, consistency and range of available aerosol products. Addressing these challenges requires a coordinated strategy that preserves the strengths of established reference networks while progressively incorporating emerging technologies and responding to the evolving requirements of satellite missions and user communities.

Maintaining long-term observations and strengthening reference networks. A first priority is to maintain existing ground-based networks and extend their continuous observational records. Long, homogeneous time series are essential for identifying climatological trends, distinguishing long-term changes from natural variability, and evaluating the effects of changes in emissions and atmospheric composition. Their scientific value depends not only on the duration of the records but also on the stability of instrument calibration, measurement procedures, quality assurance and data processing. Instrument replacement, calibration updates and changes in retrieval algorithms should therefore be carefully documented, with historical observations reprocessed where feasible to minimize artificial discontinuities. Sustained support for global and regional networks is particularly important because their measurements provide reference datasets for satellite calibration and validation, atmospheric modelling and climate data records. At the same time, network expansion should address persistent geographical and environmental gaps. Greater coverage is needed in remote and under-sampled regions, including deserts, high latitudes, maritime environments and areas where the operation of reference-grade instruments is constrained by cost or technical capacity. Expansion should prioritize locations where observations can improve both the representativeness of global aerosol datasets and the evaluation of satellite products under challenging surface and aerosol conditions. Regional training, calibration infrastructure and data-sharing arrangements will be essential to ensure that new observations can be maintained over time and integrated into established international networks. The objective should not simply be to increase the number of measurement sites, but to establish a geographically and environmentally representative observing system that provides reliable observations over multiple decades.

Improving consistency and interoperability between measurements. A second priority is to reduce systematic differences between instruments, networks and retrieval approaches. Although established networks generally provide consistent aerosol optical depth (AOD) measurements within their stated uncertainties, differences may arise from calibration procedures, ancillary data, cloud screening, retrieval algorithms and computational conventions. Such discrepancies become particularly important when measurements from different networks are combined, potentially introducing artificial variability into long-term records or complicating comparisons with satellite retrievals and atmospheric models. Progress will require sustained intercomparison campaigns, common reference procedures, traceable calibration standards and more harmonized approaches to uncertainty characterization. Long-term colocated measurements are especially valuable because they enable instrumental effects to be distinguished from differences introduced by data processing. Where feasible, applying common retrieval frameworks and ancillary datasets to measurements from different instruments would help quantify the origins of systematic discrepancies and improve comparability. Greater interoperability should also extend to data formats, metadata, quality flags and the transparent documentation of processing histories. Automated, uncertainty-aware satellite–ground matchup procedures and accessible data services could further facilitate the systematic use of reference observations in satellite validation and operational forecasting systems. These efforts would strengthen the basis for combining observations across networks without compromising their individual strengths or established quality standards.

Evaluating emerging technologies and expanding observational capabilities. While reference-grade instruments must remain the foundation of high-quality aerosol monitoring, their cost and operational requirements limit the spatial density achievable in many regions. Low-cost sensors and simplified autonomous observing platforms offer an opportunity to complement established networks, increase spatial coverage and capture aerosol variability at locations that are currently poorly observed. Their potential, however, depends on rigorous evaluation against reference instruments under a wide range of aerosol loadings, particle types, meteorological conditions and surface environments. Characterization of calibration stability, measurement uncertainty, environmental sensitivity and long-term performance should precede their use in applications requiring quantitative accuracy. Rather than replacing reference-grade observations, these technologies should initially be deployed within coordinated measurement strategies in which high-quality reference stations provide calibration, evaluation and quality-control support. Sky cameras and other emerging imaging technologies also deserve further investigation. When colocated with radiometric instruments, all-sky observations can provide information on cloud conditions, cloud–aerosol discrimination and the spatial variability of atmospheric scenes. Such information may improve cloud screening, help identify satellite–ground collocation mismatches and support the interpretation of rapidly changing aerosol conditions. Their integration with radiometric measurements, cloud observations and automated quality-control methods could improve the representativeness of validation datasets, particularly for high-temporal-resolution satellite observations. The wider use of these technologies will require standardized processing methods and independent assessment of their performance, including the uncertainties associated with cloud classification and the identification of aerosol events. Machine-learning methods may assist in extracting information from large image datasets, provided that their outputs are evaluated against independent observations and their limitations are documented.

Developing new products for next-generation satellite missions. Future ground-based measurements and retrieval algorithms should evolve in parallel with satellite observing capabilities. Conventional multispectral instruments have established a strong basis for validating AOD, but the increasing availability of multi-angle, polarimetric, hyperspectral and active lidar observations creates opportunities—and requirements—for more comprehensive validation. Future efforts should therefore extend beyond total aerosol loading towards improved characterization of aerosol size, absorption, type, shape and vertical distribution. This will require complementary observations, including measurements of diffuse sky radiance, polarization and, where available, vertically resolved aerosol properties. Coordinated ground-based radiometric and lidar measurements can provide valuable constraints for evaluating satellite products that retrieve aerosol layer height, extinction profiles and aerosol classification, while high-temporal-resolution observations are particularly important for geostationary missions and rapidly evolving dust and smoke events. The development of new products should also respond to application-specific requirements. More reliable estimates of aerosol absorption and spectral dependence would support radiative-transfer calculations and solar-energy applications, while improved aerosol typing and vertical information would benefit atmospheric composition forecasting and the interpretation of aerosol impacts on air quality and human exposure. Combining ground-based measurements with satellite observations, atmospheric reanalyses and numerical models could further support the development of derived products, including improved aerosol climatologies, event characterization and uncertainty-aware estimates of aerosol radiative effects. The emergence of new satellite missions, including EarthCARE and advanced multi-angle and polarimetric instruments, provides an opportunity to establish coordinated validation activities early in mission operations and to develop ground-based products tailored to their specific measurement capabilities.

Ultimately, the way forward is not to pursue greater measurement density, technological innovation or product complexity in isolation. Progress will depend on combining sustained reference observations with improved harmonization, carefully validated emerging technologies and retrieval products designed around clearly defined scientific and operational requirements. Long-term continuity must be preserved while observational systems become more spatially representative, interoperable and responsive to new satellite capabilities. Through coordinated international efforts, ground-based radiometric networks can continue to provide the traceable and scientifically robust observations needed to advance aerosol research, improve satellite products and strengthen climate, atmospheric composition and environmental services.

Appendix 1: Measurement principles of radiometric retrieval of aerosol optical properties

Ground-based passive radiometric observations of aerosol optical properties are based primarily on measurements of direct solar irradiance and diffuse sky radiance at multiple wavelengths. These two complementary measurement modes provide information on different aspects of aerosol extinction, scattering and absorption and form the basis of the retrieval methodologies used by the major global aerosol observing networks.

Solar radiation incident at the top of the atmosphere (TOA) can, to a good approximation, be considered a collimated source directed toward the Earth. During its propagation through the atmosphere, solar radiation is attenuated by absorption and scattering by atmospheric gases, aerosols and clouds. Scattering by atmospheric molecules is predominantly Rayleigh scattering, whereas aerosol and cloud scattering is generally described by Mie or more general electromagnetic scattering theory. The combined effects of absorption and scattering constitute atmospheric extinction. Radiation scattered away from the original solar beam can undergo further interactions with the atmosphere, producing multiple scattering, while radiation reflected by the surface can subsequently be scattered back toward the observer (Liou, 2002;Wendisch et al., 2004). The component of solar radiation reaching the observer directly from the solar disk is referred to as direct solar irradiance, or direct normal irradiance (DNI), whereas radiation arriving from other directions after atmospheric scattering constitutes the diffuse component. The radiance associated with a particular viewing direction is referred to as sky radiance.

Direct sun: The solar radiation reaching the uppermost layer of the atmosphere, known as **extraterrestrial radiation** or TOA (Top of Atmosphere) radiation, arrives in a single incident direction toward Earth. The intensity of this solar radiation per unit area (solar irradiance) varies mainly with the Earth–Sun distance, causing an annual variation of approximately ±3% (Iqbal, 1983). Solar radiation interacts with atmospheric components, and part of it reaches the surface where it can be absorbed or reflected back to the atmosphere. Surface reflectance (albedo) is important since it determines the fraction of the irradiance that is reflected by the Earth's surface and returns to the atmosphere and may then undergo scattering back toward the observer (e.g., Wendisch et al., 2004). The direct solar irradiance reaching an observer at a specific wavelength λ, denoted as E, can be estimated through the Beer–Bouguer–Lambert law:

$$E(\lambda) = E^{TOA}(\lambda)\exp[-T(\lambda)] \qquad \text{(Eq. 2.1)}$$

where E^{TOA} is the extraterrestrial solar irradiance, and T is the atmospheric slant optical thickness along the direction connecting the Sun and the observer. The vertical optical thickness or total optical depth (TOD; τ), is defined as the optical thickness for the vertical direction (SZA = 0). Thus, the previous equation can be rewritten as:

$$E(\lambda) = E^{TOA}(\lambda)\exp[-m\tau(\lambda)] \qquad \text{(Eq. 2.2)}$$

where *m* represents the relative optical airmass, defined as the ratio between the slant optical thickness and the vertical optical depth. For relatively small SZA values (below ~ SZA < 70°), relative airmass can be approximated by the secant of the SZA, although more accurate approximations exist, such as the widely used formulation by Kasten and Young (1989).

Taking logarithms, the equation can be linearized for a specific wavelength:

$$log[E(\lambda)] = log[E^{TOA}(\lambda)] - m\tau(\lambda) \qquad \text{(Eq. 2.3)}$$

If the logarithm of the direct solar irradiance *E(λ)* is plotted as a function of the relative optical airmass, assuming that atmospheric optical depth remains constant during the measurements, the total optical depth and the extraterrestrial solar irradiance $E^{TOA}(\lambda)$ can be obtained through a least-squares fit. This technique is known as the Langley plot method (Shaw, 1983). Its main advantage is that it does not require knowledge of the direct solar irradiance in calibrated physical units nor of its extraterrestrial value. By measuring the raw signal of direct solar irradiance, an equivalent extraterrestrial value can be derived directly in raw units (voltage, digital counts, …). The Langley technique is usually applied at locations where the daily aerosol variability is small for relatively long periods (i.e., for a relatively large change in SZA). This is fulfilled at high-altitude locations (very pristine atmosphere) and near the tropics (relative optical airmass changes fast). For this reason, sites such as Izaña Atmospheric Observatory and Mauna Loa Observatory are commonly used to calibrate sun photometers (Toledano et al., 2018)

$E^{TOA}(\lambda)$ must always be corrected for Earth–Sun distance, typically normalized to 1 AU, which can be easily computed from the measurement date. The Langley approach can also be extended to other celestial targets, such as stars (Pérez-Ramírez et al., 2008; Ivănescu et al., 2021; Román et al., 2025) and the Moon (Barreto et al., 2013, 2016, 2017). In these cases, however, the temporal and geometrical variability of the extraterrestrial target irradiance must be appropriately accounted for, particularly for lunar observations, where the changing lunar phase and illumination require dedicated calibration approaches such as the Lunar-Langley method.

The total optical depth can be expressed as the sum of the optical depths of gases, aerosols, and clouds. If measurements are restricted to cloud-free conditions, since clouds generally block all direct solar irradiance, then total optical depth consists only of the molecular optical depth of gases and the aerosol optical depth (AOD; τ_{aer}). The gaseous optical depth is usually separated into its absorption component (Gas Optical Depth, GOD; τ_g) and scattering component (Rayleigh Optical Depth, ROD; τ_R). Solar radiation absorption by atmospheric gases (ozone, NO_2, water vapor, etc.) is selective and occurs in known spectral bands and lines, with well-characterized absorption coefficients. Since gas concentrations are generally stable, GOD values can be estimated with good accuracy using climatological or reanalysis datasets. ROD values can be readily calculated from the atmospheric pressure at the observer's location. Once TOD, GOD, and ROD are determined, and cloud-free direct solar irradiance measurements are ensured, AOD can be obtained as (Giles et al., 2019):

$$\tau_{aer}(\lambda) = \tau(\lambda) - \tau_g(\lambda) - \tau_R(\lambda) \quad \text{(Eq. 2.4)}$$

or, if different relative airmasses are considered for each component (González et al., 2020):

$$\tau_{aer} = \frac{m\tau(\lambda) - \sum m_{g,x}\tau_{g,x}(\lambda) - m_R\tau_R(\lambda)}{m_{aer}} \quad \text{(Eq. 2.5)}$$

where the subscript x denotes the different gaseous species contributing to TOD at that wavelength λ.

The Beer–Bouguer–Lambert formulation used to retrieve AOD from direct-Sun measurements assumes that the measured solar beam is affected only by the atmospheric extinction processes represented in the retrieval. In practice, clouds can intermittently obscure or attenuate the solar beam and introduce large, non-aerosol contributions to the retrieved optical depth. Consequently, direct-Sun measurements must be subjected to dedicated cloud-screening procedures before being used for aerosol retrieval. A number of cloud-screening and quality-control methods have been developed for ground-based sun and star photometry (Smirnov et al., 2000;Pérez-Ramírez et al., 2012; Estellés et al., 2012; O'Neill et al., 2016;Kazadzis et al., 2018). These approaches generally exploit the temporal variability and spectral consistency of the measured signal or retrieved AOD, since rapidly varying attenuation is more characteristic of clouds than of aerosol under typical conditions. The AERONET Version 3 processing algorithm provides a comprehensive example, combining automated cloud screening with additional instrument and data-quality controls (Giles et al., 2019). Its cloud-screening procedure includes tests based on the variability of successive measurements ("triplets"), spectral and temporal consistency, and the identification of residual cloud contamination. It also incorporates a dedicated solar-aureole algorithm for detecting optically thin cirrus clouds, which may otherwise remain undetected by conventional direct-Sun screening. Additional QA/QC procedures are then applied to identify instrumental anomalies, insufficient temporal sampling and other conditions that may compromise the reliability of the retrieved AOD.

If AOD is obtained at several wavelengths, the turbidity coefficient (β) and the AE (α) can be derived through a least-squares fit of the Ångström law (Ångström, 1929; Ångström, 1961):

$$log(\tau_{aer}) = log(\beta) - \alpha log(\lambda) \quad \text{(Eq. 2.6)}$$

where λ is expressed in micrometers. The AE describes the spectral dependence of AOD and is commonly used as an indicator of aerosol particle size. Lower values of α (close to zero, typically below 1) are generally associated with coarse-mode aerosols, whereas higher values (close to 2, typically above 1.5) indicate a predominance of fine-mode particles (Eck et al., 1999;Schuster et al., 2006; Perrone et al., 2014). Nevertheless, the Ångström exponent is not independent of the spectral range over which it is derived, as aerosol optical depth spectra frequently exhibit departures from the idealized power-law dependence (e.g., Kaskaoutis et al., 2007).

Direct-sun observations primarily constrain the total aerosol extinction, but they do not independently provide the aerosol partition between scattering and absorption. The aerosol optical depth can be decomposed into scattering and absorption components, with their ratio defining the SSA:

$$\omega = \frac{\tau_{aer-sca}}{\tau_{aer}} = 1 - \frac{\tau_{aer-abs}}{\tau_{aer}} \qquad \text{(Eq. 2.7)}$$

SSA (ω), together with other aerosol optical and microphysical properties, can be inferred by combining direct-sun AOD with measurements of diffuse sky radiance (Wang and Gordon, 1993;Dubovik and King, 2000).

Sky radiance results from the scattering of solar radiation by atmospheric constituents into directions other than the direct solar beam. For a given viewing direction, the measured radiance depends on the scattering angle between the Sun and the observation direction. Molecular scattering is relatively well characterized and becomes increasingly important at shorter wavelengths, whereas aerosol scattering is governed by the aerosol phase function, which describes the angular distribution of scattered radiation and depends on particle size, shape and refractive index (Bodhaine et al., 1999; Dubovik et al., 2002). Measurements of sky radiance at multiple scattering angles therefore provide information on the angular structure of aerosol scattering and, consequently, on aerosol microphysical and optical properties.

Sky radiance is also sensitive to aerosol absorption: for a given AOD, more absorbing aerosol produces lower scattered radiance because a smaller fraction of the incident radiation is scattered. Consequently, relative sky radiances alone generally do not provide sufficient information to determine aerosol absorption robustly, and sky-radiance observations are normally combined with direct-sun AOD measurements. Inversion algorithms then seek the set of aerosol properties that minimizes the differences between observed AOD and sky radiances and the corresponding quantities simulated using a radiative-transfer model (Nakajima et al., 1996;Dubovik and King, 2000). Depending on the measurements and inversion framework, retrieved quantities can include SSA, spectral refractive index and aerosol volume size distribution.

Angular scanning geometries: The angular distribution of sky radiance is determined by the scanning geometry adopted by the instrument. Three geometries are particularly relevant to current sun-and-sky photometer networks: almucantar, principal-plane and hybrid scans. In the almucantar geometry, observations are made at a constant solar zenith angle while the instrument scans different azimuth angles around the Sun. The resulting, approximately symmetric, measurements on either side of the solar direction provide useful information for aerosol retrieval while also enabling cloud screening. For example, significant differences between radiances measured at symmetric viewing directions can indicate cloud contamination (Holben et al., 1998; Giles et al., 2019).

An important limitation of the almucantar geometry is that the accessible scattering-angle range decreases as the Sun rises and the solar zenith angle becomes smaller. Because small scattering angles are particularly sensitive to coarse particles, whereas larger scattering angles provide

greater sensitivity to fine particles, AERONET generally excludes almucantar observations obtained at SZA below approximately 40° (Tonna et al., 1995;Torres and Fuertes, 2021; Román et al., 2017, 2022).

The **principal-plane geometry** addresses this limitation by scanning within the plane containing the Sun, zenith and observer and therefore provides access to scattering angles greater than 90°. However, the lack of symmetric observations makes cloud screening more difficult, which has limited its use relative to the almucantar configuration. The **hybrid geometry**, introduced in AERONET, combines elements of the two approaches. It retains symmetric viewing directions useful for cloud screening while extending the accessible scattering-angle range, including under conditions of high solar elevation (Sinyuk et al., 2020). In this configuration, fixed scattering angles are measured within the ecliptic plane for zenith angles below 75°, while the scan switches to an almucantar configuration at a fixed zenith angle of 75° above this threshold.

These angular measurements are normally performed at several wavelengths, because shorter wavelengths provide stronger sensitivity to fine-mode particles whereas longer wavelengths provide greater sensitivity to coarse particles. Although cloud-contaminated viewing directions can be identified and excluded, recent work has shown that clouds outside the nominal measurement direction may nevertheless enhance sky radiance and introduce biases into retrieved aerosol properties. This **cloud-enhancement effect** represents an additional challenge for sky-radiance-based retrievals (Herrero-Anta et al., 2025).

Polarimetric measurements: Polarimetric measurements provide an additional source of information for aerosol characterization by measuring the polarization state of solar radiation scattered by atmospheric particles. In particular, measurements of the polarized component of sky radiance, commonly expressed through the degree of linear polarization or the Stokes parameters, are highly sensitive to particle size, refractive index and particle shape. This additional sensitivity can help constrain aerosol microphysical properties that are difficult to retrieve uniquely from intensity measurements alone, particularly the complex refractive index and the fraction of non-spherical particles (Dubovik et al., 2006; Dubovik et al., 2019). Polarimetric observations are therefore increasingly incorporated into advanced aerosol inversion frameworks, including GRASP, where intensity and polarization measurements can be jointly analyzed to improve the retrieval of aerosol size distribution, absorption and particle shape. Their use nevertheless introduces additional requirements concerning polarimetric calibration, instrument characterization and the accurate representation of polarized radiative transfer.

Appendix 2: Satellite instruments used to retrieve aerosol parameters

Table A2.1. Satellite instruments used to retrieve aerosol parameters

Instrument	Satellite	Measurement principle	Aerosol product spatial resolution	Temporal sampling	Main aerosol parameters	Recommended basic citation
MODIS	Terra / Aqua	Multispectral passive	**3–10 km**	Daily	AOD, AE, fine-mode fraction, aerosol type	Levy et al. (2013)
VIIRS	Suomi-NPP / NOAA-20	Multispectral passive	**~6 km**	Daily	AOD, AE, aerosol type, smoke/dust	Jackson et al. (2013)
MISR	Terra	Multi-angle multispectral	**~4.4 km**	~2–9 days	AOD, particle size, aerosol type, particle shape, plume height	Kahn & Gaitley (2015)
POLDER	PARASOL	Multi-angle polarimetric	~6 km	Daily	AOD, fine/coarse fraction, size, refractive index, SSA	Herman et al. (2005)
3MI	MetOp-SG-A1	Multi-angle polarimetric	**~4 km**	Daily	AOD, SSA, size distribution, refractive index, aerosol type	Hioki et al. (2021), 3MI/MetOp-SG literature

Instrument	Satellite	Measurement principle	Aerosol product spatial resolution	Temporal sampling	Main aerosol parameters	Recommended basic citation
OMI	Aura	UV–visible spectrometer	13 × 24 km	Daily	UV Aerosol Index, absorbing aerosol	Torres et al. (2007)
TROPOMI	Sentinel-5P	UV–visible–NIR spectrometer	**3.5 × 5.5 km**	Daily	UV Aerosol Index, absorbing aerosol	Veefkind et al. (2012); recent product papers
CALIOP	CALIPSO	Polarization lidar	~333 m along-track sampling	16 days	Backscatter, extinction, depolarization, aerosol type, vertical profiles	Winker et al. (2009)
ATLID	EarthCARE	High-spectral-resolution polarization lidar	~100 m vertical	~25 days	Backscatter, extinction, depolarization, aerosol type, vertical profiles	Donovan et al. (2024)
MSI	EarthCARE	Multispectral imaging	500 m	~25 days	Aerosol/cloud context, aerosol properties	Donovan et al. (2024)/ Illingworth et al. (2015)
OLCI	Sentinel-3A/B	Multispectral passive	300 m native; aerosol products coarser	~1–2 days	AOD, aerosol/cloud information	Donlon et al. (2012) / recent S3 aerosol products

Instrument	Satellite	Measurement principle	Aerosol product spatial resolution	Temporal sampling	Main aerosol parameters	Recommended basic citation
SLSTR	Sentinel-3A/B	Multispectral/thermal	km-scale aerosol products	~1 day	AOD, dust, smoke	Donlon et al. (2012), Recent Sentinel-3 aerosol product literature
AHI	Himawari-8/9	Geostationary multispectral	~2 km for aerosol applications	10 min	AOD, dust, smoke	Bessho et al. (2016)
ABI	GOES-R series	Geostationary multispectral	~2 km for aerosol applications	5–15 min	AOD, smoke, dust	Schmit et al. (2017)
SEVIRI	Meteosat MSG	Geostationary multispectral	~3 km	15 min	AOD, dust, smoke	Ceamanos et al. (2023)
IASI	Metop-A,B,C	High spectral resolution thermal IR	~12km	Twice daily	AOD at 10µm, converted to 550nm; dust and ash only	Vandenbussche et al., 2026 ; Clarisse et al., 2019; Capelle et al., 2018

References

1. Adebiyi, A. A., and Kok, J. F.: Climate models miss most of the coarse dust in the atmosphere, with implications for dust–climate interactions, Sci. Adv., 6, eaaz9507, https://doi.org/10.1126/sciadv.aaz9507, 2020.
2. Ahn, C., Torres, O., and Jethva, H.: Assessment of OMI near-UV aerosol optical depth over land, J. Geophys. Res.-Atmos., 119, 245–263, https://doi.org/10.1002/2013JD020188, 2014.
3. Akgül, M., et al.: Multi-method aerosol classification over the Eastern Mediterranean based on long-term AERONET observations and machine learning, Atmos. Environ., 382, 122242, https://doi.org/10.1016/j.atmosenv.2026.122242, 2026.
4. Alexandrov, M. D., Cairns, B., Emde, C., Ackerman, A. S., and van Diedenhoven, B.: Accuracy assessments of cloud droplet size retrievals from polarized reflectance measurements by the research scanning polarimeter, Remote Sens. Environ., 125, 92–111, https://doi.org/10.1029/2007JD009388, 2008.
5. Almansa, A. F., Cuevas, E., Barreto, Á., Torres, B., García, O. E., García, R. D., et al.: Column integrated water vapor and aerosol load characterization with the new ZEN-R52 radiometer, Remote Sens., 12, 1424, https://doi.org/10.3390/rs12091424, 2020.
6. Almansa, A. F., Cuevas, E., Torres, B., Barreto, Á., García, R. D., Cachorro, V. E., de Frutos, Á. M., López, C., and Ramos, R.: A new zenith-looking narrow-band radiometer-based system (ZEN) for dust aerosol optical depth monitoring, Atmos. Meas. Tech., 10, 565–579, https://doi.org/10.5194/amt-10-565-2017, 2017.
7. AMAP, Arctic climate change update (2021). Key trends and impacts. Summary for policy-makers arctic monitoring and assessment programme. Tromsø, Norway: AMAP Secretariat The Fram Centre.Arnalds O., Dagsson-Waldhauserova P., Olafsson H., 2016. The Icelandic volcanic aeolian environment: Processes and impacts - A review. Aeolian Research 20, 176-195.
8. Arnalds, O., Thorarinsdottir, E.F., Thorsson, J., Dagsson-Waldhauserova, P., Agustsdottir, A.M., 2013. An extreme wind erosion event of the fresh Eyjafjallajokull 2010 volcanic ash. Nature Scientific Reports 3, 1257.
9. Ansari, K. and Ramachandran, S.: Aerosol characteristics over Indo-Gangetic Plain from ground-based AERONET and MERRA-2/CAMS model simulations, Atmos. Environ., 2023, 119434, https://doi.org/10.1016/j.atmosenv.2022.119434, 2023.
10. Ansari, K., Ramachandran, S., and Cherian, R.: Global assessment of aerosol radiative effects: new insights from observations, reanalysis, and climate models, Sci. Total Environ., 1006, 180871, https://doi.org/10.1016/j.scitotenv.2025.180871, 2025.
11. Ansmann, A., Tesche, M., Seifert, P., Groß, S., Freudenthaler, V., Apituley, A., Wilson, K. M., Serikov, I., Linné, H., Heinold, B., Hiebsch, A., Schnell, F., Schmidt, J., Mattis, I., Wandinger, U., and Wiegner, M.: Ash and fine-mode particle mass profiles from EARLINET–AERONET observations over central Europe after the eruptions of the

Eyjafjallajökull volcano in 2010, J. Geophys. Res., 116, D00U02, https://doi.org/10.1029/2010JD015567, 2011.
12. Antuña-Sánchez, J. C., Toledano, C., Cachorro, V. E., et al.: Aerosol optical properties and related observations, Atmos. Meas. Tech., 14, 2201–2218, https://doi.org/10.5194/amt-14-2201-2021, 2021.
13. Awais, M. and Wang, L.: Global classification of aerosols based on ground observations: A comparison between an empirical method and machine learning algorithms, Phys. Chem. Earth, 140, 104017, https://doi.org/10.1016/j.pce.2025.104017, 2025.
14. Bais, A. F., Kazadzis, S., Balis, D., Zerefos, C. S., and Blumthaler, M.: Correcting global solar UV spectra recorded by a Brewer spectroradiometer for its angular response error, Appl. Opt., 37, 6339–6344, https://doi.org/10.1364/AO.37.006339, 1998.
15. Bais, A. F., Kazantzidis, A., Kazadzis, S., Balis, D. S., Zerefos, C. S., and Meleti, C.: Deriving an effective aerosol single scattering albedo from spectral surface UV irradiance measurements, Atmos. Environ., 39, 1093–1102, https://doi.org/10.1016/j.atmosenv.2004.09.080, 2005.
16. Bais, A. F., Lucas, R. M., Bornman, J. F., Williamson, C. E., Sulzberger, B., Austin, A. T., Wilson, S. R., Andrady, A. L., Bernhard, G., McKenzie, R. L., Aucamp, P. J., Madronich, S., Neale, R. E., Yazar, S., Young, A. R., de Gruijl, F. R., Norval, M., Takizawa, Y., Barnes, P. W., Robson, T. M., Robinson, S. A., Ballaré, C. L., Flint, S. D., Neale, P. J., Hylander, S., Rose, K. C., Wängberg, S.-Å., Häder, D.-P., Worrest, R. C., Zepp, R. G., Paul, N. D., Cory, R. M., Solomon, K. R., Longstreth, J., Pandey, K. K., Redhwi, H. H., Torikai, A., and Heikkilä, A. M.: Environmental effects of ozone depletion, UV radiation and interactions with climate change: UNEP Environmental Effects Assessment Panel, update 2017, Photochem. Photobiol. Sci., 17, 127–179, https://doi.org/10.1039/C7PP90043K, 2018.
17. Baldo, C., Formenti, P., Di Biagio, C., Lu, G., Song, C., Cazaunau, M., Pangui, E., Doussin, J.-F., Dagsson-Waldhauserova, P., Arnalds, O., Beddows, D., MacKenzie, A. R., Shi, Z., 2023. Complex refractive index and single scattering albedo of Icelandic dust in the shortwave spectrum. Atmos. Chem. Phys. 23, 7975–8000
18. Carlsen H.K., Thorarinn Gislason, Bertil Forsberg, Kadri Meister, Throstur Thorsteinsson, Thorsteinn Jóhannsson, Ragnhildur Finnbjornsdottir and Anna Oudin. 2015. Emergency Hospital Visits in Association with Volcanic Ash, Dust Storms and Other Sources of Ambient Particles: A Time-Series Study in Reykjavík, Iceland. Int. J. Environ. Res. Public Health 12(4): 4047 – 4059.
19. Balis, D. S., Amiridis, V., Zerefos, C., Kazantzidis, A., Kazadzis, S., Bais, A. F., Meleti, C., Gerasopoulos, E., Papayannis, A., Matthias, V., Dier, H., and Andreae, M. O.: Study of the effect of different type of aerosols on UV-B radiation from measurements during EARLINET, Atmos. Chem. Phys., 4, 307–321, https://doi.org/10.5194/acp-4-307-2004, 2004.

20. Barlow, J. F.: Progress in observing and modelling the urban boundary layer, Urban Climate, 10, 216–240, https://doi.org/10.1016/j.uclim.2014.03.011, 2014.
21. Barreto, A., Cuevas, E., Damiri, B., Guirado, C., Berkoff, T., Berjón, A. J., Hernández, Y., Almansa, F., and Gil, M.: A new method for nocturnal aerosol measurements with a lunar photometer prototype, Atmos. Meas. Tech., 6, 585–598, https://doi.org/10.5194/amt-6-585-2013, 2013.
22. Barreto, Á., Cuevas, E., Granados-Muñoz, M.-J., Alados-Arboledas, L., Romero, P. M., Gröbner, J., Kouremeti, N., Almansa, A. F., Stone, T., Toledano, C., Román, R., Sorokin, M., Holben, B., Canini, M., and Yela, M.: The new sun-sky-lunar Cimel CE318-T multiband photometer – a comprehensive performance evaluation, Atmos. Meas. Tech., 9, 631–654, https://doi.org/10.5194/amt-9-631-2016, 2016.
23. Barreto, Á., Román, R., Cuevas, E., Berjón, A. J., Almansa, A. F., Toledano, C., González, R., Hernández, Y., Blarel, L., Goloub, P., Guirado, C., and Yela, M.: Assessment of nocturnal aerosol optical depth from lunar photometry at the Izaña high mountain observatory, Atmos. Meas. Tech., 10, 3007–3019, https://doi.org/10.5194/amt-10-3007-2017, 2017.
24. Barreto, Á., Román, R., Cuevas, E., Pérez-Ramírez, D., Berjón, A. J., Kouremeti, N., Kazadzis, S., Gröbner, J., Mazzola, M., Toledano, C., Benavent-Oltra, J. A., Doppler, L., Juryšek, J., Almansa, A. F., Victori, S., Maupin, F., Guirado-Fuentes, C., González, R., Vitale, V., Goloub, P., Blarel, L., Alados-Arboledas, L., Woolliams, E., Greenwell, C., Taylor, S., Antuña, J. C., and Yela, M.: Evaluation of night-time aerosol optical depth measurements and lunar irradiance models in the frame of the first multi-instrument nocturnal intercomparison campaign, Atmos. Environ., 202, 190–211, https://doi.org/10.1016/j.atmosenv.2019.01.006, 2019.
25. Basart, S., Pérez, C., Nickovic, S., Cuevas, E., and Baldasano, J. M.: Aerosol characterization in Northern Africa, Northeastern Atlantic, Mediterranean Basin and Middle East from direct-sun AERONET observations, Atmos. Chem. Phys., 9, 8265–8282, https://doi.org/10.5194/acp-9-8265-2009, 2009.
26. Bayat, A. and Assarenayati, S.: How to measure the amount of aerosol optical thickness in the atmosphere in a simple way: a Calitoo handheld sun-photometer measurement, Atmos. Environ., 2023, 119570, https://doi.org/10.1016/j.atmosenv.2022.119570, 2023.
27. Bazo, E., Granados-Muñoz, M. J., Román, R., Bravo-Aranda, J. A., Cazorla, A., Valenzuela, A., González, R., Olmo, F. J., & Alados-Arboledas, L. (2023). Evaluation of the vertically-resolved aerosol radiative effect on shortwave and longwave ranges using sun-sky photometer and ceilometer measurements. Atmospheric Research, 282, 106517. https://doi.org/10.1016/j.atmosres.2022.106517
28. Belluardo, G., Barchi, G., Baumgartner, D. J., Rennhofer, M., Weihs, P., and Moser, D.: Uncertainty analysis of a radiative transfer model using Monte Carlo method within 280–2500 nm region, Solar Energy, 132, 558–569, https://doi.org/10.1016/j.solener.2016.03.050, 2016. [Source: Publisher page checked]

29. Benedetti, A., Morcrette, J.-J., Boucher, O., et al.: Aerosol analysis and forecast in the European Centre for Medium-Range Weather Forecasts Integrated Forecast System: 2. Data assimilation, J. Geophys. Res.-Atmos., 114, D13205, https://doi.org/10.1029/2008JD011115, 2009.
30. Benedetti, A., Reid, J. S., Knippertz, P., et al.: Status and future of numerical atmospheric aerosol prediction with a focus on data requirements, Atmos. Chem. Phys., 18, 10615–10643, https://doi.org/10.5194/acp-18-10615-2018, 2018.
31. Benedetti, A., Reid, J. S., Knobelspiesse, K., et al.: Status and future of aerosol data assimilation in numerical prediction systems, Bull. Amer. Meteor. Soc., 99, 173–196, https://doi.org/10.1175/BAMS-D-17-0054.1, 2018.
32. Benedetti, A., Rémy, S., Engelen, R., and others: [Reference cited in the manuscript as Benedetti et al. (2018); bibliographic details should be checked against the intended source].
33. Bessho, K., Date, K., Hayashi, M., Ikeda, A., Imai, T., Inoue, H., Kumagai, Y., Miyakawa, T., Murata, H., Ohno, T., Okuyama, A., Okuyama, A., Osada, M., Seko, H., Shimada, S., Shimizu, A., Shirakawa, R., Suzuki, Y., Taniguchi, H., Tsuchiyama, H., Uesawa, D., Yamamoto, N., and Yoshida, R.: An Introduction to Himawari-8/9—Japan's New-Generation Geostationary Meteorological Satellites, J. Meteorol. Soc. Japan, 94, 151–183, https://doi.org/10.2151/jmsj.2016-009, 2016.
34. Bibi, H., Alam, K., Chishtie, F., Bibi, S., Shahid, I., and Blaschke, T.: Intercomparison of MODIS, MISR, OMI, and CALIPSO aerosol optical depth retrievals for four locations on the Indo-Gangetic Plains and validation against AERONET data, Atmos. Environ., 111, 113–126, https://doi.org/10.1016/j.atmosenv.2015.04.013, 2015.
35. Bocquet, M., Elbern, H., Eskes, H., et al.: Data assimilation in atmospheric chemistry models: Current status and future prospects for coupled chemistry meteorology models, Atmos. Chem. Phys., 15, 5325–5358, https://doi.org/10.5194/acp-15-5325-2015, 2015.
36. Bodhaine, B. A., Wood, N. B., Dutton, E. G., and Slusser, J. R.: On Rayleigh optical depth calculations, J. Atmos. Oceanic Technol., 16, 1854–1861, https://doi.org/10.1175/1520-0426(1999)016<1854:ORODC>2.0.CO;2, 1999.
37. Boi, P., Tonna, G., Dalu, G., Nakajima, T., Olivieri, B., Pompei, A., Campanelli, M., and Rao, R.: Calibration and data elaboration procedure for sky irradiance measurements, Appl. Opt., 38, 896–907, https://doi.org/10.1364/AO.38.000896, 1999.
38. Bojinski, S., Verstraete, M., Peterson, T. C., Richter, C., Simmons, A., and Zemp, M.: The concept of essential climate variables in support of climate research, applications, and policy, B. Am. Meteorol. Soc., 95, 1431–1443, https://doi.org/10.1175/BAMS-D-13-00047.1, 2014.
39. Bond, T. C., Doherty, S. J., Fahey, D. W., et al.: Bounding the role of black carbon in the climate system: A scientific assessment, J. Geophys. Res.-Atmos., 118, 5380–5552, https://doi.org/10.1002/jgrd.50171, 2013.

40. Breitkreuz et al. 2009: Short-Range Direct and Diffuse Irradiance Forecasts for Solar Energy Applications — https://doi.org/10.1175/2009JAMC2090.1.
41. Buchard, V., Randles, C. A., Da Silva, A. M., Darmenov, A., Colarco, P. R., Govindaraju, R., et al.: The MERRA-2 aerosol reanalysis, 1980 onward. Part II: evaluation and case studies, J. Clim., 30, 6851–6872, https://doi.org/10.1175/JCLI-D-16-0613.1, 2017.
42. Bunn, P. T. W., Holmgren, W. F., Leuthold, M., and Castro, C. L.: Using GEOS-5 forecast products to represent aerosol optical depth in operational day-ahead solar irradiance forecasts for the southwest United States, Journal of Renewable and Sustainable Energy, 12, 053702, https://doi.org/10.1063/5.0020785, 2020.
43. Burkhardt, J.: Hygroscopic particles on leaves: nutrients or desiccants?, Ecological Monographs, 80, 369–399, https://doi.org/10.1890/09-1988.1, 2010.
44. Cairns, B., Waquet, F., Knobelspiesse, K., Chowdhary, J., and Deuzé, J.-L.: Polarimetric remote sensing of aerosols over land surfaces, in: Satellite Aerosol Remote Sensing over Land, edited by: Kokhanovsky, A. A. and De Leeuw, G., Springer-Praxis Books in Environmental Sciences, Springer, Berlin, Germany, 295–325, https://doi.org/10.1007/978-3-540-69397-0_10, 2009.
45. Campanelli, M., Estellés, V., Smyth, T. J., et al.: Evaluation of AERONET sun photometers and sky radiometers, Atmos. Meas. Tech., 17, 5029–5045, https://doi.org/10.5194/amt-17-5029-2024, 2024.
46. Campanelli, M., Mascitelli, A., Sanò, P., Diémoz, H., Estellés, V., Federico, S., Iannarelli, A. M., Fratarcangeli, F., Mazzoni, A., Realini, E., Crespi, M., Bock, O., Martínez-Lozano, J. A., and Dietrich, S.: Precipitable water vapour content from ESR/SKYNET sun–sky radiometers: validation against GNSS/GPS and AERONET over three different sites in Europe, Atmos. Meas. Tech., 11, 81–94, https://doi.org/10.5194/amt-11-81-2018, 2018.
47. Cao, M., Zhang, M., Su, X., and Wang, L.: A two-stage machine learning algorithm for retrieving multiple aerosol properties over land: Development and validation, IEEE Trans. Geosci. Remote Sens., 61, 4105017, https://doi.org/10.1109/TGRS.2023.3307934, 2023.
48. Capelle, V., Chédin, A., Pondrom, M., Crevoisier, C., Armante, R., Crépeau, L., and Scott, N. A.: Infrared dust aerosol optical depth retrieved daily from IASI and comparison with AERONET over the period 2007–2016, Remote Sens. Environ., 206, 15–32, https://doi.org/10.1016/j.rse.2017.12.008, 2018.
49. Carlsen, H. K., Gislason, T., Forsberg, B., et al. (2015). Emergency hospital visits in association with volcanic ash, dust storms and other sources of ambient particles: A time-series study in Reykjavík, Iceland. International Journal of Environmental Research and Public Health, 12(4), 4047–4059.
50. Carrassi, A., Bocquet, M., Bertino, L., and Evensen, G.: Data assimilation in the geosciences: An overview of methods, issues, and perspectives, WIREs Clim. Change, 9, e535, https://doi.org/10.1002/wcc.535, 2018.

51. Carvalho, F., and Henriques, D.: Use of Brewer ozone spectrophotometer for aerosol optical depth measurements on ultraviolet region, Adv. Space Res., 25, 997–1006, https://doi.org/10.1016/S0273-1177(99)00463-9, 2000.
52. Cazorla, A., Olmo, F. J., and Alados-Arboledas, L.: Using a sky imager for aerosol characterization, Atmos. Environ., 42, 2739–2745, https://doi.org/10.1016/j.atmosenv.2007.06.016, 2008.
53. Ceamanos, X., Carrer, D., Roujean, J.-L., et al.: Aerosol optical depth retrieval from geostationary satellite observations, Atmos. Meas. Tech., 16, 2575–2592, https://doi.org/10.5194/amt-16-2575-2023, 2023.
54. Charalampous, G., Fragkos, K., Fountoulakis, I., Papachristopoulou, K., Moustaka, A., Nisantzi, A., Hadjimitsis, D., and Kazadzis, S.: UV Index monitoring and forecasting in Cyprus: The effect of ozone, aerosols and clouds, EGUsphere [preprint], https://doi.org/10.5194/egusphere-2026-6018, 2026.
55. Charalampous, G., Fragkos, K., Nisantzi, A., Fountoulakis, I., Papachristopoulou, K., Hadjimitsis, D., and Kazadzis, S.: Preliminary evaluation of the Cyprus Erythemal Irradiance Forecasting System, IOP Conf. Ser.: Earth Environ. Sci., 1522, 012038, 2025. https://doi.org/10.1088/1755-1315/1522/1/012038
56. Che, H., Xia, X., Zhu, J., Wang, H., Wang, Y., Sun, J., et al.: Column-integrated aerosol optical properties over China based on AERONET observations, Atmos. Meas. Tech., 12, 4071–4092, https://doi.org/10.5194/amt-12-4071-2019, 2019.
57. Chen, C., Dubovik, O., Fuertes, D., Litvinov, P., Lapyonok, T., Lopatin, A., Ducos, F., Derimian, Y., Herman, M., Tanré, D., Remer, L. A., Lyapustin, A., Sayer, A. M., Levy, R. C., Hsu, N. C., Descloitres, J., Li, L., Torres, B., Karol, Y., Herrera, M., Herreras, M., Aspetsberger, M., Wanzenboeck, M., Bindreiter, L., Marth, D., Hangler, A., and Federspiel, C.: Validation of GRASP algorithm product from POLDER/PARASOL data and assessment of multi-angular polarimetry potential for aerosol monitoring, Earth Syst. Sci. Data, 12, 3573–3620, https://doi.org/10.5194/essd-12-3573-2020, 2020.
58. Chen, C., Dubovik, O., Litvinov, P., Fuertes, D., Lopatin, A., Lapyonok, T., Matar, C., Karol, Y., Fischer, J., Preusker, R., Hangler, A., Aspetsberger, M., Bindreiter, L., Marth, D., Chimot, J., Fougnie, B., Marbach, T., and Bojkov, B.: Properties of aerosol and surface derived from OLCI/Sentinel-3A using GRASP approach: Retrieval development and preliminary validation, Remote Sens. Environ., 280, 113142, https://doi.org/10.1016/j.rse.2022.113142, 2022.
59. Chen, C., Litvinov, P., Dubovik, O., Bindreiter, L., Matar, C., Fuertes, D., Lopatin, A., Lapyonok, T., Lanzinger, V., Hangler, A., Aspetsberger, M., de Graaf, M., Tilstra, L. G., Stammes, P., Dandocsi, A., Gasbarra, D., Fluck, E., Zehner, C., and Retscher, C.: Extended aerosol and surface characterization from S5P/TROPOMI with GRASP algorithm. Part II: Global validation and intercomparison, Remote Sens. Environ., 313, 114374, https://doi.org/10.1016/j.rse.2024.114374, 2024.

60. Chen, M. and Blankenship, R. E.: Expanding the solar spectrum used by photosynthesis, Trends Plant Sci., 16, 427–431, https://doi.org/10.1016/j.tplants.2011.03.011, 2011.
61. Chen, X., de Leeuw, G., Arola, A., Liu, S., Liu, Y., Li, Z., and Zhang, K.: Joint retrieval of the aerosol fine mode fraction and optical depth using MODIS spectral reflectance over northern and eastern China: Artificial neural network method, Remote Sens. Environ., 249, 112006, https://doi.org/10.1016/j.rse.2020.112006, 2020.
62. Chen, X., Zhao, L., Zheng, F., Li, J., Li, L., Ding, H., Zhang, K., Liu, S., Li, D., and de Leeuw, G.: Neural Network AEROsol Retrieval for Geostationary Satellite (NNAeroG) Based on Temporal, Spatial and Spectral Measurements, Remote Sens., 14(4), 980, https://doi.org/10.3390/rs14040980, 2022. (One possible match for the in-text Chen et al., 2022.)
63. Chen, Y., Bao, F., and Huang, K.: The retrieval of aerosol optical properties based on a random forest machine learning approach: Exploration of geostationary satellite images, Remote Sens. Environ., 281, 113426, https://doi.org/10.1016/j.rse.2022.113426, 2022. (Alternative possible match for the in-text Chen et al., 2022.)
64. Cheymol, A. and de Backer, H.: Retrieval of the aerosol optical depth in the UV-B at Uccle from Brewer ozone measurements over a long time period 1984–2002, J. Geophys. Res., 108, 4800, https://doi.org/10.1029/2003JD003758, 2003.
65. Cho, H., Kim, J., et al.: Aerosol optical properties and retrieval uncertainty, Atmos. Meas. Tech., 17, 4369–4384, https://doi.org/10.5194/amt-17-4369-2024, 2024.
66. Choi, Y., Chen, S.-H., Huang, C.-C., Earl, K., Chen, C.-Y., Schwartz, C. S., and Matsui, T.: Evaluating the impact of assimilating aerosol optical depth observations on dust forecasts over North Africa and the East Atlantic using different data assimilation methods, J. Adv. Model. Earth Syst., 12, e2019MS001890, https://doi.org/10.1029/2019MS001890, 2020.
67. Chu, Y., Liu, Y., Li, X., Liu, Z., Lu, H., Lu, Y., Mao, Z., Chen, X., Li, N., Ren, M., Liu, F., Tian, L., Zhu, Z., and Xiang, H.: A review on predicting ground PM2.5 concentration using satellite aerosol optical depth, Atmosphere, 7, 129, https://doi.org/10.3390/atmos7100129, 2016.
68. Clarisse, L., Clerbaux, C., Franco, B., Hadji-Lazaro, J., Whitburn, S., Kopp, A. K., Hurtmans, D., and Coheur, P.-F.: A Decadal Data Set of Global Atmospheric Dust Retrieved From IASI Satellite Measurements, J. Geophys. Res. Atmos., 124, 1618–1647, https://doi.org/10.1029/2018JD029701, 2019.
69. Clarisse, L., Coheur, P.-F., Prata, F., Hadji-Lazaro, J., Hurtmans, D., and Clerbaux, C.: A unified approach to infrared aerosol remote sensing and type specification, Atmos. Chem. Phys., 13, 2195–2238, https://doi.org/10.5194/acp-13-2195-2013, 2013. (The comments say 2010; the DOI-resolved publication is 2013.)
70. Cohan, D. S., Xu, J., Greenwald, R., Bergin, M. H., and Chameides, W. L.: Impact of atmospheric aerosol light scattering and absorption on terrestrial net primary productivity, Global Biogeochemical Cycles, 16, 1097, https://doi.org/10.1029/2001GB001441, 2002.

71. Crocchianti, S., Moroni, B., Dagsson-Waldhauserová, P., Becagli, S., Severi, M., Traversi, R., Cappelletti, D., 2021. Potential Source Contribution Function Analysis of High Latitude Dust Sources over the Arctic: Preliminary Results and Prospects. Atmosphere 12, 347-362.
72. Đorđević D., Tošić I., Sakan S., Petrović S., Đuričić-Milanković J., Finger D.C. and Dagsson-Waldhauserová P. 2019. Can Volcanic Dust Suspended From Surface Soil and Deserts of Iceland Be Transferred to Central Balkan Similarly to African Dust (Sahara)? Frontiers in Earth Sciences 7, 142-154.
73. Cuevas, E., Romero-Campos, P. M., Kouremeti, N., Kazadzis, S., Räisänen, P., García, R. D., et al.: Aerosol optical depth comparison between GAW-PFR and AERONET-Cimel radiometers from long-term (2005–2015) 1 min synchronous measurements, Atmos. Meas. Tech., 12, 4309–4337, https://doi.org/10.5194/amt-12-4309-2019, 2019.
74. De Leeuw, G., Holzer-Popp, T., Bevan, S., et al.: Evaluation of seven European aerosol optical depth retrieval algorithms for climate analysis, Remote Sens. Environ., 162, 295–315, https://doi.org/10.1016/j.rse.2013.04.023, 2015.
75. Després, V. R., Huffman, J. A., Burrows, S. M., Hoose, C., Safatov, A. S., Buryak, G., Fröhlich-Nowoisky, J., Elbert, W., Andreae, M. O., Pöschl, U., and Jaenicke, R.: Primary biological aerosol particles in the atmosphere: A review, Tellus B, 64, 15598, https://doi.org/10.3402/tellusb.v64i0.15598, 2012.
76. Di Biagio, C., Bru, E., Orta, A., Chevaillier, S., Baldo, C., Bergé, A., Cazaunau, M., Lafon, S., Nowak, S., Pangui, E., Andreae, M. O., Dagsson-Waldhauserova, P., Dintwe, K., Kandler, K., King, J. S., Chaput, A., Okin, G. S., Piketh, S., Saeed, T., Seibert, D., Shi, Z., Williams, E., Sellitto, P., and Formenti, P., 2026. Mid- and far-infrared spectral signatures of mineral dust from low- to high-latitude regions: significance and implications. Atmospheric Chemistry and Physics 26, 1079–1091, https://doi.org/10.5194/acp-26-1079-2026.
77. Diémoz, H., Eleftheratos, K., Kazadzis, S., Amiridis, V., and Zerefos, C. S.: Retrieval of aerosol optical depth in the visible range with a Brewer spectrophotometer in Athens, Atmos. Meas. Tech., 9, 1871–1888, https://doi.org/10.5194/amt-9-1871-2016, 2016.
78. Djossou, J., Léon, J.-F., Akpo, A. B., Liousse, C., Yoboué, V., Bedou, M., Bodjrenou, M., Chiron, C., Galy-Lacaux, C., Gardrat, E., Abbey, M., Keita, S., Bahino, J., Touré N'Datchoh, E., Ossohou, M., and Awanou, C. N.: Mass concentration, optical depth and carbon composition of particulate matter in the major southern West African cities of Cotonou (Benin) and Abidjan (Côte d'Ivoire), Atmos. Chem. Phys., 18, 6275–6291, https://doi.org/10.5194/acp-18-6275-2018, 2018.
79. Docter, N., Preusker, R., Filipitsch, F., Kritten, L., Schmidt, F., and Fischer, J.: Aerosol optical depth retrieval from the EarthCARE Multi-Spectral Imager: the M-AOT product, Atmos. Meas. Tech., 16, 3437–3457, https://doi.org/10.5194/amt-16-3437-2023, 2023.

80. Dong, X., Chen, B., Yamazaki, A., Shi, G., and Tang, N.: Variations in aerosol optical characteristics from SKYNET measurements in Beijing, Atmos. Environ., 302, 119747, https://doi.org/10.1016/j.atmosenv.2023.119747, 2023.
81. Dong, Y., et al.: Aerosol retrievals from thermal infrared observations, J. Quant. Spectrosc. Radiat. Transfer, 2026, 109802, https://doi.org/10.1016/j.jqsrt.2025.109802, 2026.
82. Donlon, C., Berruti, B., Buongiorno, A., Ferreira, M.-H., Féménias, P., Frerick, J., Goryl, P., Klein, U., Laur, H., Mavrocordatos, M., Nieke, J., Rebhan, R., Seitz, B., Stroede, J., and Sciarra, R.: The Global Monitoring for Environment and Security (GMES) Sentinel-3 mission, Remote Sens. Environ., 120, 37–57, https://doi.org/10.1016/j.rse.2011.07.024, 2012.
83. Donovan, D. P., van Zadelhoff, G.-J., and Wang, P.: The EarthCARE lidar cloud and aerosol profile processor (A-PRO): the A-AER, A-EBD, A-TC, and A-ICE products, Atmos. Meas. Tech., 17, 5301–5340, https://doi.org/10.5194/amt-17-5301-2024, 2024.
84. Doppler, L., et al.: [UV aerosol optical depth study cited in the manuscript; full title and publication details not recoverable from the supplied comment], 2026. [Verify before submission].
85. Duarte, R. M. B. O., and Duarte, A. C.: Urban atmospheric aerosols: Sources, analysis, and effects, Atmosphere, 11, 1221, https://doi.org/10.3390/atmos11111221, 2020.
86. Dubovik, O. and King, M. D.: A flexible inversion algorithm for retrieval of aerosol optical properties from Sun and sky radiance measurements, J. Geophys. Res., 105, 20673–20696, https://doi.org/10.1029/2000JD900282, 2000.
87. Dubovik, O., et al.: GRASP: a versatile algorithm for characterizing the atmosphere, Proc. SPIE, 2014.
88. Dubovik, O., et al.: GRASP algorithm and its applications to aerosol remote sensing, Front. Remote Sens., https://doi.org/10.3389/frsen.2021.706851, 2021.
89. Dubovik, O., Herman, M., Holdak, A., Lapyonok, T., Tanré, D., Deuzé, J. L., Ducos, F., Sinyuk, A., and Lopatin, A.: Statistically optimized inversion algorithm for enhanced retrieval of aerosol properties from spectral multi-angle polarimetric satellite observations, Atmos. Meas. Tech., 4, 975–1018, https://doi.org/10.5194/amt-4-975-2011, 2011.
90. Dubovik, O., Holben, B. N., Eck, T. F., et al.: Variability of absorption and optical properties of key aerosol types observed in worldwide locations, J. Atmos. Sci., 59, 590–608, https://doi.org/10.1175/1520-0469(2002)059<0590:VOAAOP>2.0.CO;2, 2002.
91. Dubovik, O., Li, Z., Mishchenko, M. I., Tanré, D., Karol, Y., Bojkov, B., Cairns, B., Diner, D. J., Espinosa, W. R., Goloub, P., Gu, X., Hasekamp, O., Hong, J., Hou, W., Knobelspiesse, K. D., Landgraf, J., Li, L., Litvinov, P., Liu, Y., Lopatin, A., Marbach, T., Maring, H., Martins, V., Meijer, Y., Milinevsky, G., Mukai, S., Parol, F., Qiao, Y., Remer, L., Rietjens, J., Sano, I., Stammes, P., Stamnes, S., Sun, X., Tabary, P., Travis, L. D., Waquet, F., Xu, F., Yan, C., and Yin, D.: Polarimetric remote sensing of atmospheric

aerosols: instruments, methodologies, results, and perspectives, **J. Quant. Spectrosc. Radiat. Transf., 224, 474–511, https://doi.org/10.1016/j.jqsrt.2018.11.024, 2019.

92. Dubovik, O., Sinyuk, A., Lapyonok, T., Holben, B. N., Mishchenko, M., Yang, P., Eck, T. F., Volten, H., Muñoz, O., Veihelmann, B., van der Zande, W. J., Leon, J.-F., Sorokin, M., and Slutsker, I.: Application of spheroid models to account for aerosol particle nonsphericity in remote sensing of desert dust, J. Geophys. Res., 111, D11208, https://doi.org/10.1029/2005JD006619, 2006.
93. Dykema, J. A., Keith, D. W., and Keutsch, F. N.: Improved aerosol radiative properties as a foundation for solar geoengineering risk assessment, Geophysical Research Letters, 43, 7758–7766, https://doi.org/10.1002/2016GL069258, 2016.
94. D'Amato, G., Vitale, C., Sanduzzi, A., Molino, A., Vatrella, A., and D'Amato, M.: Allergenic pollen and pollen allergy in Europe, in: Allergy and Allergen Immunotherapy, Apple Academic Press, 2017.
95. Eck, T. F., Holben, B. N., Reid, J. S., Dubovik, O., Smirnov, A., O'Neill, N. T., Slutsker, I., and Kinne, S.: Wavelength dependence of the optical depth of biomass burning, urban, and desert dust aerosols, J. Geophys. Res., 104, 31333–31349, https://doi.org/10.1029/1999JD900923, 1999.
96. Elsey, J., Bellouin, N., and Ryder, C.: Sensitivity of global direct aerosol shortwave radiative forcing to uncertainties in aerosol optical properties, Atmos. Chem. Phys., 24, 4065–4081, https://doi.org/10.5194/acp-24-4065-2024, 2024.
97. Eltbaakh, Y. A., Ruslan, M. H., Alghoul, M. A., Othman, M. Y., Sopian, K., and Razykov, T. M.: Solar attenuation by aerosols: An overview, Renew. Sustain. Energy Rev., 16, 4264–4276, https://doi.org/10.1016/j.rser.2012.03.053, 2012.
98. ESA STATISTICS and ACtIon4Cooling: Conclusions from the STATISTICS/ACtIon4Cooling workshop on solar radiation modification techniques, workshop held 17 June 2025, 2025. https://climate.esa.int/en/solar-radiation-modification/action4cooling/srm-workshop-conclusions/, [accessed: 10/10/2026]
99. Escribano, J., Di Tomaso, E., Jorba, O., Klose, M., Gonçalves Ageitos, M., Macchia, F., Amiridis, V., Baars, H., Marinou, E., Proestakis, E., Urbanneck, C., Althausen, D., Bühl, J., Mamouri, R.-E., and Pérez García-Pando, C.: Assimilating spaceborne lidar dust extinction can improve dust forecasts, Atmos. Chem. Phys., 22, 535–560, https://doi.org/10.5194/acp-22-535-2022, 2022.
100. Eskes, H., Tsikerdekis, A., Ades, M., et al.: Technical note: evaluation of the Copernicus Atmosphere Monitoring Service Cy48R1 upgrade of June 2023, EGUsphere [preprint], https://doi.org/10.5194/egusphere-2023-3129, 2024.
101. Estellés, V., Campanelli, M., Smyth, T. J., Utrillas, M. P., and Martínez-Lozano, J. A.: Evaluation of the new ESR network software for the retrieval of direct sun products from CIMEL CE318 and PREDE POM01 sun-sky radiometers, Atmos. Chem. Phys., 12, 11619–11630, https://doi.org/10.5194/acp-12-11619-2012, 2012.

102. Fahey, D. W., Kawa, S. R., Woodbridge, E. L., Tin, P., Wilson, J. C., Jonsson, H. H., Dye, J. E., Baumgardner, D., Borrmann, S., Toohey, D. W., Avallone, L. M., Proffitt, M. H., Margitan, J., Loewenstein, M., Podolske, J. R., Salawitch, R. J., Wofsy, S. C., Ko, M. K. W., Anderson, D. E., Schoeber, M. R., and others: In situ measurements constraining the role of sulphate aerosols in mid-latitude ozone depletion, Nature, 363, 509–514, https://doi.org/10.1038/363509a0, 1993.
103. Fan, R., Ma, Y., Jin, S., Gong, W., Liu, B., Wang, W., Li, H., and Zhang, Y.: Validation, analysis, and comparison of MISR V23 aerosol optical depth products with MODIS and AERONET observations, Sci. Total Environ., 856, 159117, https://doi.org/10.1016/j.scitotenv.2022.159117, 2023.
104. Flemming, J., Inness, A., Flentje, H., et al.: Coupling global chemistry transport models to ECMWF's Integrated Forecast System, Geosci. Model Dev., 10, 1483–1499, https://doi.org/10.5194/gmd-10-1483-2017, 2017.
105. Fougnie, B., Bracco, G., Lafrance, B., and Leroy, M.: 3MI instrument: multi-viewing, multi-channel, multi-polarization imager for MetOp-SG, J. Quant. Spectrosc. Radiat. Transfer, 219, 218–230, https://doi.org/10.1016/j.jqsrt.2018.07.008, 2018.
106. Fountoulakis, I., Bais, A. F., Fragkos, K., Meleti, C., and Zerefos, C. S.: UV aerosol optical depth measurements and related aerosol properties, Atmos. Meas. Tech., 12, 169–181, https://doi.org/10.5194/amt-12-169-2019, 2019.
107. Fountoulakis, I., Bais, A. F., Fragkos, K., Meleti, C., Tourpali, K., and Zempila, M. M.: Short- and long-term variability of spectral solar UV irradiance at Thessaloniki, Greece: effects of changes in aerosols, total ozone and clouds, Atmos. Chem. Phys., 16, 2493–2505, https://doi.org/10.5194/acp-16-2493-2016, 2016.
108. Fountoulakis, I., Kosmopoulos, P., Papachristopoulou, K., Raptis, I.-P., Mamouri, R.-E., Nisantzi, A., Gkikas, A., Witthuhn, J., Bley, S., Moustaka, A., Buehl, J., Seifert, P., Hadjimitsis, D. G., Kontoes, C., and Kazadzis, S.: Effects of aerosols and clouds on the levels of surface solar radiation and solar energy in Cyprus, Remote Sensing, 13, 2319, https://doi.org/10.3390/rs13122319, 2021.
109. Fountoulakis, I., Natsis, A., Siomos, N., Drosoglou, T., and Bais, A. F.: Deriving Aerosol Absorption Properties from Solar Ultraviolet Radiation Spectral Measurements at Thessaloniki, Greece, Remote Sensing, 11, 2179, https://doi.org/10.3390/rs11182179, 2019. [Source: Word comment reference [GC3]]
110. Fountoulakis, I., Papachristopoulou, K., Kazadzis, S., Hülsen, G., Gröbner, J., Raptis, I.-P., Kouklaki, D., Masoom, A., Kouremeti, N., Kontoes, C., and Zerefos, C. S.: Assessment of the accuracy in UV index modelling using the UVIOS2 system during the UVC-III campaign, Geosci. Model Dev., 18, 7451–7473, 2025. https://doi.org/10.5194/gmd-18-7451-2025
111. Fountoulakis, I., Tsekeri, A., Kazadzis, S., and others: A sensitivity study on radiative effects due to the parameterization of dust optical properties in models, Atmos. Chem. Phys., 24, 4915–4948, https://doi.org/10.5194/acp-24-4915-2024, 2024.

112. Fröhlich-Nowoisky, J., Kampf, C. J., Weber, B., Huffman, J. A., Pöhlker, C., Andreae, M. O., Lang-Yona, N., Burrows, S. M., Gunthe, S. S., and others: Bioaerosols in the Earth system: Climate, health, and ecosystem interactions, Atmos. Res., 182, 346–376, https://doi.org/10.1016/j.atmosres.2016.07.018, 2016.
113. Fu, G., et al.: Aerosol retrieval and validation using SPEXone observations, Geophys. Res. Lett., https://doi.org/10.1029/2024GL113525, 2025. [Full author list and title require confirmation against the DOI record.]
114. Fu, Y., Zhang, X., Li, Z., et al.: Satellite aerosol remote sensing and applications, Atmos. Meas. Tech., 16, 5863–5880, https://doi.org/10.5194/amt-16-5863-2023, 2023.
115. Garay, M. J., Kalashnikova, O. V., and Bull, M. A.: Development and assessment of a higher-spatial-resolution (4.4 km) MISR aerosol optical depth product using AERONET-DRAGON data, Atmos. Chem. Phys., 17, 5095–5106, https://doi.org/10.5194/acp-17-5095-2017, 2017.
116. García, R. D., Barreto, Á., Rey, C., Fraile-Nuez, E., González-Vega, A., León-Luis, S. F., Alcantara, A., Almansa, A. F., Guirado-Fuentes, C., González-Sicilia, P., Cachorro, V. E., and Bouchar, F.: Aerosol retrievals derived from a low-cost Calitoo sun-photometer taken on board a research vessel, Atmos. Environ., 341, 120888, https://doi.org/10.1016/j.atmosenv.2024.120888, 2025.
117. García-Pando, C. P., Thomson, M. C., Stanton, M. C., Diggle, P. J., Hopson, T., Pandya, R., Miller, R. L., and Hugonnet, S.: Meningitis and climate: From science to practice, Earth Perspect., 1, 14, https://doi.org/10.1186/2194-6434-1-14, 2014.
118. GCOS: The Global Climate Observing System Implementation Plan 2022, GCOS-244, World Meteorological Organization, Geneva, 2022.
119. Gelaro, R., McCarty, W., Suárez, M. J., Todling, R., Molod, A., Takacs, L., et al.: The Modern-Era Retrospective Analysis for Research and Applications, Version 2 (MERRA-2), J. Clim., 30, 5419–5454, https://doi.org/10.1175/JCLI-D-16-0758.1, 2017.
120. Giannadaki, D., Pozzer, A., and Lelieveld, J.: Modeled global effects of airborne desert dust on air quality and premature mortality, Atmos. Chem. Phys., 14, 957–968, https://doi.org/10.5194/acp-14-957-2014, 2014.
121. Gidarakou, M., Papayannis, A., Mylonaki, M., Kralli, E., Eleftheratos, K., Fountoulakis, I., Zografou, O., Diapouli, E., Gini, M. I., Vratolis, S., Granakis, K., Eleftheriadis, K., Evangeliou, N., Groot Zwaaftink, C., Giagka, E., Zagklis, M.-A., and Veselovskii, I.: Exceptional wildfire smoke over Greece in summer 2023: A synergistic study of aerosol optical-microphysical and UVB radiative impacts, Atmos. Chem. Phys., 26, 4313–4339, https://doi.org/10.5194/acp-26-4313-2026, 2026.
122. Gkikas, A., Proestakis, E., Amiridis, V., Kazadzis, S., Di Tomaso, E., Marinou, E., Hatzianastassiou, N., Kok, J. F., and Pérez García-Pando, C.: Quantification of the dust optical depth across spatiotemporal scales with the MIDAS global dataset (2003–2017), Atmos. Chem. Phys., 22, 3553–3578, https://doi.org/10.5194/acp-22-3553-2022, 2022.

123. Gkikas, A., Proestakis, E., Amiridis, V., Kazadzis, S., Hatzianastassiou, N., Katsanos, D., and Papadimas, C. D.: ModIs Dust AeroSol (MIDAS): a global fine-resolution dust optical depth data set, Atmos. Meas. Tech., 14, 309–336, https://doi.org/10.5194/amt-14-309-2021, 2021.
124. Gliß, J., Schmidt, J., Schuster, G. L., et al.: Evaluation of aerosol optical depth from global aerosol models and reanalyses, Atmos. Chem. Phys., 21, 87–112, https://doi.org/10.5194/acp-21-87-2021, 2021.
125. González, R., Toledano, C., Román, R., Fuertes, D., Berjón, A., Mateos, D., Guirado-Fuentes, C., Velasco-Merino, C., Antuña-Sánchez, J. C., Calle, A., Cachorro, V. E., and de Frutos, Á. M.: Daytime and nighttime aerosol optical depth implementation in CÆLIS, Geosci. Instrum. Method. Data Syst., 9, 417–433, https://doi.org/10.5194/gi-9-417-2020, 2020.
126. Goudie, A. S.: Desert dust and human health disorders, Environment International, 63, 101–113, https://doi.org/10.1016/j.envint.2013.10.011
127. Granados-Muñoz, M. J., Sicard, M., Román, R., Benavent-Oltra, J. A., Barragán, R., Brogniez, G., Denjean, C., Mallet, M., Formenti, P., Torres, B., and Alados-Arboledas, L.: Impact of mineral dust on shortwave and longwave radiation: evaluation of different vertically resolved parameterizations in 1-D radiative transfer computations, Atmospheric Chemistry and Physics, 19, 523–542, https://doi.org/10.5194/acp-19-523-2019, 2019.
128. Gratsea, M., Kazadzis, S., Bais, A., et al.: Aerosol optical depth retrievals from Brewer measurements, Atmos. Meas. Tech., 14, 749–764, https://doi.org/10.5194/amt-14-749-2021, 2021.
129. Graßl, S., Ritter, C., Wilsch, J., et al. (2024). From Polar Day to Polar Night: A Comprehensive Sun and Star Photometer Study of Trends in Arctic Aerosol Properties in Ny-Ålesund, Svalbard. Remote Sensing, 16(19), 3725. https://doi.org/10.3390/rs16193725.
130. Groot Zwaaftink, C. D., H. Grythe, H. Skov, and A. Stohl, 2016. Substantial contribution of northern high-latitude sources to mineral dust in the Arctic, Journal of Geophysical Research: Atmospheres, 121(22), 13,678-613.
131. Groß, S., Gasteiger, J., Freudenthaler, V., Schnell, F., and Wiegner, M.: Characterization of Saharan dust, marine aerosols and mixtures of biomass-burning aerosols and dust by means of multi-wavelength Raman lidar measurements during SAMUM 2, Tellus B, 63, 706–724, https://doi.org/10.3402/tellusb.v63i4.16320, 2011. [Potential match only; verify against the intended Groß et al. (2016) citation.]
132. Gröbner, J., Kazadzis, S., Kouremeti, N., et al.: Characterization of precision filter radiometers for aerosol optical depth observations, Atmos. Meas. Tech., 16, 4667–4681, https://doi.org/10.5194/amt-16-4667-2023, 2023.
133. Grönholm, T., Launiainen, S., Ahlm, L., Mårtensson, E. M., Kulmala, M., Vesala, T., and Nilsson, E. D.: Aerosol particle dry deposition to canopy and forest floor measured by

two-layer eddy covariance system, Journal of Geophysical Research: Atmospheres, 114, D04202, https://doi.org/10.1029/2008JD010663, 2009.

134. Gu, L., Baldocchi, D. D., Verma, S. B., Black, T. A., Vesala, T., Falge, E. M., and Dowty, P. R.: Advantages of diffuse radiation for terrestrial ecosystem productivity, Journal of Geophysical Research: Atmospheres, 107, ACL 2-1–ACL 2-23, https://doi.org/10.1029/2001JD001242, 2002.
135. Gueymard, C. A.: Critical analysis and performance assessment of clear sky solar irradiance models using theoretical and measured data, Sol. Energy, 51, 121–138, https://doi.org/10.1016/0038-092X(93)90074-X, 1993.
136. Gueymard, C. A.: Temporal variability in direct and global irradiance at various time scales as affected by aerosols, Solar Energy, 86, 3544–3553, https://doi.org/10.1016/j.solener.2012.01.013, 2012.
137. Gueymard, C. A. and Yang, D.: Worldwide validation of CAMS and MERRA-2 reanalysis aerosol optical depth products using 15 years of AERONET observations, Atmos. Environ., 225, 117216, https://doi.org/10.1016/j.atmosenv.2019.117216, 2020.
138. Gueymard, C., Habte, A., and Sengupta, M.: Reducing uncertainties in large-scale solar resource data: the impact of aerosols, IEEE J. Photovolt., 9, 746–753, https://doi.org/10.1109/JPHOTOV.2018.2869554, 2019.
139. Haeffelin, M., Laffineur, Q., Bravo-Aranda, J.-A., Drouin, M.-A., Casquero-Vera, J.-A., Dupont, J.-C., and De Backer, H.: Radiation fog formation alerts using attenuated backscatter power from automatic lidars and ceilometers, Atmos. Meas. Tech., 9, 5347–5365, https://doi.org/10.5194/amt-9-5347-2016, 2016.
140. Hamill, P., Giordano, M., Ward, C., Giles, D., and Holben, B.: An AERONET-based aerosol classification using the Mahalanobis distance, Atmos. Environ., 140, 213–233, https://doi.org/10.1016/j.atmosenv.2016.06.002, 2016.
141. Hanrieder, N., Wilbert, S., Mancera-Guevara, D., Buck, R., Giuliano, S., and Pitz-Paal, R.: Atmospheric extinction in solar tower plants – A review, Solar Energy, 152, 193–207, https://doi.org/10.1016/j.solener.2017.01.013, 2017.
142. Hassinen, S., Balis, D., Bauer, H., Begoin, M., Delcloo, A., Eleftheratos, K., Gimeno Garcia, S., Granville, J., Grossi, M., Hao, N., Hedelt, P., Hendrick, F., Hess, M., Heue, K.-P., Hovila, J., Jønch-Sørensen, H., Kalakoski, N., Kauppi, A., Kiemle, S., Kins, L., Koukouli, M. E., Kujanpää, J., Lambert, J.-C., Lang, R., Lerot, C., Loyola, D., Pedergnana, M., Pinardi, G., Romahn, F., van Roozendael, M., Lutz, R., De Smedt, I., Stammes, P., Steinbrecht, W., Tamminen, J., Theys, N., Tilstra, L. G., Tuinder, O. N. E., Valks, P., Zerefos, C., Zimmer, W., and Zyrichidou, I.: Overview of the O3M SAF GOME-2 operational atmospheric composition and UV radiation data products and data availability, Atmos. Meas. Tech., 9, 383–407, https://doi.org/10.5194/amt-9-383-2016, 2016.
143. Hauser, A., Oesch, D., and Foppa, N.: Aerosol optical depth over land derived from NOAA AVHRR, Geophys. Res. Lett., 32, L17811,

https://doi.org/10.1029/2005GL023579, 2005. [Title wording and author list should be checked against the publisher record.]

144. Hauser, A., Oesch, D., Foppa, N., and Wunderle, S.: NOAA AVHRR derived aerosol optical depth over land, J. Geophys. Res., 110, D08204, https://doi.org/10.1029/2004JD005439, 2005.
145. He, L., Wang, L., Lin, A., Zhang, M., and Xia, X.: VIIRS Environmental Data Record and Deep Blue aerosol products: validation, comparison, and spatiotemporal variations from 2013 to 2018 in China, Atmos. Environ., 2021. [Volume, pages, DOI, and complete author list still need verification.]
146. Herman, J., et al.: Pandora spectrometer measurements, Appl. Opt., 47, H182–H..., https://doi.org/10.1364/AO.47.00H182, 2009.
147. Herman, M., Deuzé, J.-L., Marchand, A., Roger, B., and Lallart, P.: Aerosol remote sensing from POLDER/ADEOS over the ocean: Improved retrieval using a nonspherical particle model, J. Geophys. Res., 110, D10S02, https://doi.org/10.1029/2004JD004798, 2005.
148. Hernandez-Galindo, I., Määttänen, A., Redmond Roche, B. H., Boucher, O., Irvine, P. J., and Moore, J. C.: Past field experiments of solar radiation modification: A review of the scientific and technical aspects for governance, Earth's Future, 14, e2025EF007254, https://doi.org/10.1029/2025EF007254, 2026.
149. Herrero del Barrio, C., Román, R., Herrero-Anta, S., González-Fernández, D., Carracedo, R., González, R., Gatón, J., Longarela, B., Antuña-Sánchez, J. C., Mateos, D., Toledano, C., Calle, A., Cachorro, V., and de Frutos, Á.: Cloud height mapping using multi simultaneous sky images from an all-sky camera network, EGUsphere [preprint], https://doi.org/10.5194/egusphere-2026-2694, 2026.
150. Herrero-Anta, M., et al.: [Full title and author list to verify], Atmos. Chem. Phys., 26, https://doi.org/10.5194/acp-26-1435-2026, 2026.
151. Herrero-Anta, S., Román, R., González-Fernández, D., Emde, C., Mateos, D., Herrero del Barrio, C., González, R., Dubovik, O., Toledano, C., Calle, A., Cachorro, V. E., Mayer, B., and de Frutos, Á. M.: Impact of cloud presence on sky radiances and the retrieval of aerosol properties, Atmos. Res., 317, 107938, https://doi.org/10.1016/j.atmosres.2025.107938, 2025.
152. Herrero-Anta, S., Román, R., Mateos, D., González, R., Antuña-Sánchez, J. C., et al.: Retrieval of aerosol properties from zenith sky radiance measurements, Atmos. Meas. Tech., 16, 4423–4443, https://doi.org/10.5194/amt-16-4423-2023, 2023.
153. Hicks, B. B., Saylor, R. D., and Baker, B. D.: Dry deposition of particles to canopies—a look back and the road forward, Journal of Geophysical Research: Atmospheres, 121, 14691–14707, https://doi.org/10.1002/2015JD024742, 2016.
154. Hioki, S., Riedi, J., and Djellali, M. S.: A study of polarimetric error induced by satellite motion: application to the 3MI and similar sensors, Atmos. Meas. Tech., 14, 1801–1814, https://doi.org/10.5194/amt-14-1801-2021, 2021.

155. Holben, B. N., Eck, T. F., Slutsker, I., Tanré, D., Buis, J. P., Setzer, A., Vermote, E., Reagan, J. A., Kaufman, Y. J., Nakajima, T., Lavenu, F., Jankowiak, I., and Smirnov, A.: AERONET – a federated instrument network and data archive for aerosol characterization, Remote Sens. Environ., 66, 1–16, https://doi.org/10.1016/S0034-4257(98)00031-5, 1998.
156. Hrabčák, P.: Comparison of the optical depth of total ozone and atmospheric aerosols in Poprad-Gánovce, Slovakia, Atmos. Chem. Phys., 18, 7739–7755, https://doi.org/10.5194/acp-18-7739-2018, 2018.
157. Hrabčák, P., Garcia-Suñer, M., Matos, V., et al.: 30 years of total column ozone and aerosol optical depth measurements using the Brewer spectrophotometer in Poprad-Gánovce, Slovakia, Atmos. Chem. Phys., 25, 16263–16286, https://doi.org/10.5194/acp-25-16263-2025, 2025.
158. Hsu, N. C., Jeong, M.-J., Bettenhausen, C., Sayer, A. M., Hansell, R., Seftor, C. S., Huang, J., and Tsay, S.-C.: Enhanced Deep Blue aerosol retrieval algorithm: The second generation, J. Geophys. Res.-Atmos., 118, 9296–9315, https://doi.org/10.1002/jgrd.50712, 2013.
159. Hsu, N. C., Lee, J., Sayer, A. M., Kim, W., Bettenhausen, C., and Tsay, S.-C.: VIIRS Deep Blue aerosol products over land: Extending the EOS long-term aerosol data records, J. Geophys. Res.-Atmos., 124, 4026–4053, https://doi.org/10.1029/2018JD029688, 2019.
160. Huang, J., Kondragunta, S., Laszlo, I., Liu, H., Remer, L. A., Zhang, H., Superczynski, S., Ciren, P., Holben, B. N., and Petrenko, M.: Validation and expected error estimation of Suomi-NPP VIIRS aerosol optical thickness and Ångström exponent with AERONET, J. Geophys. Res. Atmos., 121, 7139–7160, https://doi.org/10.1002/2016JD024834, 2016.
161. Huang, Y., Kok, J. F., Saito, M., and Muñoz, O.: Single-scattering properties of ellipsoidal dust aerosols constrained by measured dust shape distributions, Atmos. Chem. Phys., 23, 2557–2577, https://doi.org/10.5194/acp-23-2557-2023, 2023.
162. Huynh, H. N., and McNeill, V. F.: The potential environmental and climate impacts of stratospheric aerosol injection: A review, Environmental Science: Atmospheres, 4, 114–143, https://doi.org/10.1039/D3EA00134B, 2024.
163. Hünerbein, A., Donovan, D. P., et al.: EarthCARE aerosol and cloud retrieval products, Atmos. Meas. Tech., 17, 261–277, https://doi.org/10.5194/amt-17-261-2024, 2024.
164. ICAO: Manual on Low-Level Wind Shear and Turbulence, Doc 9817, International Civil Aviation Organization, Montreal, 2005 (first edition; the manuscript's 2019 date may refer to a later update or access date).
165. Ichoku, C., Remer, L. A., and Eck, T. F.: Quantitative evaluation and intercomparison of morning and afternoon MODIS aerosol optical depth retrievals from Terra and Aqua, J. Geophys. Res., 107, 4056, https://doi.org/10.1029/2001GL013206, 2002.

166. Ichoku, C., Remer, L. A., Eck, T. F., and Holben, B. N.: Intercomparison of aerosol optical thickness measurements from satellite and ground-based sun photometers, J. Geophys. Res., 107, AAC 1–AAC 20, https://doi.org/10.1029/2001JD001302, 2002.
167. Illingworth, A. J., Barker, H. W., Beljaars, A., et al.: The EarthCARE satellite mission—The next step forward in global measurements of clouds, aerosols, precipitation, and radiation, Bull. Am. Meteorol. Soc., 96, 1311–1332, https://doi.org/10.1175/BAMS-D-12-00227.1, 2015.
168. Ingels, M. W., Botzen, W. J. W., Aerts, J. C. J. H., Brusselaers, J., and Tesselaar, M.: The state of the art and future of climate risk insurance modeling, Annals of the New York Academy of Sciences, 1541, 100–114, https://doi.org/10.1111/nyas.15255, 2024.
169. Inness, A., Ades, M., Agustí-Panareda, A., Barré, J., Benedictow, A., Blechschmidt, A.-M., Dominguez, J. J., Engelen, R., Eskes, H., Flemming, J., Huijnen, V., Jones, L., Kipling, Z., Massart, S., Parrington, M., Peuch, V.-H., Razinger, M., Remy, S., Schulz, M., and Suttie, M.: The CAMS reanalysis of atmospheric composition, Atmos. Chem. Phys., 19, 3515–3556, https://doi.org/10.5194/acp-19-3515-2019, 2019.
170. IPCC: Climate Change 2013: The Physical Science Basis, Contribution of Working Group I to the Fifth Assessment Report of the Intergovernmental Panel on Climate Change, Cambridge University Press, Cambridge, UK and New York, NY, USA, 2013.
171. IPCC: Climate Change 2021: The Physical Science Basis, Contribution of Working Group I to the Sixth Assessment Report of the Intergovernmental Panel on Climate Change, Cambridge University Press, Cambridge, UK and New York, NY, USA, https://doi.org/10.1017/9781009157896, 2021.
172. IPCC: Climate Change 2023: Synthesis Report, Contribution of Working Groups I, II and III to the Sixth Assessment Report of the Intergovernmental Panel on Climate Change [Core Writing Team, H. Lee and J. Romero (eds.)], IPCC, Geneva, Switzerland, 2023, https://doi.org/10.59327/IPCC/AR6-9789291691647, 2023.
173. Iqbal, M.: An Introduction to Solar Radiation, Academic Press, Toronto, Canada, 408 pp., https://doi.org/10.1016/B978-0-12-373750-2.X5001-0, 1983.
174. Irie, H., Kanaya, Y., Akimoto, H., Iwabuchi, H., Shimizu, A., and Aoki, K.: Dual-wavelength aerosol vertical profile measurements by MAX-DOAS at Tsukuba, Japan, Atmos. Chem. Phys., 9, 2741–2749, https://doi.org/10.5194/acp-9-2741-2009, 2009.
175. Irrgang, C., Boers, N., Sonnewald, M., et al.: Toward neural Earth system modelling by integrating artificial intelligence in Earth system science, Nat. Mach. Intell., 3, 667–674, https://doi.org/10.1038/s42256-021-00374-3, 2021. (Second Irrgang et al. 2021 record explicitly supplied in the comments.)
176. Irrgang, C., Boers, N., Sonnewald, M., et al.: Towards trustworthy machine learning for Earth system science, Nat. Mach. Intell., 3, 792–802, https://doi.org/10.1038/s42256-021-00398-9, 2021.

177. Ivănescu, L., Baibakov, K., O'Neill, N. T., Blanchet, J.-P., and Schulz, K.-H.: Accuracy in starphotometry, Atmos. Meas. Tech., 14, 6561–6599, https://doi.org/10.5194/amt-14-6561-2021, 2021.
178. Jackson, J. M., Liu, H., Laszlo, I., Kondragunta, S., Remer, L. A., Huang, J., and Huang, H.-C.: Suomi-NPP VIIRS aerosol algorithms and data products, J. Geophys. Res. Atmos., 118, 12673–12689, 2013. (DOI not confirmed from the supplied comments.)
179. Jackson, J. M., Liu, H., Laszlo, I., Kondragunta, S., Remer, L. A., Huang, J., and Huang, H.-C.: Suomi-NPP VIIRS aerosol algorithms and data products, J. Geophys. Res.-Atmos., 118, 12673–12689, https://doi.org/10.1002/2013JD020449, 2013.
180. Jensen, E., Jónsdóttir, I., Sveinbjörnsson, E., Sigþórsson, H., Dagsson-Waldhauserová, P., 2019. Sandfok og Umferðaröryggi |Dust storms and road safety|. Skýrsla Vegagerðarinnar, 38 p.Kylling A., Groot Zwaaftink, C. D., Stohl, A., 2018. Mineral dust instantaneous radiative forcing in the Arctic. Geophysical Research Letters, 45. doi: 10.1029/2018GL077346.
181. Jethva, H., and Torres, O.: Retrieval of aerosol properties from satellite ultraviolet observations, 2019.
182. Jiang, X., Liu, Y., Yu, B., and Jiang, M.: Validation of MISR aerosol optical depth against ground-based observations, 2007. [Title and publication metadata require verification.]
183. Jickells, T. D., An, Z. S., Andersen, K. K., et al.: Global iron connections between desert dust, ocean biogeochemistry, and climate, Science, 308, 67–71, https://doi.org/10.1126/science.1105959, 2005.
184. Jickells, T. D., Baker, A. R., and Chance, R.: Atmospheric transport of trace elements and nutrients to the oceans, Philosophical Transactions of the Royal Society A, 374, 20150286, https://doi.org/10.1098/rsta.2015.0286, 2016.
185. Jickells, T. D., Buitenhuis, E., Altieri, K., et al.: A reevaluation of the magnitude and impacts of anthropogenic atmospheric nitrogen inputs on the ocean, Global Biogeochemical Cycles, 31, 289–305, https://doi.org/10.1002/2016GB005586, 2017.
186. Jiménez, P. A., and co-authors: WRF-Solar: Description and clear-sky assessment of an augmented NWP model for solar power prediction, Bulletin of the American Meteorological Society, 97, 1249–1264, https://doi.org/10.1175/BAMS-D-14-00279.1, 2016. [Check whether the citation refers to this WRF-Solar paper or another Jiménez et al. (2016) paper.]
187. Jin, J., Henzing, B., and Segers, A.: How aerosol size matters in aerosol optical depth (AOD) assimilation and the optimization using the Ångström exponent, Atmos. Chem. Phys., 23, 1641–1660, https://doi.org/10.5194/acp-23-1641-2023, 2023.
188. Jónsdóttir, A. A.: Impact of Eyjafjallajökull on tourism and international flights, doctoral dissertation, University of Iceland, 2011.

189. Kahn, R. A. and Gaitley, B. J.: An analysis of global aerosol type as retrieved by MISR, J. Geophys. Res. Atmos., 120, 4248–4281, https://doi.org/10.1002/2015JD023322, 2015.
190. Kahn, R. A., et al.: Multiangle Imaging Spectroradiometer global aerosol optical depth validation based on two years of coincident AERONET observations, J. Geophys. Res., 110, D10S04, https://doi.org/10.1029/2004JD004706, 2005.
191. Kahn, R. A., Garay, M. J., Nelson, D. L., Yau, K. K., Bull, M. A., Gaitley, B. J., Martonchik, J. V., and Levy, R. C.: Satellite-derived aerosol optical depth over dark water from MISR and MODIS: Comparisons with AERONET and implications for climatological studies, J. Geophys. Res., 112, D18205, https://doi.org/10.1029/2006JD008175, 2007.
192. Kahn, R. A., Pinty, B., Gobron, N., et al.: Aerosol remote sensing from space: current status and future directions, Rev. Geophys., 61, e2022RG000796, https://doi.org/10.1029/2022RG000796, 2023.
193. Kanakidou, M., Duce, R. A., Prospero, J. M., Baker, A. R., Benitez-Nelson, C., Dentener, F. J., Hunter, K. A., Liss, P. S., Mahowald, N., Okin, G. S., Sarin, M., Tsigaridis, K., Uematsu, M., Zamora, L. M., and Zhu, T.: Atmospheric fluxes of organic N and P to the global ocean, Global Biogeochemical Cycles, 26, GB3026, https://doi.org/10.1029/2011GB004277, 2012.
194. Kanakidou, M., Seinfeld, J. H., Pandis, S. N., Barnes, I., Dentener, F. J., Facchini, M. C., Van Dingenen, R., Ervens, B., Nenes, A., Nielsen, C. J., Swietlicki, E., Putaud, J. P., Balkanski, Y., Fuzzi, S., Horth, J., Moortgat, G. K., Winterhalter, R., Myhre, C. E. L., Tsigaridis, K., Vignati, E., Stephanou, E. G., and Wilson, J.: Organic aerosol and global climate modelling: A review, Atmos. Chem. Phys., 5, 1053–1123, https://doi.org/10.5194/acp-5-1053-2005, 2005.
195. Kanniah, K. D., Beringer, J., North, P., and Hutley, L.: Control of atmospheric particles on diffuse radiation and vegetation productivity in a tropical savanna, Atmos. Environ., [bibliographic details to be verified], 2012.
196. Karagkiozidis, D., Friedrich, M. M., Beirle, S., Bais, A., Hendrick, F., Voudouri, K. A., et al.: Retrieval of tropospheric aerosol, NO2, and HCHO vertical profiles from MAX-DOAS observations over Thessaloniki, Greece: intercomparison and validation of two inversion algorithms, Atmos. Meas. Tech., 15, 1269–1301, https://doi.org/10.5194/amt-15-1269-2022, 2022.
197. Karanikolas, A., Kouremeti, N., Campanelli, M., Estellés, V., Momoi, M., Kumar, G., Nyeki, S., and Kazadzis, S.: Intercomparison of aerosol optical depth retrievals from GAW-PFR and SKYNET sun photometer networks and the effect of calibration, Atmos. Meas. Tech., 17, 6085–6105, https://doi.org/10.5194/amt-17-6085-2024, 2024.
198. Karanikolas, A., Torres, B., Momoi, M., Herreras Giralda, M., Kouremeti, N., Gröbner, J., Doppler, L., and Kazadzis, S.: Retrieval of aerosol properties from aerosol

optical depth measurements with high temporal resolution and spectral range, Atmos. Meas. Tech., 18, 7651–7669, https://doi.org/10.5194/amt-18-7651-2025, 2025.

199. Kaskaoutis, D. G., Kambezidis, H. D., Hatzianastassiou, N., Kosmopoulos, P. G., and Badarinath, K. V. S.: Aerosol climatology: dependence of the Angstrom exponent on wavelength over four AERONET sites, Atmos. Chem. Phys., 7, 7347–7360, https://doi.org/10.5194/acpd-7-7347-2007, 2007.
200. Kasten, F. and Young, A. T.: Revised optical air mass tables and approximation formula, Appl. Opt., 28, 4735–4738, https://doi.org/10.1364/AO.28.004735, 1989.
201. Kazadzis, S., Bais, A. F., Balis, D. S., Zerefos, C. S., and others: Retrieval of downwelling UV actinic flux density spectra from spectral measurements of global and direct solar UV irradiance, J. Geophys. Res. Atmos., 105, 4857–4864, 2000. https://doi.org/10.1029/1999JD900400
202. Kazadzis, S., Bais, A. F., Kouremeti, N., Gerasopoulos, E., Garane, K., Blumthaler, M., Schallhart, B., and Cede, A.: Direct spectral measurements with a Brewer spectroradiometer: absolute calibration and aerosol optical depth retrieval, Appl. Opt., 44, 1681–1690, https://doi.org/10.1364/AO.44.001681, 2005.
203. Kazadzis, S., Bais, A., Amiridis, V., Balis, D., Meleti, C., Kouremeti, N., Zerefos, C. S., Rapsomanikis, S., Petrakakis, M., Kelesis, A., Tzoumaka, P., and Kelektsoglou, K.: Nine years of UV aerosol optical depth measurements at Thessaloniki, Greece, Atmos. Chem. Phys., 7, 2091–2101, https://doi.org/10.5194/acp-7-2091-2007, 2007.
204. Kazadzis, S., Kouremeti, N., Bais, A., Kazantzidis, A., and Meleti, C.: Aerosol forcing efficiency in the UVA region from spectral solar irradiance measurements at an urban environment, Annales Geophysicae, 27, 2515–2522, https://doi.org/10.5194/angeo-27-2515-2009, 2009.
205. Kazadzis, S., Kouremeti, N., Nyeki, S., Gröbner, J., and Wehrli, C.: The World Optical Depth Research and Calibration Center (WORCC) quality assurance and quality control of GAW-PFR AOD measurements, Geosci. Instrum. Methods Data Syst., 7, 39–53, https://doi.org/10.5194/gi-7-39-2018, 2018.
206. Kazantzidis, A., Balis, D. S., Bais, A. F., Kazadzis, S., Galani, E., Kosmidis, E., and Blumthaler, M.: Comparison of model calculations with spectral UV measurements during the SUSPEN campaign: The effect of aerosols, J. Atmos. Sci., 58, 1529–1539, 2001. https://doi.org/10.1175/1520-0469(2001)058<1529:COMCWS>2.0.CO;2
207. Khatri, P. and Takamura, T.: An algorithm to screen cloud-affected data for sky radiometer data analysis, J. Meteorol. Soc. Jpn., 87, 189–204, https://doi.org/10.2151/jmsj.87.189, 2009.
208. Khatri, P. and Takamura, T.: Factors affecting sky radiance calibration and aerosol retrievals from SKYNET observations, Atmos. Meas. Tech., 4, 2685–2697, https://doi.org/10.5194/amt-4-2685-2011, 2011.
209. Khatri, P., Iwabuchi, H., Hayasaka, T., Irie, H., Takamura, T., Yamazaki, A., Damiani, A., Letu, H., and Kai, Q.: Retrieval of cloud properties from spectral zenith radiances

observed by sky radiometers, Atmos. Meas. Tech., 12, 6037–6047, https://doi.org/10.5194/amt-12-6037-2019, 2019.

210. Khatri, P., Takamura, T., Shimizu, A., and Sugimoto, N.: Factors for inconsistent aerosol single scattering albedo between SKYNET and AERONET, J. Geophys. Res. Atmos., 121, 1859–1877, https://doi.org/10.1002/2015JD023976, 2016.
211. Khatri, P., Takamura, T., Yamazaki, A., and Uchiyama, A.: Use of 315 nm channel data of the sky radiometer to estimate the columnar ozone concentration: a preliminary study, J. Meteorol. Soc. Jpn., 92A, 185–194, https://doi.org/10.2151/jmsj.2014-A12, 2014.
212. Kikuchi, N., Nakajima, T., Kumagai, H., Kuroiwa, H., Kamei, A., Nakamura, R., and Nakajima, T. Y.: Cloud optical thickness and effective particle radius derived from transmitted solar radiation measurements: comparison with cloud radar observations, J. Geophys. Res., 111, D07205, https://doi.org/10.1029/2005JD006363, 2006.
213. Kinne, S.: The MACv2 aerosol climatology, Tellus B Chem. Phys. Meteorol., 71, 1623639, https://doi.org/10.1080/16000889.2019.1623639, 2019.
214. Kinne, S.: The MACv2 aerosol climatology, Tellus B: Chemical and Physical Meteorology, 71, 1663994, https://doi.org/10.1080/16000889.2019.1663994, 2019. [Source: Word comment reference [ID 29]]
215. Klüser, L., Martynenko, D., and Holzer-Popp, T.: Thermal infrared remote sensing of mineral dust over land and ocean: A spectral SVD-based retrieval approach for IASI, Atmos. Meas. Tech., 4, 757–773, https://doi.org/10.5194/amt-4-757-2011, 2011.
216. Kok, J. F., Adebiyi, A. A., Albani, S., and others: Contribution of the World Climate Research Programme Coupled Model Intercomparison Project Phase 6 (CMIP6) to improved dust simulations, Aerosol Sci. Technol., 55, 1–27, 2021.
217. Kok, J. F., Adebiyi, A. A., Albani, S., Balkanski, Y., Checa-Garcia, R., Chin, M., Colarco, P. R., Hamilton, D. S., Huang, Y., Ito, A., Klose, M., Li, L., Mahowald, N. M., Miller, R. L., Obiso, V., Pérez García-Pando, C., Rocha-Lima, A., and Wan, J. S.: Contribution of the world's main dust source regions to the global cycle of desert dust, Atmos. Chem. Phys., 21, 8169–8193, https://doi.org/10.5194/acp-21-8169-2021, 2021.
218. Kokhanovsky, A. A., Bréon, F.-M., Cacciari, A., Carboni, E., Diner, D., Di Nicolantonio, W., Grainger, R. G., Grey, W. M. F., Höller, R., Lee, K.-H., Li, Z., North, P. R. J., Sayer, A. M., Thomas, G. E., and von Hoyningen-Huene, W.: Aerosol remote sensing over land: A comparison of satellite retrievals using different algorithms and instruments, Atmospheric Research, 85, 372–394, https://doi.org/10.1016/j.atmosres.2007.02.008, 2007.
219. Korras-Carraca, M.-B., Hatzianastassiou, N., Matsoukas, C., and Fotiadi, A.: The regime of aerosol asymmetry parameter over Europe, the Mediterranean and the Middle East based on MODIS satellite data: evaluation against surface AERONET measurements, Atmos. Chem. Phys., 15, 13113–13132, https://doi.org/10.5194/acp-15-13113-2015, 2015.

220. Kosmopoulos, P. G., Kazadzis, S., Taylor, M., Athanasopoulou, E., Speyer, O., Raptis, P.-I., Marinou, E., Proestakis, E., Solomos, S., Gerasopoulos, E., Amiridis, V., Bais, A., and Kontoes, C.: Dust impact on surface solar irradiance assessed with model simulations, satellite observations and ground-based measurements, Atmospheric Measurement Techniques, 10, 2435–2453, https://doi.org/10.5194/amt-10-2435-2017, 2017.
221. Kouklaki, D., Charalampous, G., Moustaka, A., Papetta, A., Herrero del Barrio, C., Chadoulis, R.-T., Aslanoğlu, S. Y., Herrero-Anta, S., Mytilinaios, M., Papadimitriou, N., Anyfanti, K., Spyrou, C., Meloni, D., Fragkos, K., Derimian, Y., Di Iorio, T., Mamouri, R.-E., Amiridis, V., Solomos, S., Kazadzis, S., and Fountoulakis, I.: Dust radiative effects and impact on energy production over the Mediterranean Basin, Atmos. Meas. Tech., 19, 5633–5657, https://doi.org/10.5194/amt-19-5633-2026, 2026.
222. Kouklaki, D.; Kazadzis, S.; Raptis, I.-P.; Papachristopoulou, K.; Fountoulakis, I.; Eleftheratos, K. Photovoltaic Spectral Responsivity and Efficiency under Different Aerosol Conditions. *Energies, 16*, 6644. https://doi.org/10.3390/en16186644, 2023.
223. Kremser, S., Thomason, L. W., von Hobe, M., et al.: Stratospheric aerosol—observations, processes, and impact on climate, Reviews of Geophysics, 54, 278–335, https://doi.org/10.1002/2015RG000511, 2016.
224. Krishnaveni, A. S., Madhavan, B. L., and Ratnam, M. V.: Advancing global aerosol classification: source-compositional typology and variability from 30 years (1993–2024) of AERONET observations, Sci. Total Environ., 1007, 180918, https://doi.org/10.1016/j.scitotenv.2025.180918, 2025.
225. Kudo, R., Diémoz, H., Estellés, V., Campanelli, M., Momoi, M., Marenco, F., Ryder, C. L., Ijima, O., Uchiyama, A., Nakashima, K., Yamazaki, A., Nagasawa, R., Ohkawara, N., and Ishida, H.: Optimal use of the Prede POM sky radiometer for aerosol, water vapor, and ozone retrievals, Atmos. Meas. Tech., 14, 3395–3410, https://doi.org/10.5194/amt-14-3395-2021, 2021.
226. Kumar, A., and Mehta, M.: Retrieval and validation of aerosol optical depth from Sentinel-2 imagery, Int. J. Remote Sens., https://doi.org/10.1080/01431161.2024.2421947, 2024.
227. Laj, P., Myhre, C. L., Riffault, V., Amiridis, V., Fuchs, H., Eleftheriadis, K., Petäjä, T., Salameh, T., Kivekäs, N., Juurola, E., Saponaro, G., Philippin, S., Cornacchia, C., Alados Arboledas, L., Baars, H., Claude, A., De Mazière, M., Dils, B., Dufresne, M., Evangeliou, N., Favez, O., Fiebig, M., Haeffelin, M., Herrmann, H., Höhler, K., Illmann, N., Kreuter, A., Ludewig, E., Marinou, E., Möhler, O., Mona, L., Murberg, L. E., Nicolae, D., Novelli, A., O'Connor, E., Ohneiser, K., Petracca Altieri, R. M., Picquet-Varrault, B., van Pinxteren, D., Pospichal, B., Putaud, J.-P., Reimann, S., Siomos, N., Stachlewska, I. S., Tillmann, R., Voudouri, K. A., Wandinger, U., Wiedensohler, A., Apituley, A., Comerón, A., Gysel-Beer, M., Mihalopoulos, N., Nikolova, N., Pietruczuk, A., Sauvage, S., Sciare, J., Skov, H., Svendby, T., Swietlicki, E., Tonev, D., Vaughan, G., Zdimal, V., Baltensperger, U., Doussin, J.-F., Kulmala, M., Pappalardo, G., Sorvari Sundet, S., and

Vana, M.: Aerosol, Clouds and Trace Gases Research Infrastructure (ACTRIS): The European Research Infrastructure Supporting Atmospheric Science, Bull. Am. Meteorol. Soc., 105, E1098–E1136, https://doi.org/10.1175/BAMS-D-23-0064.1, 2024.

228. Lake, I. R., Jones, N. R., Agnew, M., Goodess, C. M., Giorgi, F., Hamaoui-Laguel, L., Semenov, M. A., Solmon, F., Storkey, J., Vautard, R., and Epstein, M. M.: Climate change and future pollen allergy in Europe, Environ. Health Perspect., 125, 385–391, https://doi.org/10.1289/EHP173, 2017.
229. Lange, A., Dykema, J. A., Vattioni, S., Niemeier, U., Rozanov, A., and von Savigny, C.: Detectability of solid particle injections into the stratosphere with satellite solar occultation instruments, Atmospheric Chemistry and Physics, 26, 13055–13067, https://doi.org/10.5194/acp-26-13055-2026, 2026.
230. Lange, A., Niemeier, U., Rozanov, A., and von Savigny, C.: Investigating the ability of satellite occultation instruments to monitor possible geoengineering experiments, Atmospheric Chemistry and Physics, 25, 11673–11688, https://doi.org/10.5194/acp-25-11673-2025, 2025.
231. Lee, D. S., Fahey, D. W., Skowron, A., et al.: The contribution of global aviation to anthropogenic climate forcing for 2000 to 2018, Atmos. Environ., 244, 117834, https://doi.org/10.1016/j.atmosenv.2020.117834, 2021. (Potential source for the manuscript's broad aviation-forcing statement; confirm whether intended instead of the ambiguous Bellouin citations.)
232. Lee, J., Hsu, N. C., Kim, W. V., Sayer, A. M., and Tsay, S.-C.: VIIRS Version 2 Deep Blue aerosol products, J. Geophys. Res.-Atmos., 129, e2023JD040082, https://doi.org/10.1029/2023JD040082, 2024.
233. Lee, W. R., Visioni, D., Wagman, B. M., Wentland, C. R., Kravitz, B., Watanabe, S., Sekiya, T., Jones, A., Haywood, J., Henry, M., and Bednarz, E. M.: G6-1.5K-SAI and G6sulfur: changes in impacts and uncertainty depending on stratospheric aerosol injection strategy in the Geoengineering Model Intercomparison Project, Atmospheric Chemistry and Physics, 26, 7463–7483, https://doi.org/10.5194/acp-26-7463-2026, 2026.
234. Levy, R. C., Mattoo, S., Munchak, L. A., Remer, L. A., Sayer, A. M., and Hsu, N. C.: The Collection 6 MODIS aerosol products over land and ocean, Atmos. Meas. Tech., 6, 2989–3034, https://doi.org/10.5194/amt-6-2989-2013, 2013.
235. Levy, R. C., Remer, L. A., Kleidman, R. G., Mattoo, S., Ichoku, C., Kahn, R., and Eck, T. F.: Global evaluation of the Collection 5 MODIS dark-target aerosol products over land, Atmos. Chem. Phys., 10, 10399–10420, https://doi.org/10.5194/acp-10-10399-2010, 2010.
236. Levy, R. C., Remer, L. A., Mattoo, S., Vermote, E. F., and Kaufman, Y. J.: Global aerosol optical properties and application to Moderate Resolution Imaging Spectroradiometer aerosol retrieval over land, J. Geophys. Res.-Atmos., 112, D13210, https://doi.org/10.1029/2006JD007815, 2007.

237. Li, C., Dubovik, O., Li, J., Fuertes, D., Lopatin, A., Litvinov, P., Lapyonok, T., Bindreiter, L., Matar, C., Chu, Y., and Tan, W.: Retrieval and validation of diurnal properties of aerosol and surface from geostationary satellite Himawari-8 using multi-pixel approach, Atmos. Meas. Tech., 18, 6609–6643, https://doi.org/10.5194/amt-18-6609-2025, 2025.
238. Li, J., Kahn, R. A., Wei, J., Carlson, B. E., Lacis, A. A., Li, Z., Li, X., Dubovik, O., and Nakajima, T.: Synergy of satellite- and ground-based aerosol optical depth measurements using an ensemble Kalman filter approach, J. Geophys. Res.-Atmos., 125, e2019JD031884, https://doi.org/10.1029/2019JD031884, 2020.
239. Li, L., Dubovik, O., Derimian, Y., Lapyonok, T., Litvinov, P., Ducos, F., Fuertes, D., Torres, B., and Chen, C.: Retrieval of aerosol components directly from satellite and ground-based measurements, Atmos. Chem. Phys., 19, 13409–13443, https://doi.org/10.5194/acp-19-13409-2019, 2019.
240. Li, X., Mauzerall, D. L., and Bergin, M. H.: Global reduction of solar power generation efficiency due to aerosols and panel soiling, Nature Sustainability, 3, 720–727, https://doi.org/10.1038/s41893-020-0553-2, 2020.
241. Li, Z., and Ginoux, P.: Satellite-based characterization of aerosol fine-mode fraction, Geophys. Res. Lett., https://doi.org/10.1029/2024GL114397, 2025.
242. Li, Z., Goloub, P., Blarel, L., Damiri, B., Podvin, T., Lecoq, R., B. et al.: Improvements for aerosol retrieval from POLDER polarization measurements, Adv. Space Res., 43, 1999–2006, https://doi.org/10.5194/angeo-27-2755-2009, 2009.
243. Li, Z., Guo, J., Ding, A., Liao, H., Liu, J., Sun, Y., Wang, T., Xue, H., Zhang, H., and Zhu, B.: Aerosol and boundary-layer interactions and impact on air quality, National Science Review, 4, 810–833, https://doi.org/10.1093/nsr/nwx117, 2017.
244. Liou, K.-N.: An Introduction to Atmospheric Radiation, 2nd ed., Academic Press, San Diego, CA, USA, 2002.
245. Litvinov, P., Chen, C., Dubovik, O., Bindreiter, L., Matar, C., Fuertes, D., Lopatin, A., Lapyonok, T., Lanzinger, V., Hangler, A., Aspetsberger, M., de Graaf, M., Tilstra, L. G., Stammes, P., Dandocsi, A., Gasbarra, D., Fluck, E., Zehner, C., and Retscher, C.: Extended aerosol and surface characterization from S5P/TROPOMI with GRASP algorithm. Part I: Conditions, approaches, performance and new possibilities, Remote Sens. Environ., 313, 114355, https://doi.org/10.1016/j.rse.2024.114355, 2024.
246. Litvinov, P., Chen, C., Dubovik, O., Zhai, S., Matar, C., Li, C., Lopatin, A., Fuertes, D., Lapyonok, T., Bindreiter, L., Dornacher, M., Lehner, A., Dandocsi, A., Gasbarra, D., and Retscher, C.: Synergetic retrieval from multi-mission spaceborne measurements for enhanced aerosol and surface characterization, Atmos. Meas. Tech., 18, 7679–7716, https://doi.org/10.5194/amt-18-7679-2025, 2025.
247. Litvinov, P., Dubovik, O., Fuertes, D., et al.: Aerosol and surface characterization using the GRASP retrieval algorithm, 2021.

248. Liu, X., et al.: Retrieval and validation of aerosol optical depth from Sentinel-3 observations, 2021.
249. Logothetis, S.-A.; Giannaklis, C.-P.; Salamalikis, V.; Tzoumanikas, P.; Raptis, P.-I.; Amiridis, V.; Eleftheratos, K.; Kazantzidis, A. Aerosol Optical Properties and Type Retrieval via Machine Learning and an All-Sky Imager. *Atmosphere, 14*, 1266. https://doi.org/10.3390/atmos14081266, 2023.
250. Logothetis, S.-A.; Salamalikis, V.; Kazantzidis, A. A Machine Learning Approach to Retrieving Aerosol Optical Depth Using Solar Radiation Measurements. *Remote Sens., 16*, 1132. https://doi.org/10.3390/rs16071132, 2024.
251. Lokshin, A., Palchan, D., Sternberg, M., Goren, T., Nakhavali, M., and Gross, A.: Atmospheric dust is a global nutrient source for plants via foliar uptake, New Phytologist, 250, 2867–2883, https://doi.org/10.1111/nph.71112, 2026.
252. Lolli, S.: Urban PM2.5 concentration monitoring: A review of recent advances in ground-based, satellite, model, and machine learning integration, Urban Clim., 63, 102566, https://doi.org/10.1016/j.uclim.2025.102566, 2025.
253. Léon, J.-F., Djossou, J., et al.: Aerosol optical properties and particulate matter in West Africa, Atmos. Chem. Phys., 21, 1815–1833, https://doi.org/10.5194/acp-21-1815-2021, 2021.
254. López-Solano, J., Redondas, A., Carlund, T., Rodriguez-Franco, J. J., Diémoz, H., León-Luis, S. F., et al.: Aerosol optical depth in the European Brewer Network, Atmos. Chem. Phys., 18, 3885–3902, https://doi.org/10.5194/acp-18-3885-2018, 2018.
255. Ma, X., et al.: Evaluation of satellite-retrieved aerosol Ångström exponent and optical properties, 2026.
256. Mahowald, N., Engelstaedter, S., Luo, C., et al.: Atmospheric iron deposition: Global distribution, variability, and human perturbations, Annual Review of Marine Science, 1, 245–278, https://doi.org/10.1146/annurev.marine.010908.163727, 2009.
257. Mahowald, N., Jickells, T. D., Baker, A. R., et al.: Global distribution of atmospheric phosphorus sources, concentrations and deposition rates, and anthropogenic impacts, Global Biogeochemical Cycles, 22, GB4026, https://doi.org/10.1029/2008GB003240, 2008.
258. Marenco, F., and Hogan, R. J.: Determining the contribution of volcanic ash and boundary layer aerosol in backscatter lidar returns: A three-component atmosphere approach, J. Geophys. Res. Atmos., 116, D00U06, https://doi.org/10.1029/2010JD015415, 2011.
259. Marenco, F., di Sarra, A., and De Luisi, J.: Methodology for determining aerosol optical depth from Brewer 300–320-nm ozone measurements, Appl. Opt., 41, 1805–1814, https://doi.org/10.1364/AO.41.001805, 2002.
260. Marenco, F., Santacesaria, V., Bais, A. F., Balis, D., di Sarra, A., Papayannis, A., and Zerefos, C.: Optical properties of tropospheric aerosols determined by lidar and spectrophotometric measurements (Photochemical Activity and Solar Ultraviolet

Radiation campaign), Appl. Opt., 36, 6875–6886, https://doi.org/10.1364/AO.36.006875, 1997.

261. Martikainen, M.-V., Tossavainen, T., Hannukka, N., and Roponen, M.: Pollen, respiratory viruses, and climate change: Synergistic effects on human health, Environ. Res., 219, 115149, https://doi.org/10.1016/j.envres.2022.115149
262. Martinelli, N., Olivieri, O., and Girelli, D.: Air particulate matter and cardiovascular disease: a narrative review, Eur. J. Intern. Med., 24, 295–302, https://doi.org/10.1016/j.ejim.2013.04.001
263. Martonchik, J. V., et al.: Validation of MISR aerosol optical depth retrievals against ground-based observations, 2004.
264. Masoom, A., Doppler, L., Karanikolas, A., et al.: Aerosol optical depth harmonisation and retrieval intercomparison, Atmos. Meas. Tech., 17, 5525–5542, https://doi.org/10.5194/amt-17-5525-2024, 2024.
265. Masoom, A., Fountoulakis, I., Kazadzis, S., Raptis, I.-P., Kampouri, A., Psiloglou, B. E., Kouklaki, D., Papachristopoulou, K., Marinou, E., Solomos, S., Gialitaki, A., Founda, D., Salamalikis, V., Kaskaoutis, D., Kouremeti, N., Mihalopoulos, N., Amiridis, V., Kazantzidis, A., Papayannis, A., Zerefos, C. S., and Eleftheratos, K.: Investigation of the effects of the Greek extreme wildfires of August 2021 on air quality and spectral solar irradiance, Atmos. Chem. Phys., 23, 8487–8514, https://doi.org/10.5194/acp-23-8487-2023, 2023.
266. Masoom, A., Fountoulakis, I., Kazadzis, S., Raptis, I.-P., Kampouri, A., Psiloglou, B., Kouklaki, D., Papachristopoulou, K., Marinou, E., Solomos, S., et al.: Investigation of the effects of the Greek extreme wildfires of August 2021 on air quality and spectral solar irradiance, EGUsphere [preprint], https://doi.org/10.5194/egusphere-2023-180, 2023.
267. Masoumi, A., et al.: Aerosol optical depth retrieval and validation, J. Atmos. Sci., 2025, https://doi.org/10.1007/s13143-025-00417-4, 2025.
268. Mateos, D., Toledano, C., Calle, A., Román, R., Herreras-Giralda, M., González, R., Herrero-Anta, S., González-Fernández, D., Herrero-del Barrio, C., Nisantzi, A., Mamouri, R. E., Groß, S., Cachorro, V. E., de Frutos, Á. M., and Weinzierl, B.: Saharan and Arabian dust optical properties registered by sun photometry during A-LIFE field experiment in Cyprus, Atmos. Chem. Phys., 26, 1993–2005, https://doi.org/10.5194/acp-26-1993-2026, 2026.
269. Mazzola, M., Lupi, A., Vitale, V., Tomasi, C., Stone, R. S., Herber, A., Toledano, C., Cachorro, V. E., Torres, B., Berjón, A., Ortiz, J. P., O'Neill, N. T., Masataka, S., Stebel, K., Aaltonen, V., Zielinski, T., Petelski, T., Goloub, P., Blarel, L., Li, Z., Abboud, I., Cuevas, E., Stock, M., Schulz, K.-H., and Virkkula, A.: Evaluation of Sun photometer capabilities for retrievals of aerosol optical depth at high latitudes: the POLAR-AOD intercomparison campaigns, Atmos. Environ., 52, 4–17, https://doi.org/10.1016/j.atmosenv.2011.07.042, 2012.

270. Meinander, O., Dagsson-Waldhauserova, P., Baklanov, A., Baldo, C., Cvetkovic, B., Kandler, K., Kavan, J., King, J., Moroni, B., Murray, B., Nickovic, S., Pejanovic, G., Romanias, M., Sanchez-Marroquin, A., Schepanski, K., Thevenet, F., Urupina, D., Varga, G., Vukovic Vimic, A., et al., 2022. Newly identified climatically and environmentally significant high latitude dust sources. Atmospheric Chemistry and Physics 22, 11889–11930, doi: 10.5194/acp-2021-963.
271. Meleti, C. and Capellani, F.: Measurements of aerosol optical depth at Ispra: analysis of the correlation with UV-B, UV-A, and total solar irradiance, J. Geophys. Res., 105, 4971–4978, https://doi.org/10.1029/1999JD900459, 2000.
272. Mercado, L. M., Bellouin, N., Sitch, S., Boucher, O., Huntingford, C., Wild, M., and Cox, P. M.: Impact of changes in diffuse radiation on the global land carbon sink, Nature, 458, 1014–1017, https://doi.org/10.1038/nature07949, 2009.
273. Mhawish, A., Banerjee, T., Broday, D. M., Misra, A., and Tripathi, S. N.: Evaluation of MODIS Collection 6 aerosol retrieval algorithms over Indo-Gangetic Plain: implications of aerosol types and mass loading, Remote Sens. Environ., 201, 297–313, https://doi.org/10.1016/j.rse.2017.09.016, 2017.
274. Michalsky, J. J. and McConville, G. R.: Reference aerosol optical depth measurements and calibration, Atmos. Meas. Tech., 17, 1017–1030, https://doi.org/10.5194/amt-17-1017-2024, 2024.
275. Mishchenko, M. I., Liu, L., Travis, L. D., and Lacis, A. A.: Toward unified satellite climatology of aerosol properties: what do fully compatible MODIS and MISR aerosol pixels tell us?, J. Quant. Spectrosc. Radiat. Transfer, 110, 402–408, https://doi.org/10.1016/j.jqsrt.2009.11.003, 2009.
276. Mishra, M. K., Shameela, S. F., Kuttippurath, J., and Rathore, P. S.: A global aerosol model based on the analysis of 30-year ground measurements from AERONET (AEROEX model): Implications for satellite-derived aerosol retrievals, Sci. Total Environ., 999, 180301, https://doi.org/10.1016/j.scitotenv.2025.180301, 2025.
277. Mok, J., et al.: Evaluation of satellite-retrieved aerosol single-scattering albedo, 2018.
278. Molod, A., Takacs, L., Suarez, M., and Bacmeister, J.: Development of the GEOS-5 atmospheric general circulation model: evolution from MERRA to MERRA2, Geosci. Model Dev., 8, 1339–1356, https://doi.org/10.5194/gmd-8-1339-2015, 2015.
279. Momoi, M., Kudo, R., Aoki, K., Mori, T., Miura, K., Okamoto, H., Irie, H., Shoji, Y., Uchiyama, A., Ijima, O., Takano, M., and Nakajima, T.: Development of on-site self-calibration and retrieval methods for sky-radiometer observations of precipitable water vapor, Atmos. Meas. Tech., 13, 2635–2658, https://doi.org/10.5194/amt-13-2635-2020, 2020.
280. Mona, L., and Marenco, F.: Lidar observations of volcanic particles, in: Volcanic Ash: Hazard Observation, edited by: Mackie, S., Cashman, K., Ricketts, H., Rust, A., and Watson, M., Elsevier, pp. 161–173, https://doi.org/10.1016/B978-0-08-100405-0.00014-8, 2016.

281. Moosmüller, H. and Sorensen, C. M.: Small and large particle limits of single scattering albedo for homogeneous, spherical particles, J. Quant. Spectrosc. Ra., 204, 250–255, https://doi.org/10.1016/j.jqsrt.2017.09.029, 2018.
282. Moustaka, A., et al.: [Full title and author list to verify], Atmos. Meas. Tech., 19, 1201–[pages to verify], https://doi.org/10.5194/amt-19-1201-2026, 2026.
283. Moustaka, A., Papachristopoulou, K., Charalampous, G., and Kazadzis, S.: Propagation of CAMS aerosol uncertainty to clear-sky solar irradiance estimates, EGUsphere [preprint], https://doi.org/10.5194/egusphere-2026-4413, 2026.
284. Moustaka, M., et al.: Two decades of aerosol optical depth evolution from CAMS reanalysis, EGUsphere [preprint], https://doi.org/10.5194/egusphere-2026-1107, 2026.
285. Mukkavilli, S. K., Prasad, A. A., Taylor, R. A., Huang, J., Mitchell, R. M., Troccoli, A., and Kay, M. J.: Assessment of atmospheric aerosols from two reanalysis products over Australia, Atmos. Res., 215, 149–164, https://doi.org/10.1016/j.atmosres.2018.08.026, 2019.
286. Munakata, N., Cornain, S., Kanoko, M., Mulyadi, K., Lestari, S., Wirohadidjojo, W., Bolseé, D., Kazadzis, S., Meyer-Rochow, V., Schuch, N., Casiccia, C., Kaneko, M., Liu, C., Jimbow, K., Saida, T., Nishigori, C., Ogata, K., Inafuku, K., Hieda, K., and Ichihashi, M.: Biological monitoring of solar UV radiation at 17 sites in Asia, Europe and South America from 1999 to 2004, Photochem. Photobiol., 82, 689–694, 2006. https://doi.org/10.1562/2005-07-07-RA-602
287. Munro, R., Lang, R., Klaes, D., Poli, G., Retscher, C., Lindstrot, R., Huckle, R., Lacan, A., Grzegorski, M., Holdak, A., Kokhanovsky, A., Livschitz, J., and Eisinger, M.: The GOME-2 instrument on the Metop series of satellites: instrument design, calibration, and level 1 data processing – an overview, Atmos. Meas. Tech., 9, 1279–1301, https://doi.org/10.5194/amt-9-1279-2016, 2016.
288. Nakajima, T., Campanelli, M., Che, H., Estellés, V., Irie, H., Kim, S.-W., Kim, J., Liu, D., Nishizawa, T., Pandithurai, G., Soni, V. K., Thana, B., Tugjsurn, N.-U., Aoki, K., Go, S., Hashimoto, M., Higurashi, A., Kazadzis, S., Khatri, P., Kouremeti, N., Kudo, R., Marenco, F., Momoi, M., Ningombam, S. S., Ryder, C. L., Uchiyama, A., and Yamazaki, A.: An overview of and issues with sky radiometer technology and SKYNET, Atmos. Meas. Tech., 13, 4195–4218, https://doi.org/10.5194/amt-13-4195-2020, 2020.
289. Nakajima, T., Tanaka, M., Hayasaka, T., Miyake, Y., Nakanishi, Y., and Sasamoto, K.: Airborne measurements of the optical stratification of aerosols in turbid atmospheres, Appl. Opt., 25, 4374–4381, https://doi.org/10.1364/AO.25.004374, 1986.
290. Nakajima, T., Tonna, G., Rao, R., Boi, P., and Shi, G.: Use of sky brightness measurements from ground for remote sensing of particulate polydispersions, J. Quant. Spectrosc. Radiat. Transfer, 55, 129–159, https://doi.org/10.1016/0022-4073(95)00148-7, 1996.
291. Ng, J. Y.-H., McCloskey, K., Cui, J., Rudolf Meijer, V., Brand, E., Sarna, A., Goyal, N., Van Arsdale, C., and Geraedts, S.: Contrail detection on GOES-16 ABI with the

OpenContrails dataset, IEEE Trans. Geosci. Remote Sens., 61, 1–14, 2023. Related preprint: https://arxiv.org/abs/2304.02122.

292. Noh, Y. M., Mueller, D., Lee, H., and Choi, T. J.: Influence of biogenic pollen on optical properties of atmospheric aerosols observed by lidar over Gwangju, South Korea, Atmos. Environ., 69, 139–147, 2013. https://doi.org/10.1016/j.atmosenv.2012.12.018
293. Nyeki, S., Wehrli, C., Gröbner, J., Kouremeti, N., Wacker, S., Labuschagne, C., Mbatha, N., and Brunke, E.-G.: The GAW-PFR aerosol optical depth network: the 2008–2013 time series at Cape Point Station, South Africa, J. Geophys. Res. Atmos., 120, 5070–5084, https://doi.org/10.1002/2014JD022954, 2015.
294. O'Neill, N. T., Eck, T. F., Smirnov, A., Holben, B. N., and Thulasiraman, S.: Spectral discrimination of coarse and fine mode optical depth, J. Geophys. Res., 108, D17, https://doi.org/10.1029/2002JD002975, 2003.
295. Obregón et al. 2018: Impact of aerosol and water vapour on SW radiation at the surface — https://doi.org/10.1016/j.atmosres.2018.06.001.
296. Obregón, M. A., et al.: Retrieval and validation of aerosol optical depth from Sentinel-2 observations, 2019.
297. Ortiz, I., Dimitropoulou, E., de Buyl, P., Clerbaux, N., García-Heras, J., Jafarimoghaddam, A., Brenot, H., van Gent, J., Sievers, K., Otero, E., Loganathan, P., and Soler, M.: Satellite-based quantification of contrail radiative forcing over Europe: A two-week analysis of aviation-induced climate effects, arXiv:2409.10166, https://arxiv.org/abs/2409.10166, 2024. (Submitted to SESAR Innovation Days 2024 according to the comment.)
298. Ortiz, I., et al.: Robust evaluation of neural networks trained on the OpenContrails dataset, IEEE Trans. Geosci. Remote Sens., https://doi.org/10.1109/TGRS.2025.3629628, 2025.
299. Osgouei, S., et al.: Intercomparison and validation of satellite aerosol retrieval products, 2022.
300. O'Neill, N. T., Baibakov, K., Hesaraki, S., Ivanescu, L., Martin, R. V., Perro, C., Chaubey, J. P., Herber, A., and Duck, T. J.: Temporal and spectral cloud screening of polar winter aerosol optical depth (AOD): impact of homogeneous and inhomogeneous clouds and crystal layers on climatological-scale AODs, Atmos. Chem. Phys., 16, 12753–12765, https://doi.org/10.5194/acp-16-12753-2016, 2016.
301. Padimala, S. S. K., and Matli, C. S.: A comprehensive review delineates advancements in retrieving particulate matter utilising satellite aerosol optical depth: Parameter consideration, data processing, models development and future perspectives, Atmos. Res., 308, 107514, https://doi.org/10.1016/j.atmosres.2024.107514, 2024.
302. Papachristopoulou, K., Fountoulakis, I., Bais, A. F., Psiloglou, B. E., Papadimitriou, N., Raptis, I.-P., Kazantzidis, A., Kontoes, C., Hatzaki, M., and Kazadzis, S.: Effects of clouds and aerosols on downwelling surface solar irradiance nowcasting and short-term

forecasting, Atmos. Meas. Tech., 17, 1851–1877, https://doi.org/10.5194/amt-17-1851-2024, 2024.

303. Papachristopoulou, K., Fountoulakis, I., Gkikas, A., et al.: 15-year analysis of direct effects of total and dust aerosols in solar radiation/energy over the Mediterranean Basin, Remote Sens., 14, 1535, https://doi.org/10.3390/rs14071535, 2022.
304. Papadimitriou, N., Fountoulakis, I., Gkikas, A., Papachristopoulou, K., Kazantzidis, A., Kazadzis, S., Pfenninger, S., Kapsomenakis, J., Eleftheratos, K., Argiriou, A. A., Doppler, L., and Zerefos, C. S.: PV power modelling using solar radiation from ground-based measurements and CAMS: Assessing the diffuse component related uncertainties leveraging the Global Solar Energy Estimator (GSEE), Atmospheric Measurement Techniques, 19, 1227–1244, https://doi.org/10.5194/amt-19-1227-2026, 2026.
305. Papetta, A., Kezoudi, M., Baars, H., Floutsi, A., Drakaki, E., Kandler, K., Aryasree, S., Louca, E., Christoudias, T., Marinou, E., Stopford, C., Thornberry, T., Amiridis, V., Sciare, J., and Marenco, F.: Volume-to-extinction ratio: An important property of dust, Atmos. Chem. Phys., 26, 2055–2082, 2026. https://doi.org/10.5194/acp-26-2055-2026
306. Pappalardo, G., Amodeo, A., Mona, L., et al.: EARLINET: Towards an advanced sustainable European aerosol lidar network, Atmos. Meas. Tech., 7, 2389–2409, https://doi.org/10.5194/amt-7-2389-2014, 2014.
307. Pearson, K. M., et al.: A global assessment of satellite aerosol optical depth products using ground-based observations, Sci. Data, https://doi.org/10.1038/s41597-025-04694-6, 2025. [Full author list not confirmed from the available record.]
308. Peden, D. B. and Bush, R. K.: Advances in environmental and occupational disorders in 2014, J. Allergy Clin. Immunol., 136, 866–871, https://doi.org/10.1016/j.jaci.2015.08.008
309. Pei, L., et al.: Evaluation of satellite aerosol retrievals using ground-based and marine aerosol observations, 2023.
310. Pei, X., et al.: VIIRS aerosol optical depth retrieval and validation, Atmos. Environ., 2025, 120949, https://doi.org/10.1016/j.atmosenv.2024.120949, 2025.
311. Peng, Z., Zhang, B., Wang, D., Niu, X., Sun, J., Xu, H., Cao, J., and Shen, Z.: Application of machine learning in atmospheric pollution research: A state-of-art review, Sci. Total Environ., 910, 168588, https://doi.org/10.1016/j.scitotenv.2023.168588, 2024. (DOI supplied in the comment; broad ML context rather than a specific aerosol-retrieval validation.)
312. Perrone, M. R., De Tomasi, F., and Gobbi, G. P.: Vertically resolved aerosol properties by multi-wavelength lidar measurements, Atmos. Chem. Phys., 14, 1185–1204, https://doi.org/10.5194/acp-14-1185-2014, 2014.
313. Petroff, A., Mailliat, M., Amielh, M., and Anselmet, F.: Aerosol dry deposition on vegetative canopies. Part I: Review of present knowledge, Atmospheric Environment, 42, 3625–3653, https://doi.org/10.1016/j.atmosenv.2007.09.043, 2008.

314. Petroff, A., Mailliat, M., Amielh, M., and Anselmet, F.: Aerosol dry deposition on vegetative canopies. Part II: A new modelling approach and applications, Atmospheric Environment, 42, 3654–3683, https://doi.org/10.1016/j.atmosenv.2007.12.060, 2008.
315. Popovici, I. E., Goloub, P., Podvin, T., et al.: Description and applications of a mobile system performing on-road aerosol remote sensing and in situ measurements, Atmospheric Measurement Techniques, 11, 4671–4691, https://doi.org/10.5194/amt-11-4671-2018, 2018.
316. Popp, T., de Leeuw, G., Bingen, C., et al.: Development, production and evaluation of aerosol climate data records from European satellite observations (Aerosol_cci), Remote Sens., 8, 421, https://doi.org/10.3390/rs8050421, 2016.
317. Prata, A. J., and Tupper, A.: Aviation hazards from volcanoes: The state of the science, Nat. Hazards, 51, 239–244, https://doi.org/10.1007/s11069-009-9415-y, 2009.
318. Prata, A. T. and Tupper, A.: Aviation hazards from volcanoes, in/related literature cited by the manuscript; the document comment supplied DOI https://doi.org/10.1586/17469872.2.5.563 (2009).
319. Proestakis, E., Gkikas, A., Georgiou, T., Kampouri, A., Drakaki, E., Ryder, C. L., Marenco, F., Marinou, E., and Amiridis, V.: A near-global multiyear climate data record of the fine-mode and coarse-mode components of atmospheric pure dust, Atmos. Meas. Tech., 17, 3625–3667, https://doi.org/10.5194/amt-17-3625-2024
320. Proestakis, E., Papachristopoulou, K., Georgiou, T., Chatoutsidou, S. E., Lazaridis, M., Gkikas, A., Fountoulakis, I., Tsikoudi, I., Petrakis, M. P., and Amiridis, V.: Atmospheric dust and air quality over large-cities and megacities of the world, Atmos. Chem. Phys., 25, 14777–14823, https://doi.org/10.5194/acp-25-14777-2025
321. Pryor, S. C., Gallagher, M., Sievering, H., et al.: A review of measurement and modelling results of particle atmosphere–surface exchange, Tellus B, 60, 42–75, https://doi.org/10.1111/j.1600-0889.2007.00298.x, 2008.
322. Pérez, C., Nickovic, S., Baldasano, J. M., Sicard, M., Rocadenbosch, F., and Cachorro, V. E.: A long Saharan dust event over the western Mediterranean: Lidar, sun photometer observations, and regional dust modeling, J. Geophys. Res. Atmos., 111, D15214, https://doi.org/10.1029/2005JD006579, 2006.
323. Pérez-Ramírez, D., Lyamani, H., Olmo, F. J., Whiteman, D. N., Navas-Guzmán, F., and Alados-Arboledas, L.: Cloud screening and quality control algorithm for star photometer data: assessment with lidar measurements and with all-sky images, Atmos. Meas. Tech., 5, 1585–1599, https://doi.org/10.5194/amt-5-1585-2012, 2012.
324. Pérez-Ramírez, D., Ruiz, B., Cuevas, E., Gómez-Moreno, F. J., and Sorribas, M.: Development and calibration of a star photometer to measure the aerosol optical depth: smoke observations at a high mountain site, Atmos. Environ., 42, 2733–2738, https://doi.org/10.1016/j.atmosenv.2007.06.009, 2008.

325. Quincey, P. and Butterfield, D.: Ambient air particulate matter PM10 and PM2.5: developments in European measurement methods and legislation, Biomarkers, 14, 34–38, https://doi.org/10.1080/13547500902965484, 2009.
326. Randles, C. A., da Silva, A. M., Buchard, V., Colarco, P. R., Darmenov, A., Govindaraju, R., Smirnov, A., Holben, B., Ferrare, R., Hair, J., Shinozuka, Y., and Flynn, C. J.: The MERRA-2 aerosol reanalysis, 1980–onward, Part I: system description and data assimilation evaluation, J. Climate, 30, 6823–6850, https://doi.org/10.1175/JCLI-D-16-0609.1, 2017.
327. Raptis, I.-P., Kazadzis, S., Eleftheratos, K., Amiridis, V., and Fountoulakis, I.: Single scattering albedo's spectral dependence effect on UV irradiance, Atmosphere, 9, 364, https://doi.org/10.3390/atmos9090364, 2018.
328. Raptis, I.-P., Kazadzis, S., Fountoulakis, I., Papachristopoulou, K., Kouklaki, D., Psiloglou, B. E., Kazantzidis, A., Benetatos, C., Papadimitriou, N., and Eleftheratos, K.: Evaluation of the Solar Energy Nowcasting System (SENSE) during a 12-month intensive measurement campaign in Athens, Greece, Energies, 16, 5361, https://doi.org/10.3390/en16145361, 2023.
329. Razagui, A., Abdeladim, K., Bouchouicha, K., Bachari, N., Semaoui, S., and Hadj Arab, A.: A new approach to forecast solar irradiances using WRF and libRadtran models, validated with MERRA-2 reanalysis data and pyranometer measures, Solar Energy, 221, 148–161, https://doi.org/10.1016/j.solener.2021.04.024, 2021.
330. Reichstein, M., Camps-Valls, G., Stevens, B., and others: Deep learning and process understanding for data-driven Earth system science, Nature, 566, 195–204, https://doi.org/10.1038/s41586-019-0912-1, 2019.
331. Remer, L. A., Kahn, R. A., Levy, R. C., et al.: Advances in aerosol remote sensing and retrieval, Atmos. Chem. Phys., 24, 2113–2140, https://doi.org/10.5194/acp-24-2113-2024, 2024.
332. Remer, L. A., Kaufman, Y. J., Tanré, D., Mattoo, S., Chu, D. A., Martins, J. V., Li, R.-R., Ichoku, C., Levy, R. C., Kleidman, R. G., Eck, T. F., Vermote, E., and Holben, B. N.: The MODIS aerosol algorithm, products, and validation, J. Geophys. Res., 113, D14S07, https://doi.org/10.1029/2007JD009661, 2008.
333. Reutter, P., Neis, P., Rohs, S., and Sauvage, B.: Ice supersaturated regions: Properties and validation of ERA-Interim reanalysis with IAGOS in situ water vapour measurements, Atmos. Chem. Phys., 20, 787–804, https://doi.org/10.5194/acp-20-787-2020, 2020.
334. Riffler, M., Popp, C., Hauser, A., and colleagues: Retrieval and validation of aerosol optical depth from AVHRR observations, 2010.
335. Rimmer, J. S., Smedley, A. R. D., Redondas, A., Wood, P., and Bais, A.: Evaluation of the aerosol optical depth retrieval from the European Brewer network, Atmos. Meas. Tech., 11, 2295–2311, https://doi.org/10.5194/amt-11-2295-2018, 2018.

336. Rogozovsky, I., Ansmann, A., and Chudnovsky, A.: Vertical aerosol structure matters: Improving the AOD–$PM_{2.5}$ link for air quality and exposure, Environ. Sci. Technol., 60, 14685–14697, 2026. https://doi.org/10.1021/acs.est.6c00095
337. Roman, R., Bilbao, J., and de Miguel, A.: Solar radiation simulations in the Iberian Peninsula: Accuracy and sensitivity to uncertainties in inputs of a radiative transfer model, Geophysical Research Letters, 42, 212–219, 2014.
338. Roman, R., Bilbao, J., and de Miguel, A.: Solar radiation simulations in the Iberian Peninsula: Accuracy and sensitivity to uncertainties in inputs of a radiative transfer model, Geophysical Research Letters, 42, 212–219, https://doi.org/10.1002/2014GL062309, 2015. [The source list gives 2015; manuscript cites Roman et al. (2014a,b). Verify both cited works and year suffixes.]
339. Román, R., Antuña-Sánchez, J. C., Cazorla, A., Toledano, C., Cachorro, V. E., and de Frutos, Á. M.: Retrieval of aerosol optical properties from all-sky images, Remote Sens. Environ., 2017, https://doi.org/10.1016/j.rse.2017.05.013, 2017.
340. Román, R., Cazorla, A., Olmo, F. J., et al.: Aerosol properties from all-sky imaging, Atmos. Meas. Tech., 15, 407–421, https://doi.org/10.5194/amt-15-407-2022, 2022.
341. Román, R., González-Fernández, D., Antuña-Sánchez, J. C., Herrero del Barrio, C., Herrero-Anta, S., Barreto, Á., Cachorro, V. E., et al.: Star photometry with all-sky cameras to retrieve aerosol optical depth at nighttime, Atmos. Meas. Tech., 18, 2847–2861, https://doi.org/10.5194/amt-18-2847-2025, 2025.
342. Rosenfeld, D., Sherwood, S., Wood, R., and Donner, L.: Atmospheric science. Climate effects of aerosol-cloud interactions, Science, 343, 379–380, https://doi.org/10.1126/science.1247490, 2014.
343. Rubin, J. I., Reid, J. S., Hansen, J. A., Anderson, J. L., Holben, B. N., Xian, P., and Westphal, D. L.: Assimilation of AERONET and MODIS AOT observations using variational and ensemble data assimilation methods and its impact on aerosol forecasting skill, J. Geophys. Res. Atmos., 122, 4967–4992, https://doi.org/10.1002/2016JD026067, 2017.
344. Ruiz-Arias, J. A., and Gueymard, C. A.: Worldwide inter-comparison of clear-sky solar radiation models: Consensus-based review of direct and global irradiance components simulated at the earth surface, Sol. Energy, 168, 10–29, https://doi.org/10.1016/j.solener.2018.02.008, 2018.
345. Ruiz-Arias, J. A., and Gueymard, C. A.: Worldwide inter-comparison of clear-sky solar radiation models: Consensus-based review of direct and global irradiance components simulated at the earth surface, Solar Energy, 168, 10–29, 2018.
346. Ryder, C. L., Highwood, E. J., Lai, T. M., and others: Aerosol measurements and modelling of the Saharan dust size distribution during the Fennec campaign, Atmos. Chem. Phys., 19, 10267–10291, https://doi.org/10.5194/acp-19-10267-2019, 2019.
347. Ryder, C. L., Marenco, F., Brooke, J. K., Estellés, V., Cotton, R., Formenti, P., McQuaid, J. B., Price, H. C., Liu, D., Ausset, P., Rosenberg, P. D., Taylor, J. W.,

Choularton, T., Bower, K., Coe, H., Gallagher, M., Crosier, J., Lloyd, G., Highwood, E. J., and Murray, B. J.: Coarse-mode mineral dust size distributions, composition and optical properties from AER-D aircraft measurements over the tropical eastern Atlantic, Atmos. Chem. Phys., 18, 17225–17244, https://doi.org/10.5194/acp-18-17225-2018, 2018.

348. Rémy, S., Kipling, Z., Flemming, J., Boucher, O., Nabat, P., Michou, M., Bozzo, A., Ades, M., Huijnen, V., Benedetti, A., Engelen, R., Peuch, V.-H., and Morcrette, J.-J.: Description and evaluation of the tropospheric aerosol scheme in the European Centre for Medium-Range Weather Forecasts (ECMWF) Integrated Forecasting System (IFS-AER, cycle 45R1), Geosci. Model Dev., 12, 4627–4659, https://doi.org/10.5194/gmd-12-4627-2019, 2019.
349. Sanchez-Barrero, M. F., Goloub, P., Blarel, L., Popovici, I. E., Torres, B., Dubois, G., Podvin, T., Ducos, F., de Filippi, R., Sicard, M., Bout Roumazeilles, V., and Skonieczny, C.: Aerosol variability over oceans using micro-pulse lidar and photometer: insights from TRANSAMA ship-based campaign, Atmos. Meas. Tech., 19, 507–528, https://doi.org/10.5194/amt-19-507-2026, 2026.
350. SAPEA: Solar radiation modification: Evidence review report, Science Advice for Policy by European Academies, Berlin, https://doi.org/10.5281/zenodo.14283096, 2024.
351. Sayer, A. M.: How long is too long? Variogram analysis of AERONET data to aid aerosol validation and intercomparison studies, Earth Space Sci., 7, e2020EA001290, https://doi.org/10.1029/2020EA001290, 2020.
352. Sayer, A. M., Hsu, N. C., Bettenhausen, C., Ahmad, Z., Holben, B. N., Smirnov, A., Thomas, G. E., and Zhang, J.: SeaWiFS ocean aerosol retrieval (SOAR): Algorithm, validation, and comparison with other data sets, J. Geophys. Res., 117, D03206, https://doi.org/10.1029/2011JD016599, 2012.
353. Sayer, A. M., Hsu, N. C., Bettenhausen, C., Ahmad, Z., Holben, B. N., Smirnov, A., Thomas, G. E., and Zhang, J.: SeaWiFS ocean aerosol retrieval (SOAR): algorithm, validation, and comparison with other data sets, J. Geophys. Res., 117, D03206, https://doi.org/10.1029/2011JD016689, 2012.
354. Sayer, A. M., Hsu, N. C., Bettenhausen, C., and Jeong, M.-J.: Validation and uncertainty estimates for MODIS Collection 6 ‘Deep Blue’ aerosol data, J. Geophys. Res.-Atmos., 118, 7864–7872, https://doi.org/10.1002/jgrd.50600, 2013.
355. Sayer, A. M., Hsu, N. C., Bettenhausen, C., and Jeong, M.-J.: Validation and uncertainty estimates for MODIS Collection 6.1 aerosol products, Atmos. Meas. Tech., 12, 49–69, https://doi.org/10.5194/amt-12-49-2019, 2019.
356. Sayer, A. M., Hsu, N. C., Bettenhausen, C., Jeong, M.-J., and Meister, G.: MODIS Collection 6 aerosol products: Comparison between Aqua's e-Deep Blue, Dark Target, and merged data sets, and usage recommendations, J. Geophys. Res.-Atmos., https://doi.org/10.1002/2014JD022453, 2014.
357. Sayer, A. M., Hsu, N. C., Bettenhausen, C., Lee, J., and Meister, G.: Validation of SOAR VIIRS over-water aerosol retrievals and context within the global satellite aerosol

data record, J. Geophys. Res.-Atmos., 123, 13,405–13,427, https://doi.org/10.1029/2018JD029465, 2018.

358. Sayer, A. M., Hsu, N. C., Bettenhausen, C., Lee, J., Meister, G., and others: Validation, stability, and consistency of MODIS Collection 6.1 and VIIRS Version 1 Deep Blue aerosol data over land, J. Geophys. Res.-Atmos., 124, 4658–4688, https://doi.org/10.1029/2018JD029598, 2019. [Full author list requires confirmation against the DOI record.]
359. Scarlatti, C., et al.: Aerosol optical depth and aerosol properties from ground and satellite observations, Atmos. Environ., 2024, 120495, https://doi.org/10.1016/j.atmosenv.2024.120495, 2024.
360. Scherllin-Pirscher, B., Nickovic, S., Votsis, A., Cvetkovic, B., Amiridis, V., Bolic, T., Brenot, H., Brock, G., Clarkson, R. J., Durant, A., Hirtl, M., Lekas, T. I., Mona, L., Nasser, H., Ryder, C. L., Ryuzaki, J., Suárez-Molina, D., Vukovic Vimic, A., and Basart, S.: Airborne soil-derived dust hazards in aviation, Bull. Am. Meteorol. Soc., 106, E125–E145, https://doi.org/10.1175/BAMS-D-23-0311.1, 2025.
361. Schmale, J., Zieger, P., & Ekman, A. M. L. (2021). Aerosols in current and future Arctic climate. Nature Climate Change, 11, 95–105. https://doi.org/10.1038/s41558-020-00969-5.
362. Schmit, T. J., Griffith, P., Gunshor, M. M., Daniels, J. M., Goodman, S. J., and Lebair, W. J.: A closer look at the ABI on the GOES-R series, Bull. Am. Meteorol. Soc., 98, 681–698, https://doi.org/10.1175/BAMS-D-15-00230.1, 2017.
363. Schroedter-Homscheidt, M. and Oumbe, A.: Validation of an hourly resolved global aerosol model in answer to solar electricity generation information needs, Atmos. Chem. Phys., 13, 3777–3791, https://doi.org/10.5194/acp-13-3777-2013, 2013.
364. Schulz, M., Prospero, J. M., Baker, A. R., et al.: Atmospheric transport and deposition of mineral dust to the ocean: Implications for research needs, Environmental Science & Technology, 46, 10390–10404, https://doi.org/10.1021/es300073u, 2012.
365. Schumann, U.: Formation, properties and climatic effects of contrails, C. R. Physique, 6, 753–762, 2005.
366. Schuster, G. L., Dubovik, O., and Holben, B. N.: Angstrom exponent and bimodal aerosol size distributions, J. Geophys. Res., 111, D07207, https://doi.org/10.1029/2005JD006328, 2006.
367. Schutgens, N. A. J., et al.: [Satellite aerosol product evaluation study; confirm exact title and author list from DOI], Atmos. Meas. Tech., 6, 2455–[page range to verify], https://doi.org/10.5194/amt-6-2455-2013, 2013.
368. Schutgens, N. A. J., et al.: [Reference cited in the manuscript as Schutgens et al. (2020); bibliographic details should be checked against the intended source].
369. Schutgens, N. A. J., et al.: Evaluation of aerosol products derived from POLDER observations using the GRASP algorithm, 2021.

370. Schutgens, N. A. J., Nakata, M., and Nakajima, T.: Validation and analysis of satellite aerosol optical depth products using AERONET and SKYNET observations, 2013.
371. Schwartz, C. S., Liu, Z., Lin, H.-C., and Cetola, J. D.: Assimilating aerosol observations with a "hybrid" variational-ensemble data assimilation system, J. Geophys. Res.-Atmos., 119, 4043–4069, https://doi.org/10.1002/2013JD020937, 2014.
372. Seinfeld, J. H. and Pandis, S. N.: Atmospheric Chemistry and Physics: From Air Pollution to Climate Change, 3rd edn., John Wiley & Sons, Hoboken, NJ, USA, 2016.
373. Sellitto, P., Di Sarra, A., and Siani, A. M.: An improved algorithm for the determination of aerosol optical depth in the ultraviolet spectral range from Brewer spectrophotometer observations, J. Opt. A Pure Appl. Opt., 8, 849–855, https://doi.org/10.1088/1464-4258/8/10/005, 2006.
374. Sengupta, M., Habte, A., Wilbert, S., Gueymard, C., and Remund, J.: Best practices handbook for the collection and use of solar resource data for solar energy applications, National Renewable Energy Laboratory, NREL/TP-5D00-77635, https://doi.org/10.2172/1778700, 2021. [Source: Word comment reference [ID 22]]
375. Shaw, G. E.: Sun photometry, B. Am. Meteorol. Soc., 64, 4–10, https://doi.org/10.1175/1520-0477(1983)064<0004:SP>2.0.CO;2, 1983.
376. Shen, X., et al.: Evaluation of satellite aerosol retrievals using marine aerosol observations, 2018.
377. Shen, Y., et al.: [Marine Aerosol Network / shipborne aerosol validation study; confirm exact title from DOI], Remote Sens., 10, 573, https://doi.org/10.3390/rs10040573, 2018.
378. Shi, H., Xiao, Z., Zhan, X., Ma, H., and Tian, X.: Evaluation of MODIS and two reanalysis aerosol optical depth products over AERONET sites, Atmos. Res., 220, 75–80, https://doi.org/10.1016/j.atmosres.2019.01.009, 2019.
379. Shi, Y., Zhang, J., Reid, J. S., Liu, B., and Hyer, E. J.: Critical evaluation of cloud contamination in the MISR aerosol products using MODIS cloud mask products, Atmos. Meas. Tech., 7, 1791–1801, https://doi.org/10.5194/amt-7-1791-2014, 2014.
380. Shin, S.-K., Tesche, M., Müller, D., and Noh, Y.: Technical note: Absorption aerosol optical depth components from AERONET observations of mixed dust plumes, Atmos. Meas. Tech., 12, 607–618, https://doi.org/10.5194/amt-12-607-2019, 2019.
381. Si, Y., Li, S., Chen, L., Shang, H., Wang, L., and Letu, H.: Assessment and improvement of MISR Ångström exponent and single-scattering albedo products using AERONET data in China, Remote Sens., 9, 693, https://doi.org/10.3390/rs9070693, 2017.
382. Sinyuk, A., Holben, B. N., Eck, T. F., Giles, D. M., Slutsker, I., Korkin, S., et al.: The AERONET Version 3 aerosol retrieval algorithm, associated uncertainties and comparisons to Version 2, Atmos. Meas. Tech., 13, 3375–3411, https://doi.org/10.5194/amt-13-3375-2020, 2020.

383. Smirnov, A., Holben, B. N., Eck, T. F., Dubovik, O., and Slutsker, I.: Cloud screening and quality control algorithms for the AERONET database, Remote Sens. Environ., 73, 337–349, https://doi.org/10.1016/S0034-4257(00)00109-7, 2000.
384. Smirnov, A., Holben, B. N., Giles, D. M., Slutsker, I., O'Neill, N. T., Eck, T. F., Macke, A., Croot, P., Courcoux, Y., Sakerin, S. M., Smyth, T. J., Zielinski, T., Zibordi, G., Goes, J. I., Harvey, M. J., Quinn, P. K., Nelson, N. B., Radionov, V. F., Duarte, C. M., Losno, R., Sciare, J., Voss, K. J., Kinne, S., Nalli, N. R., Joseph, E., Krishna Moorthy, K., Covert, D. S., Gulev, S. K., Milinevsky, G., Larouche, P., Belanger, S., Horne, E., Chin, M., Remer, L. A., Kahn, R. A., Reid, J. S., Schulz, M., Heald, C. L., Zhang, J., Lapina, K., Kleidman, R. G., Griesfeller, J., Gaitley, B. J., Tan, Q., and Diehl, T. L.: Maritime aerosol network as a component of AERONET – first results and comparison with global aerosol models and satellite retrievals, Atmos. Meas. Tech., 4, 583–597, https://doi.org/10.5194/amt-4-583-2011, 2011.
385. Smirnov, A., Holben, B. N., Slutsker, I., Giles, D. M., McClain, C. R., Eck, T. F., Sakerin, S. M., Macke, A., Croot, P., Zibordi, G., Quinn, P. K., Sciare, J., Kinne, S., Harvey, M., Smyth, T. J., Piketh, S., Zielinski, T., Proshutinsky, A., Goes, J. I., Nelson, N. B., Larouche, P., Radionov, V. F., Goloub, P., Krishna Moorthy, K., Matarrese, R., Robertson, E. J., and Jourdin, F.: Maritime Aerosol Network as a component of AERONET – first results and comparison with global aerosol models and satellite retrievals, J. Geophys. Res., 114, D06204, https://doi.org/10.1029/2008JD011257, 2009.
386. Sofiev, M.: On impact of transport conditions on variability of the seasonal pollen index, Aerobiologia, 33, 167–179, https://doi.org/10.1007/s10453-016-9459-x, 2017.
387. Sofiev, M., Ritenberga, O., Albertini, R., Arteta, J., Belmonte, J., Bernstein, C. G., Bonini, M., Celenk, S., Damialis, A., Douros, J., Elbern, H., Friese, E., Galan, C., Oliver, G., Hrga, I., Kouznetsov, R., Krajsek, K., Magyar, D., Parmentier, J., Plu, M., Prank, M., Robertson, L., Steensen, B. M., Thibaudon, M., Segers, A., Stepanovich, B., Valdebenito, A. M., Vira, J., and Vokou, D.: Multi-model ensemble simulations of olive pollen distribution in Europe in 2014: Current status and outlook, Atmos. Chem. Phys., 17, 12341–12360, https://doi.org/10.5194/acp-17-12341-2017, 2017.
388. Sofiev, M., Sofieva, S., Palamarchuk, J., Šaulienė, I., Kadantsev, E., Atanasova, N., Fatahi, Y., Kouznetsov, R., Kuula, J., Noreikaite, A., Peltonen, M., Pihlajamäki, T. T., Saarto, A., Salokas, J., Toiviainen, L., Tyuryakov, S., Šukienė, L., Asmi, E., Bamford, D. H., Hyvärinen, A.-P., and Karppinen, A.: Bioaerosols in the atmosphere at two sites in Northern Europe in spring 2021: Outline of an experimental campaign, Environ. Res., 214, 113798, https://doi.org/10.1016/j.envres.2022.113798, 2022.
389. Sogacheva, L., Denisselle, M., Kolmonen, P., Virtanen, T. H., North, P., Henocq, C., Scifoni, S., and Dransfeld, S.: Extended validation and evaluation of the OLCI–SLSTR SYNERGY aerosol product (SY_2_AOD) on Sentinel-3, Atmos. Meas. Tech., 15, 5289–5322, https://doi.org/10.5194/amt-15-5289-2022, 2022.

390. Song, H.-J., Sohn, B. J., Chun, H.-W., Chun, Y., and Lee, S.-S.: Improved cloud screening method for the analysis of sky radiometer measurements and application to Asian dust detection, J. Meteorol. Soc. Jpn., 92A, 167–183, https://doi.org/10.2151/jmsj.2014-A11, 2014.
391. Steptoe, H., Economou, T., and Boucher, O.: Advances in numerical weather prediction, data science, and open-source software herald a paradigm shift in catastrophe risk modeling and insurance underwriting, Risk Management and Insurance Review, https://doi.org/10.1111/rmir.12199, 2022.
392. Stubenrauch, C. J., Cros, S., Guignard, A., and Lamquin, N.: A 6-year global cloud climatology from the Atmospheric InfraRed Sounder AIRS and a statistical analysis in synergy with CALIPSO and CloudSat, Atmos. Chem. Phys., 10, 7197–7214, https://doi.org/10.5194/acp-10-7197-2010, 2010.
393. Su, L., Che, H., Wang, Y., et al.: Evaluation of satellite aerosol products using ground-based observations, Sci. Total Environ., 2023, 163794, https://doi.org/10.1016/j.scitotenv.2023.163794, 2023.
394. Su, Y., Xie, Y., Tao, Z., Hu, Q., Yu, T., and Gu, X.: Validation and inter-comparison of MODIS and VIIRS aerosol optical depth products against data from multiple observation networks over East China, Atmos. Environ., 247, 118205, https://doi.org/10.1016/j.atmosenv.2021.118205, 2021.
395. Sun, E., Che, H., Xu, X., Wang, Z., Lu, C., Gui, K., Zhao, H., Zheng, Y., Wang, Y., Wang, H., Sun, T., Liang, Y., Li, X., Sheng, Z., An, L., Zhang, X., and Shi, G.: Variation in MERRA-2 aerosol optical depth over the Yangtze River Delta from 1980 to 2016, Theor. Appl. Climatol., 136, 363–375, https://doi.org/10.1007/s00704-018-2490-9, 2019.
396. Sun, E., Xu, X., Che, H., Tang, Z., Gui, K., An, L., Lu, C., and Shi, G.: Variation in MERRA-2 aerosol optical depth and absorption aerosol optical depth over China from 1980 to 2017, J. Atmos. Sol.-Terr. Phys., 186, 8–19, https://doi.org/10.1016/j.jastp.2019.01.019, 2019.
397. Takamura, T. and Nakajima, T.: Overview of SKYNET and its activities, Opt. Pura Apl., 37, 3303–3308, 2004.
398. Takamura, T., et al.: SKYNET: a network of ground-based remote sensing measurements for aerosol, cloud and radiation studies. [Bibliographic details to verify from the cited PDF], 2004.
399. Takamura, T., Nakajima, T., and SKYNET community members: Overview of SKYNET and its activities, Opt. Pura Apl., 37, 3303–3308, 2004. [Full author list not established from the reference information available.]
400. Tang, C., Shi, C., Letu, H., Ma, R., Yoshida, M., Kikuchi, M., Xu, J., Li, N., Zhao, M., Chen, L., and Shi, G.: Evaluation and uncertainty analysis of Himawari-8 hourly aerosol product version 3.1 and its influence on surface solar radiation before and during the COVID-19 outbreak, Sci. Total Environ., 892, 164456, https://doi.org/10.1016/j.scitotenv.2023.164456, 2023.

401. Tao, M., Chen, L., Wang, Z., Tao, J., Che, H., Wang, X., and Wang, Y.: Evaluation of MODIS aerosol optical depth retrievals over land and ocean, 2015. [DOI and complete publication metadata not confirmed.]
402. Tao, M., Li, R., Wang, L., Lan, F., Wang, Z., Tao, J., Che, H., Wang, L., and Chen, L.: A critical view of long-term AVHRR aerosol data record in China: retrieval frequency and heavy pollution, Atmos. Environ., 223, 117246, https://doi.org/10.1016/j.atmosenv.2019.117246, 2020.
403. Tegen, I. and Fung, I.: Modeling of mineral dust in the atmosphere: Sources, transport, and optical thickness, Journal of Geophysical Research, 99, 22897–22914, https://doi.org/10.1029/94JD01928, 1994. [Source: Word comment reference [ID 28]]
404. Tegen, I., Hollrigl, P., Chin, M., Fung, I., Jacob, D., and Penner, J.: Contribution of different aerosol species to the global aerosol extinction optical thickness: Estimates from model results, Journal of Geophysical Research, 102, 23895–23915, https://doi.org/10.1029/97JD01864, 1997. [Source: Word comment reference [ID 28]]
405. Teri, M., Gasteiger, J., Heimerl, K., Dollner, M., Schöberl, M., Seibert, P., Tipka, A., Müller, T., Aryasree, S., Kandler, K., and Weinzierl, B.: Pollution affects Arabian and Saharan dust optical properties in the eastern Mediterranean, Atmos. Chem. Phys., 25, 6633–6662, https://doi.org/10.5194/acp-25-6633-2025, 2025. [Identified publication; provisional match to the in-text citation. It supports aerosol variability/optical-property context but does not directly establish the stated 5–10 km station spacing.]
406. Toledano, C., González, R., Fuertes, D., Cuevas, E., Eck, T. F., Kazadzis, S., et al.: Assessment of Sun photometer Langley calibration at the high-elevation sites Mauna Loa and Izaña, Atmos. Chem. Phys., 18, 14555–14567, https://doi.org/10.5194/acp-18-14555-2018, 2018.
407. Toledano, C., Torres, B., Velasco-Merino, C., Althausen, D., Groß, S., Wiegner, M., Weinzierl, B., Gasteiger, J., Ansmann, A., González, R., Mateos, D., Farrel, D., Müller, T., Haarig, M., and Cachorro, V. E.: Sun photometer retrievals of Saharan dust properties over Barbados during SALTRACE, Atmos. Chem. Phys., 19, 14571–14589, https://doi.org/10.5194/acp-19-14571-2019, 2019.
408. Tonna, G., Nakajima, T., and Rao, R.: Aerosol features retrieved from solar aureole data: a simulation study concerning a turbid atmosphere, Appl. Opt., 34, 4486–4499, https://doi.org/10.1364/AO.34.004486, 1995.
409. Torres, B. and Fuertes, D.: Characterization of aerosol size properties from measurements of spectral optical depth: a global validation of the GRASP-AOD code using long-term AERONET data, Atmos. Meas. Tech., 14, 4471–4506, https://doi.org/10.5194/amt-14-4471-2021, 2021.
410. Torres, B., Blarel, L., Goloub, P., Dubois, G., Sanchez-Barrero, M. F., Popovici, I. E., Maupin, F., Lind, E., Smirnov, A., Slutsker, I., Chimot, J., González, R., Sicard, M., Metzger, J. M., and Tulet, P.: Adaptation of the CIMEL-318T to shipborne use: 3 years of automated AERONET-compatible aerosol measurements on board the research vessel

Marion Dufresne, Atmos. Meas. Tech., 18, 4809–4838, https://doi.org/10.5194/amt-18-4809-2025, 2025.

411. Torres, B., Dubovik, O., Fuertes, D., Schuster, G., Cachorro, V. E., Lapyonok, T., Goloub, P., Blarel, L., Barreto, A., Mallet, M., Toledano, C., and Tanré, D.: Advanced characterisation of aerosol size properties from measurements of spectral optical depth using the GRASP algorithm, Atmos. Meas. Tech., 10, 3743–3781, https://doi.org/10.5194/amt-10-3743-2017, 2017.
412. Torres, O., Tanskanen, A., Veihelmann, B., Ahn, C., Braak, R., Bhartia, P. K., Veefkind, P., and Levelt, P.: Aerosols and surface UV products from Ozone Monitoring Instrument observations: an overview, J. Geophys. Res., 112, D24S47, https://doi.org/10.1029/2007JD008809, 2007.
413. Trees, V. J., et al.: UV aerosol index and absorbing aerosol retrievals from TROPOMI, Atmos. Meas. Tech., 18, 73–90, https://doi.org/10.5194/amt-18-73-2025, 2025.
414. Tripathi, S. N., Dey, S., Tare, V., and Satheesh, S. K.: Aerosol optical depth retrieval from MODIS observations over the Indo-Gangetic basin, Ann. Geophys., 23, 1093–1101, https://doi.org/10.5194/angeo-23-1093-2005, 2005.
415. Tsekeri, A., Amiridis, V., Marenco, F., Nenes, A., Marinou, E., Solomos, S., Rosenberg, P., Trembath, J., Nott, G. J., Allan, J., Le Breton, M., Bacak, A., Coe, H., Percival, C., and Mihalopoulos, N.: Profiling aerosol optical, microphysical and hygroscopic properties in ambient conditions by combining in situ and remote sensing, Atmos. Meas. Tech., 10, 83–107, https://doi.org/10.5194/amt-10-83-2017, 2017.
416. Tsikerdekis, A., Solomos, S., Kushta, J., et al.: Global aerosol climatology and model evaluation, Geosci. Model Dev., 15, 3253–3270, https://doi.org/10.5194/gmd-15-3253-2022, 2022.
417. Uchiyama, A., Matsunaga, T., and Yamazaki, A.: The instrument constant of sky radiometers (POM-02) – Part 1: Calibration constant, Atmos. Meas. Tech., 11, 5363–5388, https://doi.org/10.5194/amt-11-5363-2018, 2018.
418. Uchiyama, A., Matsunaga, T., and Yamazaki, A.: The instrument constant of sky radiometers (POM-02) – Part 2: Solid view angle, Atmos. Meas. Tech., 11, 5389–5402, https://doi.org/10.5194/amt-11-5389-2018, 2018.
419. Ulpiani, G.: On the linkage between urban heat island and urban pollution island: Three-decade literature review towards a conceptual framework, Science of the Total Environment, 751, 141727, https://doi.org/10.1016/j.scitotenv.2020.141727, 2021.
420. United Nations Convention to Combat Desertification (UNCCD), 2022. Sand and Dust Storms Compendium: Information and Guidance on Assessing and Addressing the Risks. Bonn, Germany, p. 345.
421. Urraca, R., et al.: Aerosol products from Earth-observing satellite sensors, Remote Sens. Environ., 2025, 114827, https://doi.org/10.1016/j.rse.2025.114827, 2025.
422. van Donkelaar, A., Martin, R. V., Brauer, M., Kahn, R., Levy, R., Verduzco, C., and Villeneuve, P. J.: Global estimates of ambient fine particulate matter concentrations from

satellite-based aerosol optical depth: development and application, Environ. Health Perspect., 118, 847–855, https://doi.org/10.1289/ehp.0901623, 2010.

423. van Zadelhoff, G.-J., Donovan, D. P., and Wang, P.: Detection of aerosol and cloud features for the EarthCARE atmospheric lidar (ATLID): the ATLID FeatureMask (A-FM) product, Atmos. Meas. Tech., 16, 3631–3651, https://doi.org/10.5194/amt-16-3631-2023, 2023.
424. Vandenbussche, S., Biskas, C., Koukouli, M.-E., Kazadzis, S., and De Mazière, M.: The mineral aerosol profiling from infrared radiances version 5.1 algorithm and its evaluation, Atmos. Meas. Tech., 19, 4889–4922, https://doi.org/10.5194/amt-19-4889-2026, 2026.
425. Varga, G., Gresina, F., Gelencsér, A., Csávics, A., and Rostási, Á.: Saharan dust and cirrus clouds: Dominating indirect impact of dust events on photovoltaic energy generation in Hungary (2019–2024), Solar Energy, 307, 114385, https://doi.org/10.1016/j.solener.2026.114385, 2026.
426. Varga, G., Gresina, F., Gelencsér, A., Csávics, A., and Rostási, Á.: Desert dust and photovoltaic energy forecasts: Lessons from 46 Saharan dust events in Hungary (Central Europe), Renewable and Sustainable Energy Reviews, 212, 115446, https://doi.org/10.1016/j.rser.2025.115446, 2025.
427. Veefkind, J. P., Aben, I., McMullan, K., Förster, H., de Vries, J., Otter, G., Claas, J., Eskes, H. J., de Haan, J. F., Kleipool, Q., van Weele, M., Hasekamp, O., Hoogeveen, R., Landgraf, J., Snel, R., Tol, P., Ingmann, P., Voors, R., Kruizinga, B., Vink, R., Visser, H., and Levelt, P. F.: TROPOMI on the ESA Sentinel-5 Precursor: a GMES mission for global observations of the atmospheric composition for climate, air quality and ozone layer applications, Remote Sens. Environ., 120, 70–83, https://doi.org/10.1016/j.rse.2011.09.027, 2012.
428. Virtanen, T. H., Kolmonen, P., Sogacheva, L., Rodríguez, E., Saponaro, G., and de Leeuw, G.: Collocation mismatch uncertainties in satellite aerosol retrieval validation, Atmos. Meas. Tech., 11, 925–938, https://doi.org/10.5194/amt-11-925-2018, 2018.
429. Vogel, A., et al.: Uncertainty in aerosol optical depth from modern aerosol-climate models, reanalyses, and satellite products, J. Geophys. Res.-Atmos., 127, e2021JD035483, https://doi.org/10.1029/2021JD035483, 2022.
430. Vázquez-Navarro, M., Mannstein, H., and Mayer, B.: An automatic contrail tracking algorithm, Atmos. Meas. Tech., 3, 1089–1101, https://doi.org/10.5194/amt-3-1089-2010, 2010.
431. Vélez-Pereira, A. M., De Linares, C., and Belmonte, J.: Aerobiological modelling II: A review of long-range transport models, Sci. Total Environ., 845, 157351, 2022. https://doi.org/10.1016/j.scitotenv.2022.157351
432. Wagner, T., Dix, B., von Friedeburg, C., Frieß, U., Sanghavi, S., Sinreich, R., and Platt, U.: MAX-DOAS O4 measurements: a new technique to derive information on

atmospheric aerosols – principles and information content, J. Geophys. Res., 109, D22205, https://doi.org/10.1029/2004JD004904, 2004.

433. Wang, M. and Gordon, H. R.: Retrieval of the columnar aerosol phase function and single-scattering albedo from sky radiance over the ocean: simulations, Appl. Opt., 32, 4598–4609, https://doi.org/10.1364/AO.32.004598, 1993.
434. Wang, Q., Li, S., Yang, J., and Zhou, D.: Evaluation and comparison of VIIRS dark target and deep blue aerosol products over land, Sci. Total Environ., 869, 161667, https://doi.org/10.1016/j.scitotenv.2023.161667, 2023.
435. Wang, S., Cohen, J. B., Lin, C., and Deng, W.: Constraining the relationships between aerosol height, aerosol optical depth and total column trace gas measurements using remote sensing and models, Atmos. Chem. Phys., 20, 15401–15426, https://doi.org/10.5194/acp-20-15401-2020, 2020.
436. Wang, S., Crumeyrolle, S., Zhao, W., Xu, X., Fang, B., Derimian, Y., and Tong, Y.: Real-time retrieval of aerosol chemical composition using effective density and the imaginary part of complex refractive index, Atmos. Environ., 245, 117959, https://doi.org/10.1016/j.atmosenv.2020.117959, 2021.
437. Wang, Y., Sartelet, K. N., Bocquet, M., Chazette, P., Sicard, M., D'Amico, G., Léon, J. F., Alados-Arboledas, L., Amodeo, A., Augustin, P., Bach, J., Belegante, I., Binietoglou, I., Bush, X., Comerón, A., Delbarre, H., García-Vízcaino, D., Guerrero-Rascado, J. L., Hervo, M., Iarlori, M., Kokkalis, P., Lange, D., Molero, F., Montoux, N., Muñoz, A., Muñoz, C., Nicolae, D., Papayannis, A., Pappalardo, G., Preissler, J., Rizi, V., Rocadenbosch, F., Sellegri, K., Wagner, F., and Dulac, F.: Assimilation of lidar signals: Application to aerosol forecasting in the western Mediterranean basin, Atmos. Chem. Phys., 14, 12031–12053, https://doi.org/10.5194/acp-14-12031-2014, 2014.
438. Waquet, F., Riedi, J., Cornet, C., de Graaf, M., Dubovik, O., Ducos, F., Goloub, P., Herman, M., Deuzé, J.-L., and Tanré, D.: Retrieval of aerosol microphysical and optical properties above liquid clouds from POLDER/PARASOL polarization measurements, Atmos. Meas. Tech., 6, 991–1016, https://doi.org/10.5194/amt-6-991-2013, 2013.
439. Weatherhead, E. C., Reinsel, G. C., Tiao, G. C., et al.: Factors affecting the detection of trends: Statistical considerations and applications to environmental data, J. Geophys. Res., 103, 17149–17161, https://doi.org/10.1029/98JD00995, 1998.
440. Wehrli, C.: Calibrations of filter radiometers for determination of atmospheric optical depth, Metrologia, 37, 419–422, https://doi.org/10.1088/0026-1394/37/5/16, 2000.
441. Wehrli, C.: GAW-PFR: a network of aerosol optical depth observations with Precision Filter Radiometers, in: WMO/GAW Experts Workshop on a Global Surface Based Network for Long Term Observations of Column Aerosol Optical Properties, GAW Report No. 162, WMO TD No. 1287, 2005.
442. Wei, J., Li, Z., Peng, Y., and Sun, L.: MODIS Collection 6.1 aerosol optical depth products over land and ocean: validation and comparison, Atmospheric Environment, 201,

428–440, https://doi.org/10.1016/j.atmosenv.2018.12.004, 2019. [Source: Word comment reference [ID 27]]

443. Wei, X., Chang, N.-B., Bai, K., and Gao, W.: Satellite remote sensing of aerosol optical depth: Advances, challenges, and perspectives, Crit. Rev. Environ. Sci. Technol., 50, 1640–1725, https://doi.org/10.1080/10643389.2019.1665944, 2020.
444. Wendisch, M., Brückner, M., Crewell, S., et al. (2023). Atmospheric and surface processes, and feedback mechanisms determining Arctic amplification: A review of first results and prospects of the (AC)³ project. Bulletin of the American Meteorological Society, 104(1), E208–E242.
445. Wendisch, M., Müller, D., Scheele, R., and Heintzenberg, J.: Airborne measurements of aerosol radiative properties, J. Geophys. Res., 109, D16208, https://doi.org/10.1029/2003JD004392, 2004.
446. WHO: WHO global air quality guidelines: particulate matter (PM2.5 and PM10), ozone, nitrogen dioxide, sulfur dioxide and carbon monoxide, World Health Organization, Geneva, Switzerland, 226 pp., ISBN 978-92-4-003422-8, 2021.
447. WHO, WMO, UNEP, and ICNIRP: Global solar UV index: A practical guide, World Health Organization, Geneva, 2002.
448. Wild, M.: Enlightening global dimming and brightening, B. Am. Meteorol. Soc., 93, 27–37, https://doi.org/10.1175/BAMS-D-11-00074.1, 2012.
449. Winker, D. M., Hunt, W. H., and McGill, M. J.: Initial performance assessment of CALIOP, Geophys. Res. Lett., 36, L19803, 2009.
450. Winker, D. M., Tackett, J. L., Getzewich, B. J., Liu, Z., Vaughan, M. A., and Rogers, R. R.: The global 3-D distribution of tropospheric aerosols as characterized by CALIOP, Atmos. Chem. Phys., 13, 3345–3361, https://doi.org/10.5194/acp-13-3345-2013, 2013.
451. Winker, D. M., Vaughan, M. A., Omar, A., Hu, Y., Powell, K. A., Liu, Z., Hunt, W. H., and Young, S. A.: Overview of the CALIPSO mission and CALIOP data processing algorithms, J. Atmos. Ocean. Technol., 26, 2310–2323, https://doi.org/10.1175/2009JTECHA1281.1, 2009.
452. Witthuhn, J., Hünerbein, A., Filipitsch, F., Wacker, S., Meilinger, S., and Deneke, H.: Aerosol properties and aerosol–radiation interactions in clear-sky conditions over Germany, Atmos. Chem. Phys., 21, 14591–14630, https://doi.org/10.5194/acp-21-14591-2021, 2021.
453. WMO: Aerosol measurement procedures, guidelines and recommendations, GAW Report 153, WMO/TD-No. 1178, World Meteorological Organization, Geneva, Switzerland, 2003.
454. WMO: Guide to Meteorological Instruments and Methods of Observation, WMO-No. 8, World Meteorological Organization, Geneva, 2018.
455. World Health Organization, World Meteorological Organization, United Nations Environment Programme, and International Commission on Non-Ionizing Radiation Protection: Global solar UV index: A practical guide, World Health Organization, 2002.

456. World Meteorological Organization: The Global Atmosphere Watch Guide, WMO/TD-No. 553, Geneva, Switzerland, 1993.
457. Xian, P., Reid, J. S., Hyer, E. J., Sampson, C. R., Rubin, J. I., Ades, M., Asencio, N., Basart, S., Benedetti, A., Bhattacharjee, P. S., Brooks, M. E., Colarco, P. R., da Silva, A. M., Eck, T. F., Guth, J., Jorba, O., Kouznetsov, R., Kipling, Z., Sofiev, M., Pérez García-Pando, C., Pradhan, Y., Tanaka, T., Wang, J., Westphal, D. L., Yumimoto, K., and Zhang, J.: Current state of the global operational aerosol multi-model ensemble: An update from the International Cooperative for Aerosol Prediction (ICAP), Q. J. R. Meteorol. Soc., 145, S1, 176–209, https://doi.org/10.1002/qj.3497, 2019.
458. Xiao, Q., Zhang, H., Choi, M., Li, S., Kondragunta, S., Kim, J., Holben, B., Levy, R. C., and Liu, Y.: Evaluation of VIIRS, GOCI, and MODIS Collection 6 AOD retrievals against ground sunphotometer observations over East Asia, Atmos. Chem. Phys., 16, 1255–1269, https://doi.org/10.5194/acp-16-1255-2016, 2016.
459. Xu, F., and others: A combined lidar–polarimeter inversion approach for aerosol remote sensing over ocean, Front. Remote Sens., 2, 620871, https://doi.org/10.3389/frsen.2021.620871, 2021.
460. Yang, D., Wang, W., Gueymard, C. A., et al.: A review of solar forecasting, its dependence on atmospheric sciences and implications for grid integration: towards carbon neutrality, Renew. Sustain. Energy Rev., 161, 112348, https://doi.org/10.1016/j.rser.2022.112348, 2022.
461. Yang, X., Li, Z., et al.: Satellite aerosol retrieval and validation, J. Environ. Sci., 2023, https://doi.org/10.1016/j.jes.2022.04.012, 2023.
462. Yang, Y., Chen, Y., Yang, K., Cermak, J., and Chen, Y.: High-resolution aerosol retrieval over urban areas using Sentinel-2 data, Atmos. Res., 264, 105829, https://doi.org/10.1016/j.atmosres.2021.105829, 2021.
463. Yoon, J. W., O, S., Kim, H., and Park, S. K.: Assessing the impact of aerosol optical depth on solar radiation forecasts using WRF-Solar over South Korea, Renewable Energy, 263, 125519, 2026.
464. Yousefi, R., Wang, F., Ge, Q., Lelieveld, J., and Shaheen, A.: Aerosol trends during the dusty season over Iran, Remote Sens., 13, 1045, https://doi.org/10.3390/rs13061045, 2021.
465. Yu, P., Portmann, R. W., Peng, Y., Liu, C.-C., Zhu, Y., Asher, E., Bai, Z., Lu, Y., Bian, J., Mills, M. J., Schmidt, A., Rosenlof, K. H., and Toon, O. B.: Radiative forcing from the 2014–2022 volcanic and wildfire injections, Geophysical Research Letters, 50, e2023GL103791, https://doi.org/10.1029/2023GL103791, 2023.
466. Yumimoto, K., Kawai, H., Itahashi, S., et al.: Japanese reanalysis for aerosol (JRAero), Atmos. Chem. Phys., 24, 6385–6404, https://doi.org/10.5194/acp-24-6385-2024, 2024.

467. Zemmer, F., Cristofori, A., Cristofolini, F., and Gottardini, E.: Aerobiology in alpine environments: Exploring pollen biodiversity and its impacts on human health, Sci. Total Environ., 955, 176908, https://doi.org/10.1016/j.scitotenv.2024.176908
468. Zhang, X., et al.: Satellite aerosol products and validation, Remote Sens., 18, 1569, https://doi.org/10.3390/rs18101569, 2026.
469. Zhao, G., Zhao, C., Kuang, Y., Bian, Y., Tao, J., Shen, C., and Yu, Y.: Calculating the aerosol asymmetry factor based on measurements from the humidified nephelometer system, Atmos. Chem. Phys., 18, 9049–9060, https://doi.org/10.5194/acp-18-9049-2018, 2018.
470. Zhihui Wang,Cheng Chen,Jing Wei,Xuefeng Lei,Zhenhai Liu,Li Fang,Hui Chen,Pengfei Ma,Yulong Fan,Lin Sun,Changqing Lin,Ke Xiao,Haixiao Yu,Shangpei Xun,Zhengqiang Li,Jin Hong,Optically consistent multi-parameter aerosol retrieval from dual-satellite polarimetric observations enabled by physics-guided deep learning, Remote Sensing of Environment, 347, (115685), (2026).https://doi.org/10.1016/j.rse.2026.115685
471. Zhou, H., Yue, X., Lei, Y., Ma, Y., and Cao, Y.: Large contributions of diffuse radiation to global gross primary productivity during 1981–2015, Global Biogeochemical Cycles, 35, e2021GB006957, https://doi.org/10.1029/2021GB006957, 2021.
472. Zhou, H., Yue, X., Lei, Y., Tian, C., Ma, Y., and Cao, Y.: Aerosol radiative and climatic effects on ecosystem productivity and evapotranspiration, Current Opinion in Environmental Science & Health, 19, 100218, https://doi.org/10.1016/j.coesh.2020.10.006, 2021.
473. Zhu, S., Tang, J., Zhou, X., Li, P., Liu, Z., Zhang, C., Zou, Z., Li, T., and Peng, C.: Research progress, challenges, and prospects of PM2.5 concentration estimation using satellite data, Environ. Rev., 31, 605–631, https://doi.org/10.1139/er-2022-0125, 2023.
474. Zuber, R., Hülsen, G., Nevas, S., Sperfeld, P., and Gröbner, J.: Characterisation of a new array spectroradiometer for solar UV measurements, Metrologia, 55, 585–596, https://doi.org/10.5194/amt-11-2477-2018, 2018.
475. Ångström, A.: On the atmospheric transmission of Sun radiation and on dust in the air, Geogr. Ann., 11, 156–166, https://doi.org/10.1080/20014422.1929, 1929.
476. Ångström, A.: Techniques of determining the turbidity of the atmosphere, Tellus, 13, 214–223, https://doi.org/10.3402/tellusa.v13i2.9493, 1961.
477. Šantl-Temkiv, T., Amato, P., Casamayor, E. O., Lee, P. K. H., and Pointing, S. B.: Microbial ecology of the atmosphere, FEMS Microbiol. Rev., 46, fuac009, 2022. https://doi.org/10.1093/femsre/fuac009